ABSTRACT

Introduction

The stability along joint planes is one of the most important characteristics of a rock mass forming the foundation of a concrete dam. The shear strength of discontinuities within the foundation rock is probably the most important characteristic.

Objectives and Purpose of the study

The objectives of this research project were to determine and to analyse the shear strength of joints in a number of rock types, sampled at different locations, and to link these strengths to the condition in the foundations of dams and, in particular, the condition of the surfaces of the rock joints. The information so obtained can then serve as a databank for the design of new dams and for the evaluation of the safety of existing dams.

Stages of investigation

The study was carried out in four identifiable phases. The first phase that took place during 1992 and 1993 was a literature study in order to determine the shear strength characteristics of different rock types world-wide and in southern Africa. The literature study was updated during 2002/3. During this stage a visit was undertaken to the UK, Norway and the USA to study shear apparatus and the rock testing methods in these countries. The second phase was to determine the shear strength characteristics of important southern African rock types. During the period 1993 to 1995 the shear apparatus and surface-scanning device to be used in the third stage were designed and constructed. The third phase (1994 to 1999) comprised of direct shear tests on NX-size borehole core samples and the testing and characterisation of large shear surfaces. The last phase (1999 to 2003) consisted of updating the literature survey and compilation of the thesis.

Several delays were encountered mainly due to the following reasons: (a) the late delivery of the large shearbox and subsequent problems with the computer controlling the shearbox, (b) resignation of the technician working full-time on the project and (c) illness of the researcher during 1996.

It was impossible to determine the true peak and residual shear strength due to practical limitations. Sa discussed in chapter four the peak values are therefore approximated by

determining the "maximum post-peak" strength, whilst residual values were approximated by "minimum post-peak" values.

Format of the thesis

The text of the thesis starts by stating the problems to be investigated, followed by Chapter two containing the findings of a literature study. Chapter three describes the experimental stage of the study: the methods used and a description of the equipment. Chapter four contains the presentation and discussion of the results. This is followed by Chapter five showing a classification of shear strength using a geotechnical characterization of the joint surface followed by Chapters six and seven with the conclusions, recommendations and references. The Compact Disc (CD) contains the appendices (reports, graphs and photo's) in electronic format.

Results

A literature study on the test methods and shear strength characteristics of different rock types was conducted. It was found that although shear strength characteristics of rock material have been investigated on a regular basis for civil and other engineering applications, this information is not readily available to the engineering community at large for safety use in dams. It is often regarded as confidential information by clients and filed for possible use against claims. This document is probably the most comprehensive source of shear strength characteristics of southern African rock types available today.

This report describes the shear strength characteristics of quartzite, shale, sandstone, dolerite, mudstone, granite, rhyolite and tillite. Chapter four describes each of these rock types in detail. These rock types were selected because they cover a very large portion of the surface area of southern Africa, and as such, many dams and other civil engineering structures have been built on them.

Emphasis was placed on the shear strength parameters of joints, especially the angle of friction. Two types of joints are recognised in nature: (a) joints with no or little fill material where the shear strength is determined by the characteristics of the rock material and (b) joints with fill material where the shear strength is determined by the characteristics of the fill material. The major part of this research concentrated on joints with no or little fill material listed under (a).

The three major characteristics determining the shear strength parameters of this type of joint are (i) the base shear strength of the rock material, (ii) the roughness profile along the joint surface and (iii) the hardness of the material on the joint surface.

The basic shear strength parameters of the different rock materials were determined as part of the determination of rock material characteristics. The basic angle of friction obtained for the different materials corresponds very well to those published in the literature. The values for cohesion obtained through testing is zero to very small.

As part of this research project, a laser-scanning device was developed. This device measure the x, y and z co-ordinates on a rock joint surface on a grid pattern. This information can be analyzed with software on a computer to produce a contour diagram of the joint surface area. From this contour diagram, joint roughness profiles were obtained. These, as well as profiles obtained with a carpenter's comb, were compared visually, with an overlay, to typical roughness profiles as published by Barton (1977).

The relationship between joint roughness coefficient (JRC) and shear displacement was investigated during this study. The influence of high normal stresses were not taken into consideration as testing was limited to normal stresses with a maximum of 1 MPa. An exponential regression was fitted to the points plotted. After a cumulative shear displacement of more than 2,0 meter will be required to smooth the joint surface as a result of friction. It was found that after a shear displacement of 2,0 meters the friction angle was equal to the residual friction angle.

Conclusions

This study provides a guide to shear strength characteristics of several important rock types in southern Africa for planning and preliminary design of dams. It is probably the most comprehensive document describing the rock material, the testing procedure, and the shear strength characteristics of so many rock types in southern Africa.

This research project was the first attempt to determine the shear strength characteristics of joints in southern African rock types with a large shear apparatus.

This study also contributes to the knowledge on shear strength of southern African rocks, in particular on (i) the sampling and preparation of specimens for testing in the large shear apparatus, (ii) the measurement of the roughness of the joint surfaces and (iii) the testing procedure and (iv) interpretation and application of friction angle as design parameter in the analysis of stability of dam foundations. The shear strength characteristics of the rock joints of southern African rocks are described joints were classified using a geotechnical description of the joint surface. Geotechnical parameters include rock type, roughness, hardness, and a description of fill joint material was used in the classification. This classification is a first attempt to use these parameters and further work still needs to be done in this regard.

Further research

It is recommended that a project be initiated to investigate the shear strength of southern African rock types in further detail. Such an investigation can build on the knowledge obtained in this investigation. It is important to keep the variables such as rock type, weathering, and hardness to a minimum to investigate influence of joint roughness. An appropriate rock type to start with could be mudstone from the Qeduzisi Dam area near Ladysmith. This is a relative soft rock with smooth joints that gave low shear strength results during testing. These results of this study could be confirmed. The investigation could then be extended to other rock types once the influence of roughness has been established.

Acknowledgement

The author whishes to express his gratitude to the Water Research Commission for funding this project and hope that the report will contribute to dams and other civil engineering structures being built more cost effectively and safely.

Contributions by the following persons are acknowledged:

Prof G Pegram of the Department of Civil Engineering of the University of Natal who assisted with the development and building of the laser scanning device.

Mr. UW Vogler who assisted with the interpretation of the test results of the different phases of testing.

Mr. A van der Walt of the Department of Water Affairs and Forestry for the assistance with the design and building as well as the use of the large shear box.

Prof A van Schalkwyk for his guidance and contribution to enhancing the quality of the final thesis.

CONTENTS

LIST OF FIGURES

LIST OF TABLES

LIST OF SYMBOLS AND ACRONYMS

A = cross-sectional area (m^2)

c = cohesion (kPa, MPa)

d = diameter (m)

E_t = Tangent modulus (GPa)

E_{av} = Average modulus (GPa)

E_{sec} = Secant Modulus (GPa)

g = acceleration due to gravity (9,81 ms^{-2})

l = length (m)

m = meter (m)

N = Newton

ν = Poisson's ratio

ρ = density (kg/m^3)

γ = unit weight (kN/m^3)

σ = normal stress (MPa)

τ = shear stress (MPa)

ϕ = friction angle (degrees)

ϕ_b = basic friction angle (degrees)

ϕ_r = residual friction angle (degrees)

ISRM = International Society for Rock Mechanics

JCS = Joint wall compressive strength (MPa)

JRC = Joint roughness coefficient

PLSI = Point load strength index

SHI = Shear strength index

UCS = Uniaxial compressive strength (MPa)

XRD = X-ray diffraction

CHAPTER ONE

INTRODUCTION AND MOTIVATION

1.1 Objectives of the study

The engineering characteristics of rocks and particularly, the shear strength of joints (discontinuities) in rock masses play a key role in civil engineering and specifically in the design and safety evaluation of dams. Civil engineers are confronted with the problem of shear strength when designing excavations in rock masses for structures such as dam foundations, cuttings in rock for roads (slopes), tunnels etc.

To evaluate the stability of a dam foundation, the shear strength of those joints with the most unfavourable orientations relative to the applied loads is required. Determination of the orientation of joints in a foundation by means of a joint survey is relatively easy. From this, the most unfavourably oriented joints can be selected. The design parameters for shear strength of these joints are usually not available during the early stages of the design and it is thus necessary to estimate these. It is therefore the aim of this investigation to provide a guideline for the estimation of these shear strength characteristics as accurately as possible.

The objective of this research project was to determine and to analyse the shear strength of joints in a number of rock types, sampled at different locations and to classify these strengths in accordance with joint surface parameters. The information so obtained serves as a data bank of shear strength parameters for the design of new dams and for the evaluation of the safety of existing dams in South Africa.

The shear strength of joints in rock is also of importance for the design of slopes in rock for roads and railways and for mining excavations as well as for the design of tunnels for civil and mining engineering applications. The information presented in this report will therefore also be of use to engineers in the design of such structures.

1.2 Motivation

A large proportion of South Africa's economically most active population lives in the Gauteng Province, which is situated on a watershed. Furthermore, South Africa is a relatively dry country that necessitates that water storage dams have to be built in suitable riverbeds from where the water has to be transferred to the end users by means of pump stations, pipelines, tunnels and canals. A number of major water schemes have been constructed, e.g. the Drakensberg Pumped Storage Scheme, the Orange-Fish River Scheme and the Lesotho Highlands Water Project currently under construction. Increasing the capacity of existing schemes will become necessary and further, similar schemes will have to be constructed in the future to satisfy the ever-increasing demand for water in the RSA. A number of dams in our country have reached ages of 40 years and more with the result that their safety and stability will have to be re-evaluated.

The stability of a dam depends on its design, on the materials and methods used during its construction and on the stability of the foundations on which it is built. The characteristics of the rocks and particularly the shear resistance of the joints in the rocks are very important design parameters. The latter parameter has generally not received the necessary attention, mainly because it cannot be determined quickly and cheaply. An additional explanation is that obtaining representative rock samples is very difficult and often only the more competent materials survive the sampling processes.

A large number of rock types occur in southern Africa. These include igneous, sedimentary and metamorphic rocks. A database including the widest range is thus preferable. The types of rocks tested include in this investigation were: sandstone of the Cape Supergroup; post-Karoo dolerite; mudstone, sandstone, of the Karoo Supergroup; and granite of the Basement Complex.

1.3 The history of the study conducted

The duration of the study was ten years, from 1992 until 2002. This study formed part of a more extensive study to determine the engineering characteristics of important southern African rock types with the emphasis on the shear strength of concrete dam foundations (Geertsema, 2000). The Water Research Commission (WRC) was the main funder of this project.

The study has been executed in five distinct phases. The first phase, took place between 1992 and 1993 and consisted of a literature survey with the aim of collecting and studying data on the engineering properties of different types of rock from southern Africa and elsewhere, as well as of worldwide origin. The literature study was updated during 2002-2003. During this phase the United Kingdom, Norway and the United States were visited by the author, to study inter alia their methods of determination of the engineering characteristics of rocks and particularly also their equipment for shear testing. During the same period, the Department of Water Affairs and Forestry (DWAF) designed a large shear box. The shear box was built during 1993 – 1995. This shear box was used for testing of large samples during this research project.

During the second phase a sampling programme was undertaken and the general engineering properties of the sampled southern African types of rocks were determined. During 1995 a scanning apparatus was developed and built. This apparatus scans the surface of a rock specimen and can produce a contour map of the scanned surface, which can be used to describe quantitatively the surface topography and thus the roughness of the rock joints to be tested.

The third phase, from 1994 to 1999, consisted of an intensive testing programme during which NX-size (54,5 mm diameter) cores were used to determine the shear strength (basic and residual) of the selected rock materials. In addition, the large specimens collected for testing in the large shear box at the DWAF were characterised and a number of these were tested.

During the fourth phase a number of shear tests on large specimens were conducted at the DWAF – (both 'wet' and 'dry').

The last phase conducted between 1999 and 2000 included a sampling and testing programme of three specimen of granite. The purpose of this phase was to apply the knowledge and experience gained during the previous part of the project, to calibrate the results obtained previously. This thesis was written during 2001 and 2002. Additions were made during 2003.

The investigation experienced a number of serious delays for which the main reasons were:
(a) The large shear box developed by the DWAF was delivered late and in addition, problems were experienced with its computerised control system.
(b) The resignation of the technician who had been appointed in a full-time capacity to work on the project.
(c) The illness of the researcher during 1996.

As a result of the test machine being new, and that a learning curve had to be followed by the investigators to familiarise themselves with the equipment, more time was spent on this phase that was anticipated. The taking of large rock samples was also more complicated as originally anticipated. Just as these problems were being solved the researcher fell ill. The result of this sequence of events led to a situation where data could only be analysed after the testing programme was almost completed. A second attempt was made after consultation with a consultant to put the available already tested samples through a further set of tests. It should be emphasised that a specific sample could only be tested once to determine the peak shear strength. All these factors contributed to a rather small number of rock samples that could ultimately be tested.

1.4 Outline of the thesis

Chapter one of this thesis describes the objectives, the motivation for the project as well as the problem of determining the shear strength of joints in rock. This is followed by a description of a literature survey that describes the principal of shear, factors influencing shear strength, results of previous studies and work done by the Norwegian Geotechnical Institute. The following chapter deals with the rock types tested as well as the determination of the shear characteristics. Chapter four describes the interpretation and discussion of the results. This chapter also describes a tool for experienced engineering geologists or rock mechanics engineers to determine the contribution to the angle of friction by the joint surface

characteristics. By adding the basic friction angle the total friction angle is obtained. Chapter five describes the classification of shear strength and an estimation of the shear strength by making use of the geotechnical description of the joint surfaces. The next two chapters present conclusions and recommendations. The thesis closes with a list of literature references.

Appendices are available in the back of the thesis in electronic format on compact disc.

CHAPTER TWO
LITERATURE STUDY ON THE SHEAR STRENGTH OF JOINTS IN ROCK

2.1 Introduction

Discontinuities such as bedding planes, joints, shear zones and faults form part of any rock mass. The behaviour of the rock mass at shallow depth, where stresses are relatively low, is largely controlled by sliding of blocks of rock on joints (discontinuities).
There are a number of factors that influence the shear strength of joints in rock and are mainly concerned with the character of the joint surface. These factors include: the roughness of the joint surface, hardness of the joint surface, the presence and pressure of water, the presence of fill material, type of fill material and the thickness of fill material.

2.2 Discontinuities in rock

Discontinuities occurring in any rock mass are the result of the formation of the rock mass or movement in the crust of the earth. According to Jennings (1971) two sets of discontinuities are recognized namely (i) major or through going features and (ii) minor or secondary features. Major features include bedding planes, faults, contacts and dykes, all of which can be traced over long distances. These joints are important in the analysis of stability of slopes. Minor features are of limited length such as cross joint in sedimentary rocks

Types of joints

Sedimentary rock normally has **bedding planes** as a major discontinuity. The origin of these joints are from the deposition of mechanical or chemical sediments.
Stress relief joints form as a result of erosion of weathered rock and soil materials. **Tension joints** are the result of cooling and crystallization of igneous rock.
Shear joints is the result of faulting and shear in the rock mass as result tectonic movement.

Characteristics of joints

The **orientation** of a joint plane in relation to other joint planes and the direction of disturbing force will determine if parts of a rock mass are free to slide.

Joint **spacing** is a measure of the closeness of joints in a specific set and will effect the shear strength of a rock mass.

Hardness is determined by the **wall rock type** or degree of alteration of the joint wall Weathered or filled joints will have lower shear strength than unweathered hard joint surfaces.

Waviness is a contributor to higher shear strength over larger areas such as dam foundations.

Roughness can be described in terms of (i) asperities (small-scale roughness) (ii) large protrusions (intermediate roughness) and (iii) waviness or undulations (large-scale roughness).

Filling of joints with alteration products can have a negative effect on the shear strength of joints.

The **water condition** on the joint surface has a influence on the mechanical behaviour or the joint surface. The presence of water and water under pressure normally reduces shear strength.

2.3 The principles of shear

The principle of shear and shear strength is described as follows by Cutnell and Johnson (2001): Experiments have shown that when a body is pressed against a surface, and a force **F** attempts to slide the body along the surface, the resulting frictional force has three properties:

a. If the body does not move, then the static frictional force **fs** and the component of **F** that is parallel to the surface are equal in magnitude, and **fs** is directed opposite that component of **F.**

b. The magnitude of **fs** has a maximum value of **fs max** that is given by:

$$\mathbf{fs,\ max} = \mu_s N \quad \ldots\ldots\ldots\ldots\ldots\ldots\ldots\ldots\ldots (2.1)$$

c. where μs is the coefficient of static friction, and N is the magnitude of the normal force. If the magnitude of the component of **F** that is parallel to the surface exceeds **fs, max** then the body begins to slide along the surface. Just before this point is reached, the factor of safety is equal to one.

If the body begins to slide along the surface, the magnitude of the frictional force rapidly decreases to a value $\mathbf{f_k}$ given by: $\mathbf{f_k} = \mu_k \mathbf{N}$ .....(2.2)

where μ_k is the coefficient of kinetic friction. Thereafter during sliding, the kinetic frictional force f_k is given by equation 2.2

This principal could be demonstrated by the following example: Figure 2.1 shows a slab of rock resting on an other slab of rock separated by a natural joint tilted at an angle θ with the horizontal. By using a tilt testing apparatus it is found that when θ is increased to 30°, the top slab begins to slide down the joint plane. What is the coefficient of static friction between the bottom and top rock slabs?

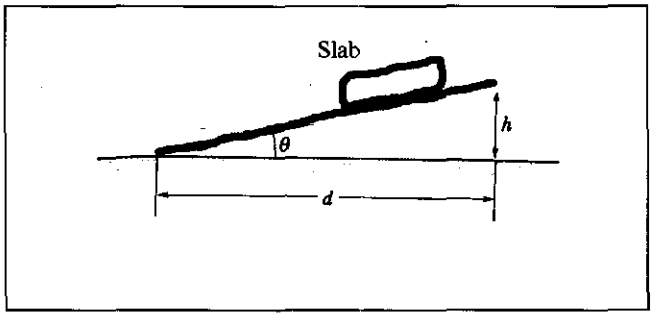

Figure 2.1 **A slab of rock resting on another slab of rock separated by a natural joint tilted at an angle θ with the horizontal. (After Cutnell and Johnson (2001) modified)**

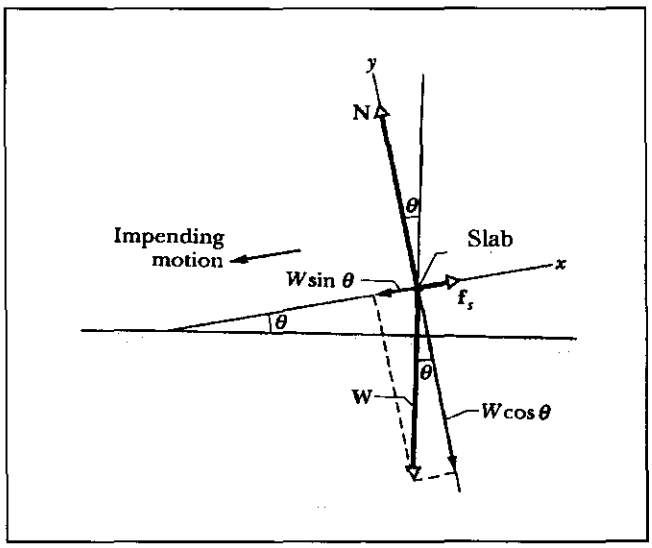

Figure 2.2 **A free-body diagram of a slab of rock when it is on the verge of sliding. (After Cutnell and Johnson (2001) modified)**

Figure 2.2 is a free-body diagram for the slab when it is on the verge of sliding. The forces on the slab is the normal force N, pushing outward from the plane of the book, the weight W of the slab on top, and the frictional force F_s, which points up the plane, because the impending motion is down the plane. Since the slab is in equilibrium, the net force acting on it must be zero. From Newton's second law, we have:

$$\Sigma F = f_s + W + N = 0 \quad \ldots\ldots\ldots\ldots\ldots\ldots\ldots\ldots \quad (2.3)$$

For the x components, this vector equation gives us:

$$\Sigma F_x = f_s - W \sin\theta = 0$$

or $$f_s = W \sin\theta \quad \ldots\ldots\ldots\ldots\ldots\ldots\ldots\ldots\ldots\ldots \quad (2.4)$$

For the y components, we have

$$\Sigma F_y = N - W \cos\theta = 0$$

or $$N = W \cos\theta \quad \ldots\ldots\ldots\ldots\ldots\ldots\ldots\ldots\ldots\ldots \quad (2.5)$$

When the slab is on the verge of sliding, the magnitude of the static frictional force acting on it, has its maximum value $\mu_s N$. Substituting this into equation 2.4 and dividing by equation 2.5, we obtain:

$$f_s / N = \mu_s N / N = W \sin\theta / W \cos\theta = \tan\theta$$

or $$\mu_s = \tan\theta \quad \ldots\ldots\ldots\ldots\ldots\ldots\ldots\ldots\ldots\ldots \quad (2.6)$$

The coefficient of static friction for a joint set with a slope of 30° is thus tan 30°.

If a body slides or attempts to slide over a surface, a bonding between the body and the surface resists the motion. The resistance is considered to be a single force called the frictional force or simply **friction**. The force runs parallel to the surface, opposite the direction of the intended motion. The frictional force is a force acting between the surface atoms of one body and those of the other. When two surfaces are placed together, only the high points touch each other. The actual microscopic area of contact is much less than the apparent macroscopic contact area, perhaps by a factor of 10^4. (after Halliday, D (1993)). Many contact points cold weld together. (If two highly polished and carefully cleaned metal surfaces are brought together in a very good vacuum, they cannot be made to slide over each other, instead they cold-weld together, instantly forming a single piece of metal.) When surfaces move across each other, there is a continuous rupturing and reforming of contact areas or welds. This is illustrated in Figure 2.3

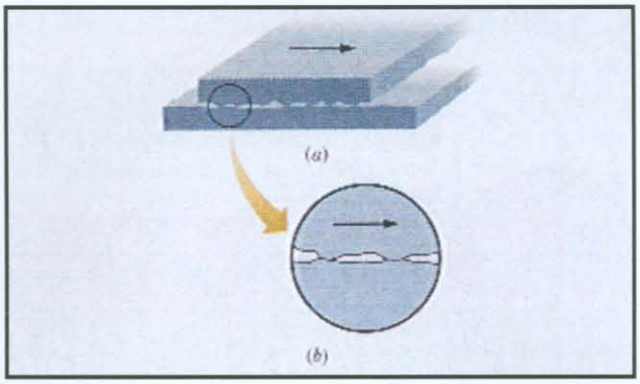

Figure 2.3 **Continuous rupturing and reforming of contact areas as surfaces move across each other. (After Cutnell and Johnson, 2001)**

2.4 Shear strength of planar joint surfaces in rock

A number of samples (at least three) are required for shear testing, ISRM (1974). Each sample contains a through-going plane (discontinuity) that could be used to apply a normal and shear load to, for testing.

The bedding plane is absolutely planar, having no surface irregularities or undulations. As illustrated in Figure 2.4, each specimen is subjected to a stress σ_n normal to the bedding plane, and shear stress τ, required to cause a displacement δ.

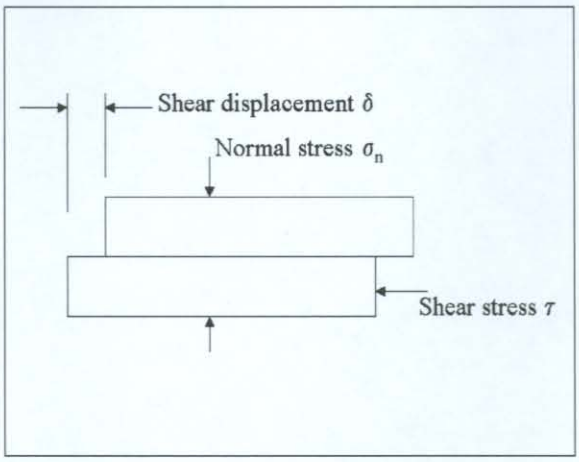

Figure 2.4 **Schematic representation of displacement and stresses on joint plane.**

The shear stress will increase rapidly until the peak strength is reached. This corresponds to the sum of the strength of the cementing material bonding the two halves of the bedding plane together and the frictional resistance of the matching surfaces. As the displacement continues, the shear stress will fall to some residual value that will then remain constant, even for large shear displacements. This basic test method and theory is described by Hoek, E (2000).

Plotting the peak and residual shear strengths for different normal stresses results in the two lines illustrated in Figure 2.5. For planar discontinuity surfaces the experimental points will generally fall along straight lines. The peak strength line has a slope of ϕ and an intercept of c on the shear strength axis. The residual strength line has a slope of ϕ_r. The relationship between the peak shear strength τ_p and the normal stress σ_n can be represented by the **Mohr-Coulomb** equation:

$$\tau_p = c + \sigma_n \tan \phi \quad \ldots\ldots\ldots\ldots\ldots\ldots\ldots\ldots (2.7)$$

(τ_p = peak shear strength, c = cohesion intercept, ϕ = friction angle of the joint wall (discontinuity wall), σ_n = normal stress).

Discontinuities of geological origin that intersect almost all near-surface rock masses are referred to as joints. The most important external factor affecting shear strength is the magnitude of the effective normal stress (σ_n) acting across the joint. In many rock engineering problems in civil engineering the maximum effective normal stress will lie in the range 0.1 to 2.0 MPa for those joints considered critical for stability (in mining engineering this value can be much bigger). This effective normal stress is about three orders of magnitude lower than those used by tectonophysicists when studying the shear strength faults under stress levels of for example 100 to 2000 MPa. In consequence, the literature contains shear strength data for rock joints spanning a stress range of at least four orders of magnitude. It is partly for this reason that opinions concerning shear strength vary so widely to the results of shear strength investigations on rock joints. If Equation (2.7) is applied to the results of shear tests on rough joints, under both high normal stress and low normal stress, one finds the tectonophysicists recording a cohesion intercept of tens of MPa and a friction angle of perhaps only 20°, while the rock slope engineer finds that he has a friction angle of perhaps 70° and zero cohesion.

Figure 2.5 shows a graph of shear stress vs. shear displacement that illustrates peak and residual shear strength. (Patton, 1966).

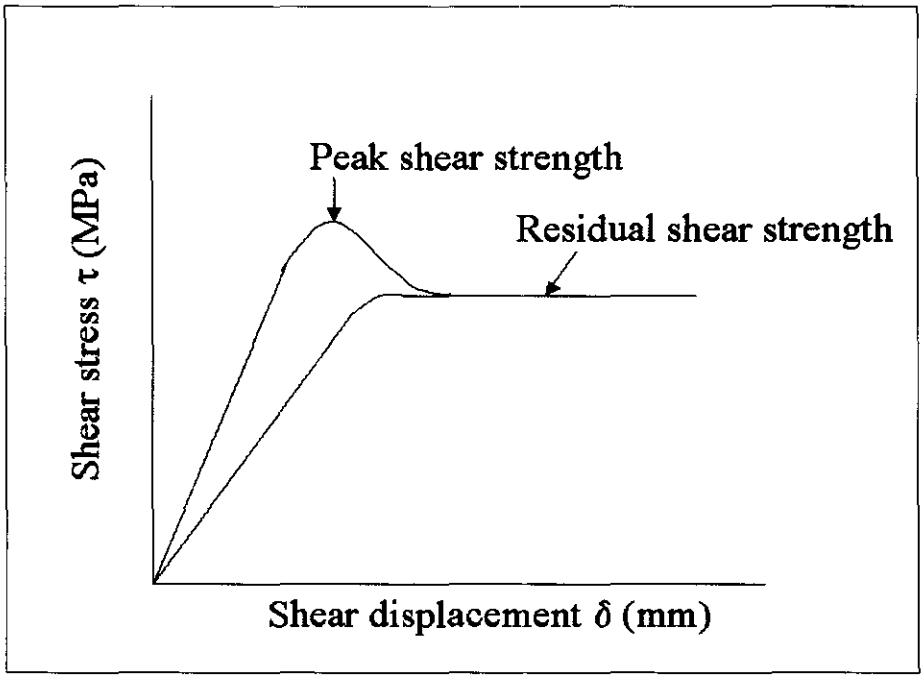

Figure 2. 5 Shear stress vs. displacement illustrating peak residual shear strength

The peak shear strength envelopes for non-planar rock joints are strongly curved. This curved envelope also has the effect that it seems as if there is some cohesion present. This is called the apparent cohesion. (See figure 2.6 where cohesion is indicated by (c)). This fact has been known for many years, however many engineers still describe shear strength as if they were rock properties in terms of Coulomb's constants ϕ and c. Both are in fact stress dependent variables. They are also scale dependent.

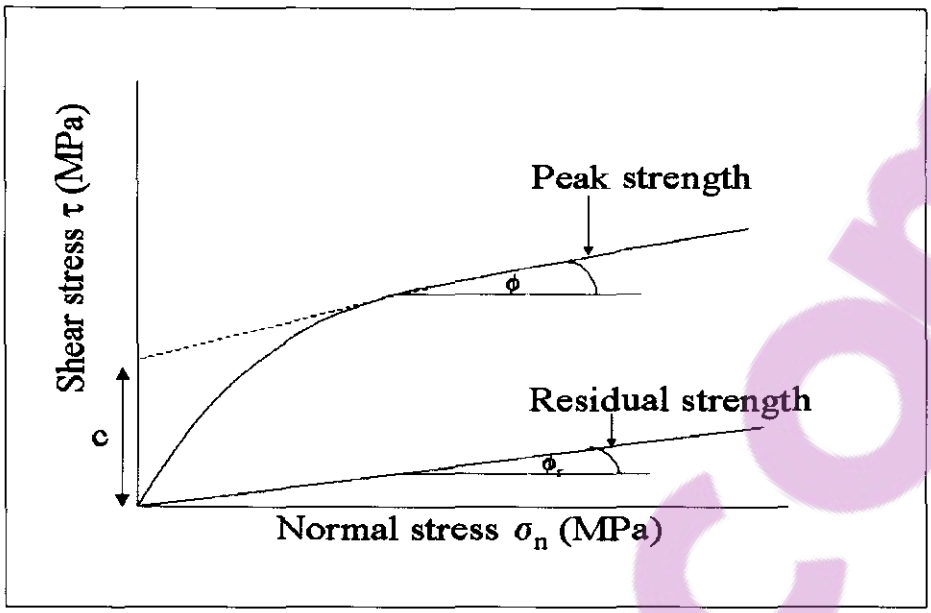

Figure 2. 6 **Graph of shear strength vs. normal stress illustrating angle of friction and cohesion**

In the case of residual shear strength, the cohesion c is zero and the relationship between ϕ_r and σ_n is as follows:

$$\tau_r = \sigma_n \tan \phi_r \quad \ldots\ldots\ldots\ldots\ldots\ldots\ldots\ldots (2.8)$$

where ϕ_r = residual friction angle of the joint

In shear tests on soils, the stress levels are generally an order of magnitude lower than those involved in rock testing and the cohesive strength of a soil is a result of the adhesion of the soil particles. In rock mechanics, true cohesion occurs when cemented surfaces are sheared. However, in many practical applications, the term cohesion is used for convenience and it refers to a mathematical quantity related to surface roughness. Cohesion is simply the intercept on the τ axis at zero normal stress.

The basic friction angle ϕ_b is a quantity that is fundamental to the understanding of the shear strength of discontinuity surfaces. This is approximately equal to the residual friction angle ϕ_r but it is generally measured by testing sawn or ground rock surfaces. These tests, which can be carried out on surfaces as small as 50 mm diameter, will produce a straight line plot defined by the equation :

$$\tau_r = \sigma_n \tan \phi_b \quad \ldots\ldots\ldots\ldots\ldots\ldots\ldots\ldots (2.9)$$

where ϕ_b = basic friction angle of the joint

The basic friction angle (ϕ_b) is the friction angle of rock material based on the base strength exhibited by flat unweathered rock surfaces which are prepared by a diamond saw. In some cases these surfaces are sandblasted between tests.

A useful list of basic friction angle values (ϕ_b) was compiled by Barton and Choubey (1977) from work done by Coulson (1971) and is shown in Table 2.1.

ROCK TYPE	BASIC FRICTION ANGLE (ϕ_b) (Degrees)	REFERENCE
A. Sedimentary Rocks		
Sandstone	26 - 35	Patton, 1966
Sandstone	31 - 33	Krsmanovic, 1967
Sandstone	31 - 34	Coulson, 1972
Siltstone	31 – 33	Coulson, 1972
B. Igneous Rocks		
Basalt	35 - 38	Coulson, 1972
Granite (Fine)	31 - 35	Coulson, 1972
Granite (Coarse)	31 - 35	Coulson, 1972
Porphyry	31	Barton, 1971
Dolerite	36	Richards, 1975
C. Metamorphic Rocks		
Gneiss	26 - 29	Coulson, 1972
Slate	25 – 30	Barton, 1971

Table 2. 1 **Basic friction angles of various unweathered rocks (Barton and Choubey, 1977 after Coulson, 1971)**

The friction angles obtained are applicable to unweathered joint surfaces and will not be applicable to weathered rock joints unless the level of effective normal stress applied is high enough for the thin layers of weathered rock to be worn away, thereby allowing contact between the fresher underlying rock (Richards, 1975). Under low levels of effective normal stress the thin layers of weathered material, perhaps less than 1 mm in thickness, may continue to control the shear strength past peak strength and even for displacements up to residual strength. Barton and Choubey (1977) also describe the tilt test as a means to determine the base shear strength of joints. The residual tilt test is basically a shear test under very low normal stress. Most specimens slide at a joint surface tilt angle of about 30° that correspond to a normal stress of approximately of 1 to 5 kPa.

2.5 Shear strength of rough joint surfaces in rock

A natural discontinuity surface in hard rock is never as smooth as a sawn or ground surface of the type used for determining the basic friction angle. The undulations and asperities on a natural joint surface have a significant influence on its shear behaviour . Generally, this surface roughness increases the shear strength of the surface, and this strength increase is extremely important in terms of the stability of excavations in rock.

Patton (1966) demonstrated this influence by means of an experiment in which he carried out shear tests on 'saw-tooth' specimens such as the one illustrated in Figure 2.7. Shear displacement in these specimens occurs as a result of the surfaces moving up the inclined faces, causing dilation (an increase in volume) of the specimen.

The shear strength of Patton's saw-tooth specimens can be represented by:

$$\tau = \sigma_n \tan (\phi_b + i) \quad \ldots\ldots\ldots\ldots\ldots\ldots\ldots\ldots (2.10)$$

where ϕ_b is the basic friction angle of the surface and i is the angle of the saw-tooth face.

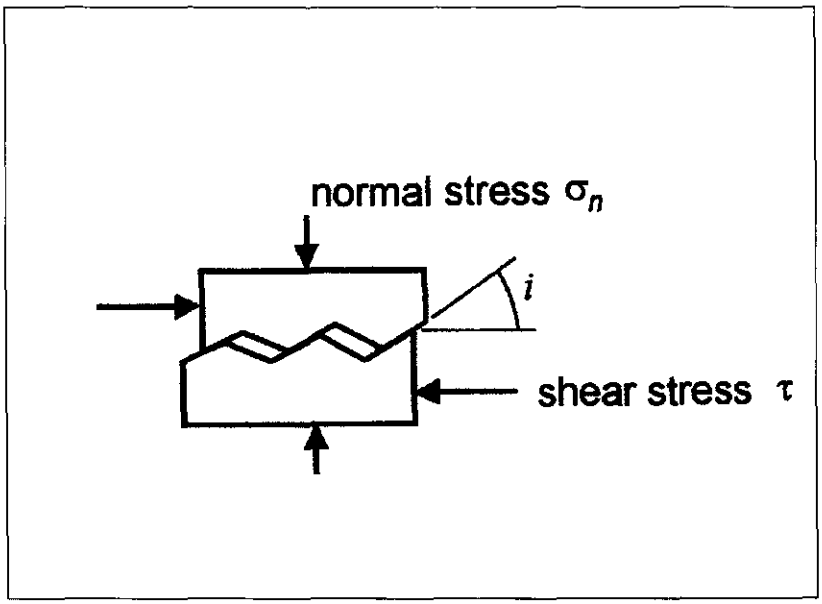

Figure 2.7 **Saw- tooth asperity roughness by Patton (1966)**

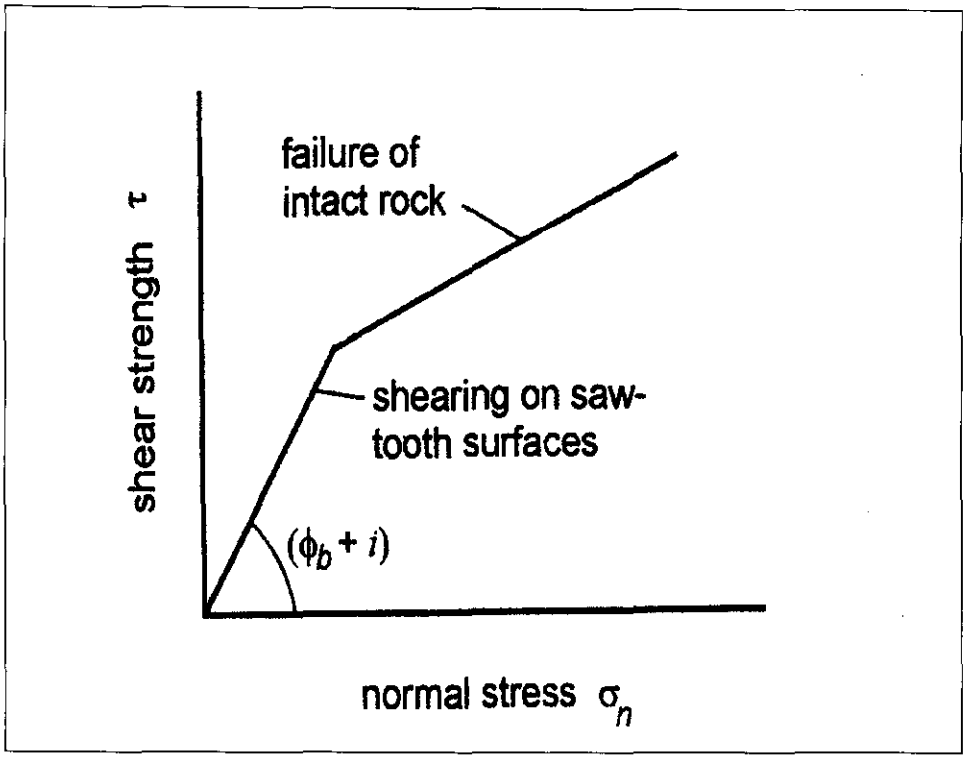

Figure 2.8 **Shear strength envelope by Patton (1966)**

Many researchers have studied the roughness as important parameter in the determination of shear strength. Initially researchers [Barton and co-workers (1971a, 1971b, 1972, 1974, 1976, 1977, and 1983, Maksimovic (1996), Zhao (1997a and 1997b), Fox et al (1998), Kulatilake (1999), Yong (2000), Lee et al (2001) and Seidel (2002)] studied two dimensional roughness.

Most of these authors studied a two dimensional profile and defined joint roughness. The joint roughness coefficient (JRC) is a number that can be estimated by comparing the appearance of a discontinuity surface with standard profiles published by Barton and others. One of the most useful of these profile sets was published by Barton and Choubey (1977) and is reproduced in Figure 4.2.

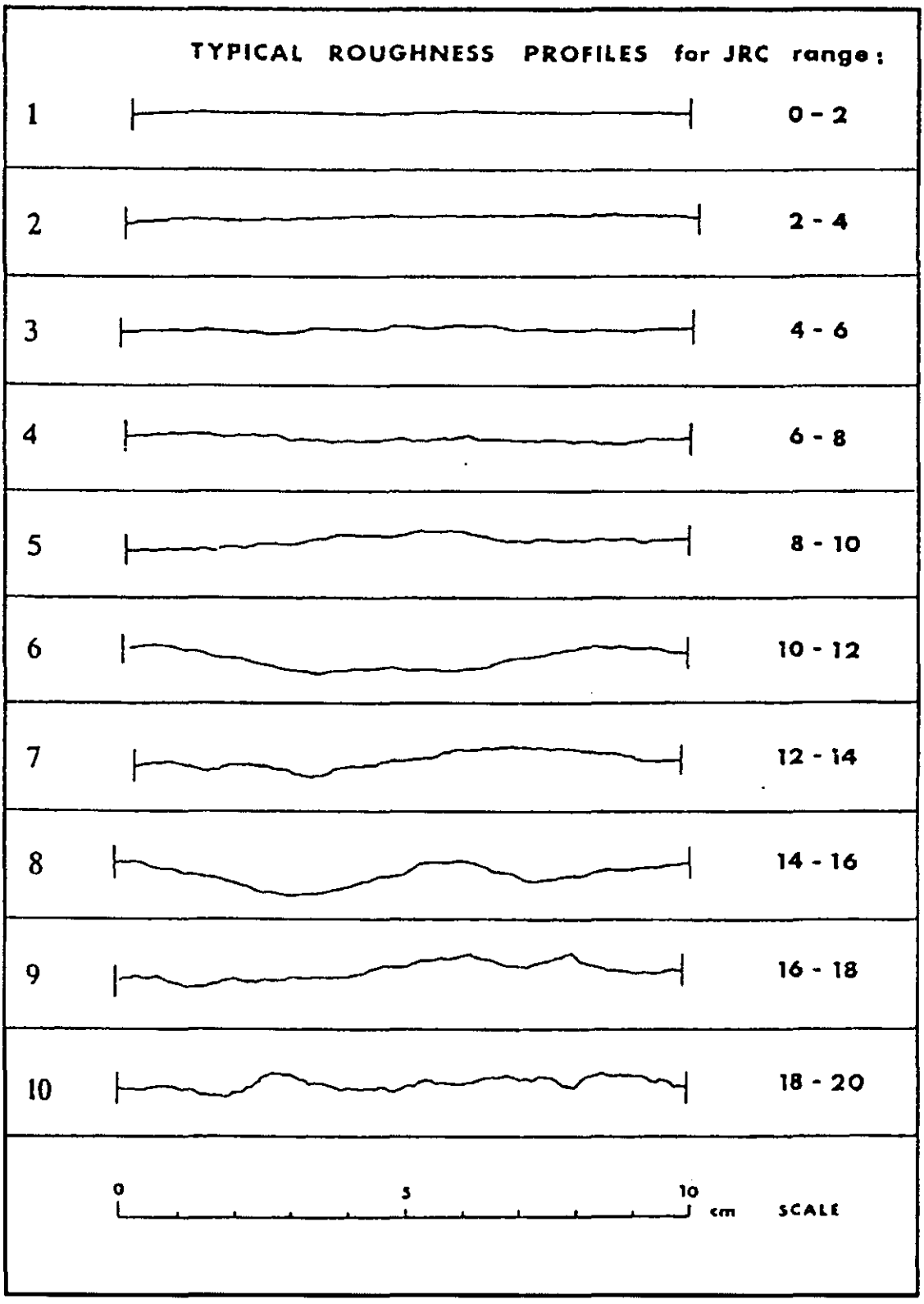

(vertical scale = horizontal scale)

Figure 2. 9 **Typical roughness profiles (After Barton and Choubey, 1977)**

The surface topography of joints vary widely in any given rock mass according to Bandis, (1993). Individual features can be classified as (i) asperities (small-scale roughness) (ii) large protrusions (intermediate roughness) and (iii) undulations (large-scale roughness). The effects of these broad classes of roughness on shear strength are related to the length of joint under consideration. Asperities with a base length of 1-2 mm will influence the strength of a 10 cm long joint, but will have no effect on a 100 cm long joint. Hence, a distinction is more meaningful if expressed with reference to the joint size. For example, the following base length to joint length percent ratios could be suggested: < 0.5% for small, 0.5-2% for intermediate and >2% for large-scale roughness. Many small-scale discontinuities that fit exactly give not unimportant effects.

Roughness measurements can be made by continuous profiling, recordings of peaks and recessions with respect to the mean plane at prescribed intervals, or field measurements of inclinations along selected profile lengths. The instruments used may vary from LVDTs, wire gauges, compass and base plates or any other practical devices to applications of photographic and photogrammetric methods [Maertz (1990)].

Several methods according to Barton and Choubey (1977) are used for the quantitative analysis of roughness, including estimation of:

(i) maximum and median angle i = arc tan $(2a/L)$, where a = amplitude and L = base length of irregularity
(ii) arithmetic mean of peaks and recessions with respect of the mean joint plane
(iii) amplitude index equal to the ratio of the sum of projected asperities over the total length of profile

If a joint profile is analysed geometrically by measuring inclinations i and D the relationship between them will be found as shown in Figure 2.3 (a) and 2.3 (b), also known as Rengers envelope (Rengers, 1971and Fecker and Rengers, 1971)

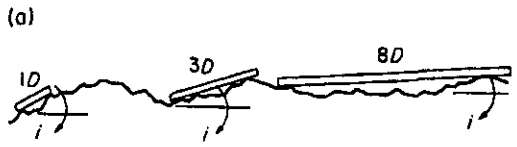

Figure 2.10 (a) Geometrical scale effects in joint roughness (By Bandis, 1993 after Fecker and Rengers, 1971)

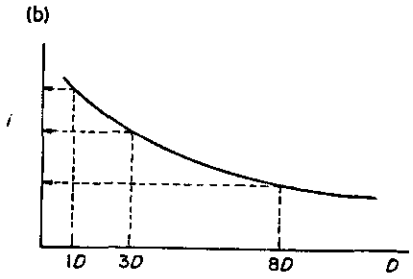

Figure 2.10(b) Inclination (i) vs. measured distance (D) (By Bandis, 1993 after Fecker and Rengers, 1971)

In the first experimental demonstration of the surface geometry scale effect, a tilt-tested long joint was found to slide at a smaller inclination angle than smaller samples sectioned from the same surface (Barton and Choubey, 1977). Recent studies of roughness scale effect and fractal dimension also indicate an apparent increase in roughness with decreasing base length (Maertz and Franklin, 1990). The roughness profiles of long joints apparently have been shown not to be fractal objects, confirming a roughness scale effect.

An immediate practical implication of the above concerns the choice of the 'correct' *i* value to be used in equation (Barton, 1974), for cases of shear-overriding behaviour. However,

further complications arise when asperity failures are also involved, as will soon be discussed.

No established method is available for recognizing the correct sampling steps for *i* determinations. A safe assumption may be that large-scale waviness will provide the component *i* (see Figure 2.6(a). That may be true in some cases of large-scale shear failures or when surface weathering effects smooth the smaller scale features. On the other hand rock masses at or near the surface the blocks resting on a shear plane will probably possess the freedom to move more or less independently thus maintaining contact with all scales of roughness. The freedom for block movement will obviously depend on the stiffness of the rock mass and generally increase as the block size or joint spacing decrease.

Barton and Bandis (1991) confirmed the latter through experimental studies on multiply jointed block assemblies. One conclusion from those studies was that the geometrical scale effect on roughness would probably be limited to the joint lengths corresponding to the average block size as specified by the spacing of the cross-joints. The latter may be envisaged as lines or potential 'hinges' (albeit stiff ones) in the rock mass, above and below a shear plane, which hinder continued scale effects when multiple rock masses are considered. Hence, the average cross-joint spacing may in some cases be an optimum.

Because dams are large structures, individual features like asperities (small scale roughness), large protrusions (intermediate roughness) and undulations (large scale roughness) all contribute to the roughness of discontinuities in the foundation. The effects of these broad classes of roughness on shear strength are related to the length of joint under consideration.

Roughness of joint surfaces is one of the most important factors that determine the shear strength of such surfaces. Barton and Choubey developed the joint roughness coefficient (JRC) as measure of joint roughness.

For many rock-engineering projects, it is necessary to have a good indication of the shear strength of the joints required for design purposes. A method was developed for estimating the JRC by measuring the roughness. Table 2.2 and Figure 2.9 gives a description of the 10 surfaces. (Barton and Choubey, 1977). The descriptions of roughness, i.e. "undulating" and " planar" refer to small and intermediate scale features, respectively.

Sample	Rock type	Description of joint	JRC
1	Slate	smooth, planar: cleavage joints, iron stained	0.4
2	Aplite	smooth, planar: tectonic joints, unweathered	2.8
3	Gneiss (muscovite)	undulating, planar: foliation joints unweathered	5.8
4	Granite rough	planar: tectonic joints, slightly weathered	6.7
5	Granite rough	planar: tectonic joints, slightly weathered	9.5
6	Hornfels (nodular)	rough, undulating: bedding joints, calcite coatings	10.8
7	Aplite	rough, undulating: tectonic joints, slightly weathered	12.8
8	Aplite	rough, undulating: relief joints, partly oxidized	14.5
9	Hornfels (nodular)	rough, irregular: bedding joints, calcite coatings	16.7
10	Soapstone	rough, irregular: artificial tension fractures, fresh surfaces	18.7

Table 2.2 Descriptive classification of Rock Joints (After Barton and Choubey, 1977)

The crude estimates of JRC (5, 10 and 20) given by Barton (1971) were proposed as a preliminary guide for those unable to investigate the parameter JRC more closely. Ideally, three profiles are measured on each specimen and the JRC values are grouped in the following ranges 0-2, 2-4 etc. up to 18-20. An attempt is then made to select the most typical profiles of each group. In all cases where the mean joint plane is not within ± 1° of horizontal when placed in the shear box, the shear strengths and corresponding JRC values must be corrected to the horizontal plane.

The appearance of the discontinuity surface is compared visually with the profiles shown and the JRC value corresponding to the profile which most closely matches that of the discontinuity surface is chosen. In the case of small scale laboratory specimens, the scale of the surface roughness will be approximately the same as that of the profiles illustrated. However, in the field the length of the surface of interest may be several metres or even tens of metres and the JRC value must be estimated for the full scale surface.

Recently researchers [Roko et al (1997), Scavia and Re (1999), Geertsema (2000), Gentier et al (2000), Grasselli (2002) and Duzgun et al (2002)] began to study three dimensional characterization of joint surfaces. They attempted to quantify the joint surface and find some

relation to the shear strength. Further work in this field has the potential to deliver interesting results.

Another factor contributing to the shear strength over larger areas such as dam foundations is waviness of joint surfaces. Hack et. al. (2002) developed large-scale roughness profiles for slope stability probability classification. This is presented in Figure 2.11. These roughness profiles can be used in the determination of the contribution to friction angle of the waviness

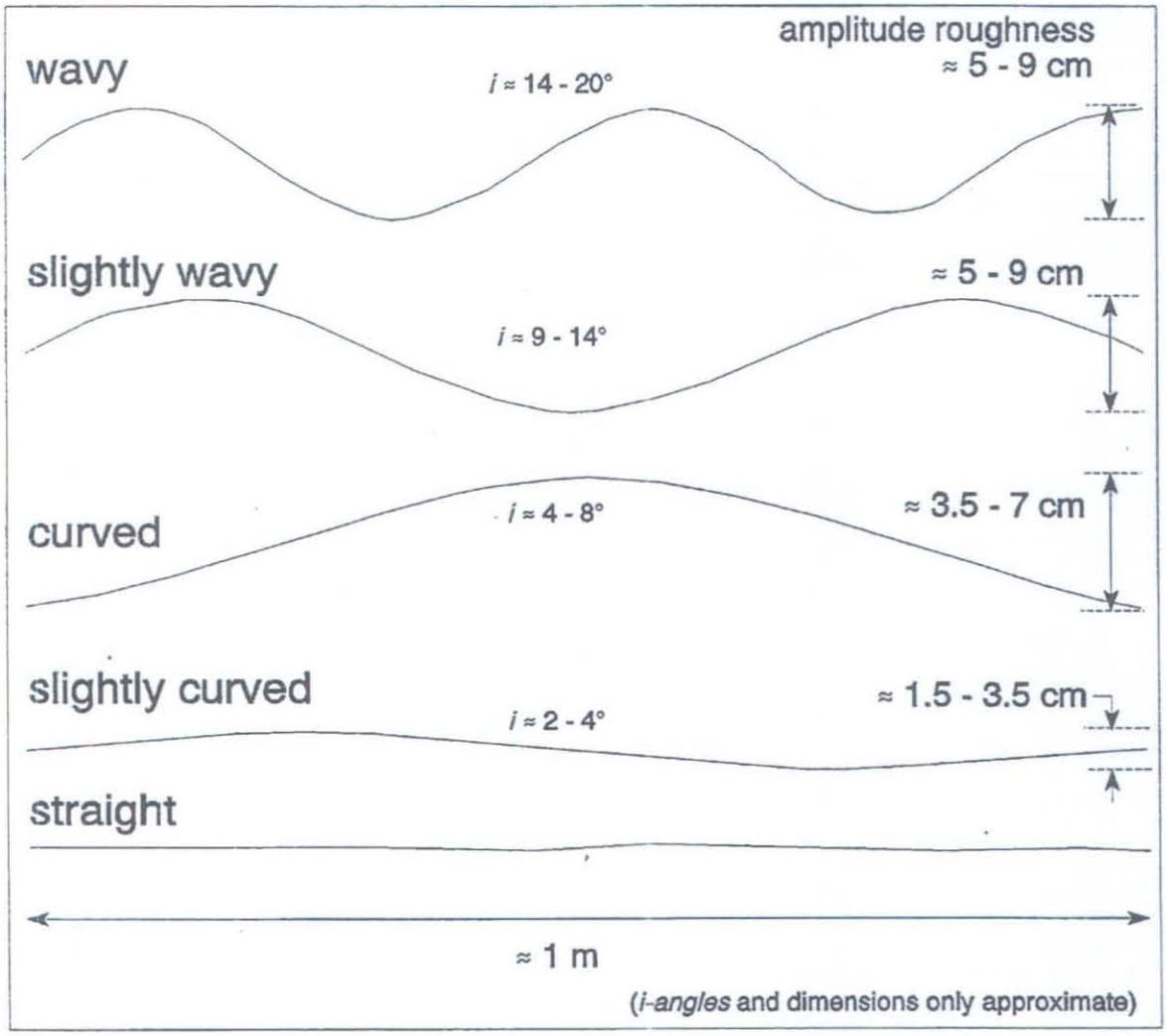

Figure 2.11 Large-scale roughness profiles used for the slope stability probability classification – After Hack et. al. (2002)

2.6 Determination of joint wall hardness.

Researchers such as Barton and Choubey (1977), Szwedzicki (1998), Katz et al (2000) and van Loon (2003) have studied joint wall hardness.

Barton and Choubey (1977) studied hardness of joint surfaces and stated that the measurement of this parameter is of fundamental importance in rock engineering since it is largely the wall characteristics that control the strength and deformation properties of the rock joints. They describe hardness of joint surfaces as joint wall compressive strength (JCS). The importance of the parameter is accentuated if the joint walls are weathered, since then the *JCS* value may be only a small fraction of the uniaxial compressive strength of the rock material associated with the majority of the rock mass, as typically sampled by borehole core. The depth of penetration of weathering into joint walls depends on the rock type, in particular on its permeability. A permeable rock will tend to be weakened throughout; while impermeable rocks will just develop weakened joint walls leaving relatively unweathered rock in the interior of each block.

Barton and Choubey (1977) propose that the weathering process of a rock mass can be summarized in the following simplified stages:

(i) the formation of the joint is intact in unweathered rock and the JCS value is the same as the uniaxial compressive strength, σ_c

(ii) slow reduction of joint wall strength occur if joints are water-conducting and the *JCS* becomes less than σ_c

(iii) common intermediate stage occur with weathered, water conducting joints and impermeable rock blocks between and the JCS becomes some fraction of σ_c.

(iv) penetration of joint weathering effect into rock blocks with progressive reduction of σ_c from the walls of the blocks inwards and the *JCS* continues to reduce slowly.

(v) advanced stage of weathering occur and more uniformly reduced σ_c drops to the same level as the *JCS* with the rock mass permeable throughout.

The *JCS* values corresponding to stages (i) and (v) can be obtained by conventional unconfined compression tests on intact cylinders or from point load tests on rock core or irregular lumps though there might be sampling problems in the case of stage (v). Point load testing has been described in detail by Broch and Franklin (1972). In view of the fact that point load tests can be performed on core discs down to a few centimetres in thickness, it

might also be possible to use this test for stage (iv) on the core pieces on each side of deeply weathered joints. However, the *JCS* values relevant to stages (ii) and (iii) cannot be evaluated by these standard rock mechanics tests. The thickness of material controlling shear strength may be as little as a fraction of a millimeter (for planar joints) up to perhaps a few millimeters (for rough, weathered joints) with the limits depending on the ratio JCS/σ_c that basically controls the amount of asperity damage for a given joint roughness.

Barton and Choubey (1977) state that the Schmidt hammer provides the ideal solution to determine JCS. The Schmidt hammer is a simple device for recording the rebound of a spring loaded plunger after its impact with a surface. The L-hammer used here (L for light, impact energy = 0.075 mkg) is described by the manufacturers as being "suitable for testing small and impact-sensitive parts of concrete or artificial stone". It is suitable for measuring *JCS* values down to about 20 MPa and up to at least 300 MPa. A wide ranging assessment of the suitability of the Schmidt hammer for use in rock mechanics was done by Miller (1965) as reported by Barton and Choubey (1977). He found a reasonable correlation between the rebound number (range 10 to 60) and the unconfined compressive strength (σ_c) of the rock. However, a better correlation was obtained when he multiplied the rebound number by the dry density of the rock.

$$\text{Log}_{10}(\sigma_c) = 0.00088\,\phi\,R + 1.01 \quad \text{.....(2.11)}$$

where (σ_c) = unconfined compressive strength of surface material (MPa)

ϕ = dry unit weight of rock (kN/m³), and

R = rebound number

Example:

$$\text{Log}_{10}(\sigma_c) = 0.00088\,\phi\,R + 1.01$$

$$\text{Log}_{10}(\sigma_c) = 0.00088 * 27 * 48 + 1.01$$

$$\sigma_c = 141 \text{ MPa}$$

Deere and Miller (1966) investigated the relationship between Schmidt hardness and the uniaxial compressive strength of rock. Figure 2.12 presents this relationship. Suppose that a vertical downwards held type L-hammer gave a reading of 48 on a rock with a unit weight of 27 kN/m³, the uniaxial compressive strength σ_c is given by the graph as 140 ±50 MPa . Note that the hammer should always be perpendicular to the rock surface.

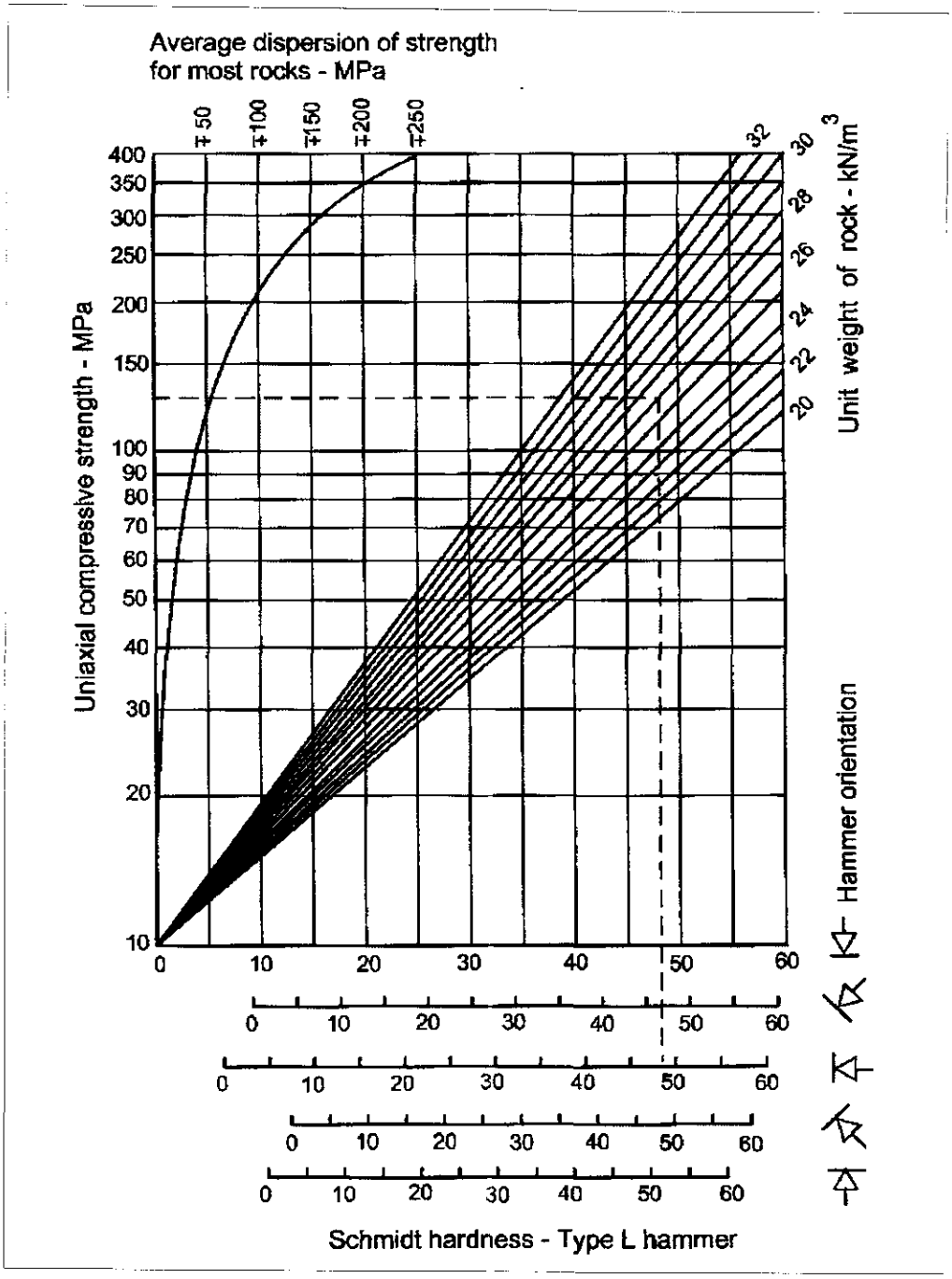

Figure 2. 12 **The relationship between Schmidt hardness and the uniaxial compressive strength of rock (After Deere and Miller 1966 as reported by Barton and Choubey, 1977)**

2.7 Joint matching

Joints in a rock mass are formed at various stages and times, and have been subjected to different methods of alteration which affect the joint surface geometrical and mechanical properties. As a result of these alterations, joints will present different surface profiles on each side and different degrees of matching according to Zhao (1997). It is common for joints to be equally rough but mismatched due to alteration and dislocation. He developed the joint matching coefficient (JMC) based on the percentage of joint surface in contact as an independent joint surface geometrical parameter. The JMC is used with the joint roughness coefficient (JRC) in order to describe the geometrical properties and to assess the hydro mechanical behaviour of joints. It has also been demonstrated that joint matching is an important factor governing the aperture, normal closure, stiffness, shear strength and hydraulic conductivity of joints.

When Barton's JRC-JCS shear strength criterion was used by Zhao (1997) for the interpretation and prediction of shear strength of natural joints, it was found the this model tends to over predict the shear strength for those natural joints with less matched surfaces. To overcome this shortcoming, a new JRC-JMC shear strength criterion is proposed in order to include the effects of both joints surface roughness and joint matching in the form of:

$$\tau = \sigma_n \tan [JRC \cdot JMC \cdot \log_{10} (JCS/\sigma_n) + \phi_r] \quad \ldots\ldots\ldots\ldots (2.12)$$

Where τ = peak shear strength; σ_n = effective normal stress; JRC = joint roughness coefficient; JCS = joint wall compressive strength; ϕ_r = residual friction angle; JMC = joint matching coefficient

The JMC should be set at 0,3 for any measured JMC < 0,3. This is a modification of the existing JRC-JCS criterion.

2.8 Infilling of joints

In practice, the assumption that the minimum shear strength of an infilled rock joint is the shear strength of the filler itself is frequently made. De Toledo et al. (1993) tested flat saw-cut and polished surfaces of limestone and basalt in shear boxes using different soils as the

infilling material. The ratio of the shear strength of the infilled joint to that of the soil alone varied between 0,61 and 0,95, which means that an infilled joint is normally weaker than the soil that constitutes its filler. The magnitude of the strength reduction seems to be a function of the surface roughness and of the clay minerals present in the soil. Other authors like Amadei, (1990) have also found boundary effects.

When comparing published results in the literature it is important to remember that there are according to de Toledo et. al. (1993), eight basic parameters to be considered in the study of the shear strength of infilled joints. Some parameters relate to the material properties, some to the joint itself and the geological formation to which the joint belongs, and others to the equipment and the particular problem under consideration.

Table 2.3 summarizes the parameters involved in both drained and undrained shear strengths, which should be borne in mind in the testing of infilled joints. Some of these parameters will be discussed in the following paragraphs.

a. Material parameters	Infilling properties Infilling thickness Joint stress history Rock properties Joint wall roughness Orthogonal joints
b. Equipment parameters	Rate of shear Stiffness of the shearing equipment

Table 2. 3 **Parameters controlling the shear strength of infilled discontinuities (After De Toledo et al, 1993)**

Sun et al. (1981) performed shear box tests on joints in concrete blocks filled with clayey sand and sandy clay with variable normal stresses and filler thicknesses. The failure surfaces occurred either at the top or at the bottom concrete contact or as a combination of both surfaces. Pereira (1990), using mainly sand filling between two flat granite blocks, also

reported failure along the joint walls due to the rolling of sand grains. Solid walls affect the strength of a joint in two ways namely:

- in clay, fillers sliding occurs along the contact due to the particle alignment
- where as, in sands the rolling of grains seems to be the major factor responsible for the greater weakness of a joint as compared with its filler.

The magnitude of the influence of surface roughness depends on the particle size of the soil. In a simple form, when sand is considered as infilling material, the influence of the rock wall may begin to be felt when its surface is smoother than the roughness of the sand surface defined by its particle size distribution. This is because dilation is reduced.

According to De Toledo et al (1993) the shear strength characteristics of rock discontinuities have been studied for a long time but a complete understanding of the mechanisms and of the parameters controlling the process has never been reached. Infilled joints are likely to be the weakest elements of any rock mass in which they occur and exert a dominant influence on its behavior. The behavior of infilled rock joints in shear has been investigated for decades. Many results of field and laboratory tests had been published since the 1960's and these results were reviewed by Barton (1974). From then on, investigations became more systematic and concentrated mainly on laboratory testing.

Different materials and test procedures were employed in an attempt to study the influence of filler thickness on peak shear strength. Other physical properties were studied less frequently, mainly because of experimental difficulties. Previously published test results lead to contradictory conclusions so far as the influence of filler thickness is concerned.

A laboratory investigation always has to choose between testing real joints and artificially created ones. Natural joints, either filled or unfilled, are virtually impossible to use in systematic research, but the benefits of adopting either a copy of a natural joint or a regularly profiled one are clear. The friction of the discontinuity wall of natural, tension and artificially cut joints will be different because, for example, the cutting process may have changed the discontinuity surface mineral and crystal structure by melting, whereas natural discontinuity walls have been subjected to water percolation weathering, ect. This causes major differences in friction angle and one would expect it to be of major influence on the research and

interpretation of the research results. It is a matter of choice between the study of the behavior of the interaction of infill with a real joint shape as opposed to the study of infill within a boundary whose geometry is well constrained but made from real rock material. Idealized profiles allow a better understanding of specific joint properties, yet both methods of testing laboratory-prepared joints may face serious shortcomings, such as inappropriate representation of an infilled joint in the field. In most cases laboratory shear box tests have been adopted for this work with sample sizes of 50 -250 mm and normal stresses of 20-1500 kPa, producing results relevant to conditions of zero normal stiffness, i.e. constant normal stress. Peak shear strength was always investigated and in some cases residual strength was also studied. However, the ability of equipment to study the residual strength of joints infilled with soil is limited by maximum displacements, which may lead to significant errors.

Kutter (1974), using a simplified rotary machine, showed the need to use large displacements in order to define properly the residual strength of an unfilled and rough rock joint. In fact, displacements of up to 100 mm are usually required to achieve the residual strength in soils Lupini, Skinner & Vaughan, (1981) and as much as 200 mm have been observed for some rough unfilled rock joints. It is doubtful whether a shear box apparatus or the ring shear apparatus is capable of producing a correct measure of the residual shear strength characteristics of natural infilled joints.

Research tests are generally conducted on natural joints, and on model infill joint material. Several authors, whose results on the latter can be divided into two categories, have studied the influence of filler thickness. The first category includes the matching toothed joints that have a ratio filler thickness to asperity height t/a of less than three. The second category comprises planar joints using either saw-cut, sandblasted or polished surfaces, where t/a is usually much greater than three.

Ladanyi & Archambault (1977) performed direct shear tests using kaolin clay between two series of juxtaposed concrete blocks. Different asperity heights and different normal stresses were used. The results obtained seem to confirm results obtained by Goodman (1970).

2.9 Shear strength equations

The equation, $\tau = \sigma_n \tan(\phi_b + i)$, is valid at low normal stresses where shear displacement is due to sliding along the inclined surfaces. At higher normal stresses, the strength of the intact material will be exceeded and the asperities will tend to break off, resulting in a shear strength behaviour which is more closely related to the intact material strength than to the frictional characteristics of the surfaces.

While Patton' s (1966) approach has the merit of being very simple, it does not reflect the reality that changes in shear strength with increasing normal stress are gradual rather than abrupt. Barton and his co-workers (1973, 1976, 1977, 1990) studied the behaviour of natural rock joints and have proposed that the equation can be re-written as:

$$\tau = \sigma_n \tan [JRC \log_{10} (JCS/\sigma_n) + \phi_b] \quad \text{.....(2.13)}$$

Where τ = peak shear strength; σ_n = effective normal stress

JRC = joint roughness coefficient; *JCS* = joint wall compressive strength

ϕ_b = basic friction angle (obtained from residual shear tests on flat unweathered rock surfaces)

Barton and Bandis (1982) and Barton (1991), based on extensive laboratory testing of joints, and joint replicas, and a study of the literature at the time, proposed a scale correction for JRC as presented in equation 2.14:

$$JRC_n = JRC_0 (Ln / L_0)^{-0.02JRC_0)} \quad \text{..... (2.14)}$$

where JRC_0 and L_0 refer to the JRC and length of 100mm diameter laboratory scale samples and JRC_n and L_n refer to in situ specimen.

Barton and Bandis (1982) argued that the average joint wall compressive strength of large surfaces is likely to have greater possibility of weaknesses and JCS would decres with increasing scale. They proposed equation 2.15 as correction for JCS:

$$JCS_n = JcCS_0 (Ln / L_0)^{-0.03JCS_0)} \ldots\ldots\ldots\ldots\ldots (2.15)$$

where JCS_0 and L_0 refer to the JCS and length of 100mm diameter laboratory scale samples and JCS_n and L_n refer to in situ specimen.

CHAPTER THREE
THE EXPERIMENTAL STAGE OF THE STUDY

3.1 Rock types tested

During the planning stage of the study of the shear strength of joints in rock it was envisaged to select as many of the rock types covering the surface and near surface in southern Africa as possible. Potential sites where rock material samples could be taken were identified. These sites were in most cases dam sites, although road cuttings and quarry sites were also included. Various rock types were sampled and subsequently tested. Figure 3.1 shows the origins of the samples discussed in this chapter.

Figure 3. 1 **Location where samples of rock material with joints were taken**

Block samples for shear testing in the large shear box were taken at the sites of dams under construction as well as at one road cutting. The purpose of the large scale testing was to determine the peak and residual shear strength and the influence of the surface characteristics (mainly hardness and roughness) and scale on the shear strength. Large shear tests were carried out on block samples with surface areas ranging from approximately 100 x 100 mm to 300 x 300 mm. Table 3.1 presents the rock types and origins of the block samples that were tested.

During the taking of large-scale samples for shear test care must be taken as not to damage the shear surface. Large shear tests were carried out on block samples with surface areas ranging from approximately 100 x 100 mm to 300 x 300 mm. The samples are extremely sensitive to disturbance during sample taking, transportation, preparation, and testing. During sampling, transportation and preparation of samples extreme care was taken as not to damage samples and it can be reported that damage to surfaces were very limited and it can be stated that joint surfaces tested were very similar to joints conditions in situ, with the exception of moisture content. Samples were taken from the sites that were of a small enough size to fit the laboratory shear box so that cutting and associated damage to the shear surface was limited to a minimum. Generally joint fill material got dried out during the period between sample taking and testing that could have been as much as eighteen (18) months. During the final phase of testing water as added to the shear box to test the shear strength under saturated conditions.

ROCK TYPE	GEOLOGICAL SUCCESSION	SITE
Basalt	Karoo Supergroup	Lesotho Highlands Water Scheme
Dolerite	Post Karoo	Qedusizi Dam, Ladysmith
Granite	Archaean	Driekoppies Dam
Sandstone	Natal Group	N3 Cutting, Darnall
Mudstone(Shale)	Karoo Supergroup	Qedusizi Dam, Ladysmith
Quartzite	Cape Supergroup	Skuifraam Dam site, Franschhoek
Granite	Archaean	Nandoni Dam

Table 3. 1 **Selected rock types (large rock samples) tested with the large shear box**

Only six rock types were tested in the large shear box apparatus due to the difficulties in obtaining samples as well as the duration of the testing process. The quartzite samples from Skuifraam dam site, Franschoek were very brittle and disintegrated during sample preparation and testing. No results for this rock type could be obtained. Samples tested went through three phases of testing. The first phase was carried out dry and could, in hindsight, be seen as part of the learning curve for the new large shear apparatus. The second phase was carried out after problems with the machine were eliminated. Each sample was tested three times dry and then three times under saturated conditions. Eventually third phase tests were conducted on three additional granite specimens.

3.2 Apparatus used in testing

The different apparatus used in this research is discussed in this paragraph.

3.2.1 Shear boxes

Two types of shear tests were conducted. The tests were conducted on

(i) samples with saw cut surfaces tested on a modified soil shear box and

(ii) large samples with natural joint surfaces tested on the large shear box of the Department of Water Affairs and Forestry.

3.2.1.1 The small shear box.

Basic shear strength and shear strength of joints (peak and residual) of NX size core samples were tested on this test apparatus. A Soiltech soil shear box was modified for this purpose. The original sample box was removed and replaced by a clamp mechanism to accommodate the NX size rock core samples. The bottom sample holder is fixed to the frame of the apparatus while the upper sample holder can move along the line of shear. The normal load is applied through a yoke and hanger system where the normal load is increased by adding additional weights. The shear load is applied by a motorized worm drive acting on a load cell transferring the load to the upper sample holder assembly. Vertical dilation and horizontal movements are measured by means of linear variable displacement transducers (LVDT's).

Three loading cycles were carried out on each sample. Normal stresses of 55 kPa, 105 kPa and 1,55 MPa were applied and the corresponding shear loads were measured.

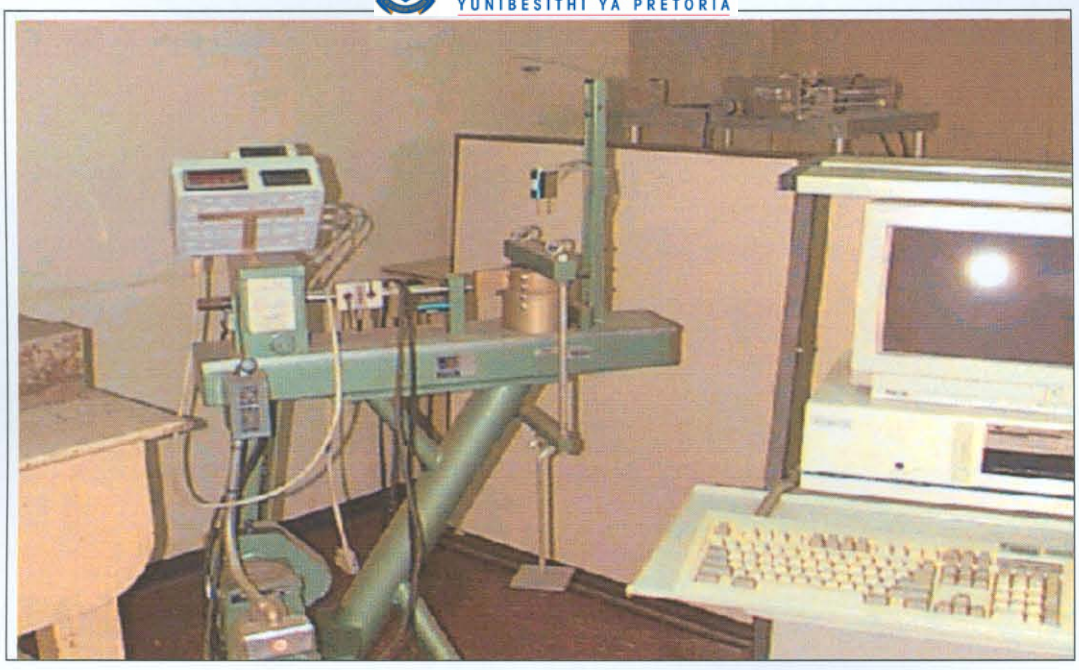

Figure 3. 2 The modified soil shear box for shear testing of NX-size rock core samples.

The shear process is computer controlled and data retrieval is done through a data acquisition unit connected to a PC. Figure 3.2 shows the laboratory set-up. The maximum displacement was 10 mm. After each cycle the upper sample holder containing the sample was returned to its original position before applying the next higher load. The measurements are illustrated in graphic form as shear load vs. shear displacement and shear stress vs. normal stress available in Appendices A and B. Results of the testing are discussed in chapter four. Raw data in the form of tables and graphs are in Appendixes A and B.

3.2.1.2 Large shear box of the Department of Water Affairs and Forestry

The apparatus

The machine was designed and built in such a way, that specimens of rock or soil of a maximum size of 350 x 350 mm can be tested under normal loads of up to 200 kN and shear loads of up to 500 kN - illustrated in Figure 3.3.

The machine consists essentially of an arrangement to accommodate the specimen to be tested, a mechanism to apply different constant vertical loads on the specimen and a mechanism to apply shear loads, in a direction perpendicular to the normal load.

Figure 3.3 **The large shear testing machine**

A line drawing of the machine is presented in Figure 3.4 (side view) and Figure 3.5 (front view). Suitable instrumentation to measure and record forces and displacements is also provided.

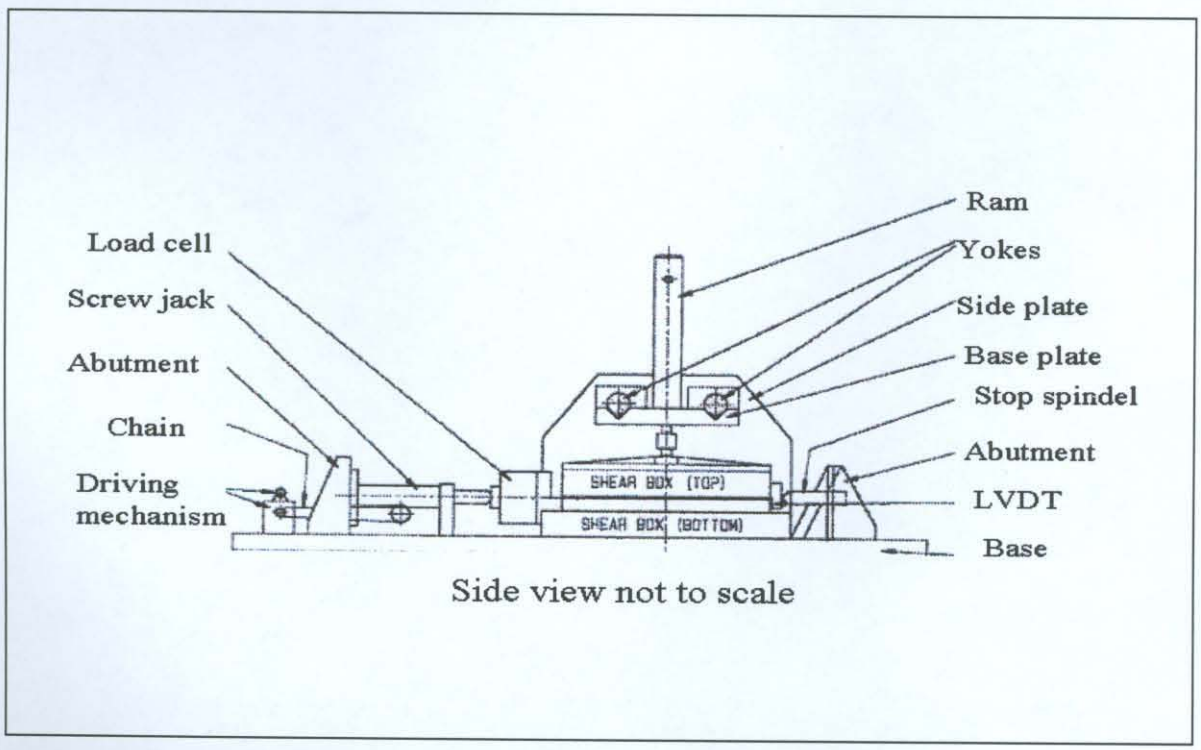

Figure 3.4 **Schematic sketch of large shear testing machine (side view)**

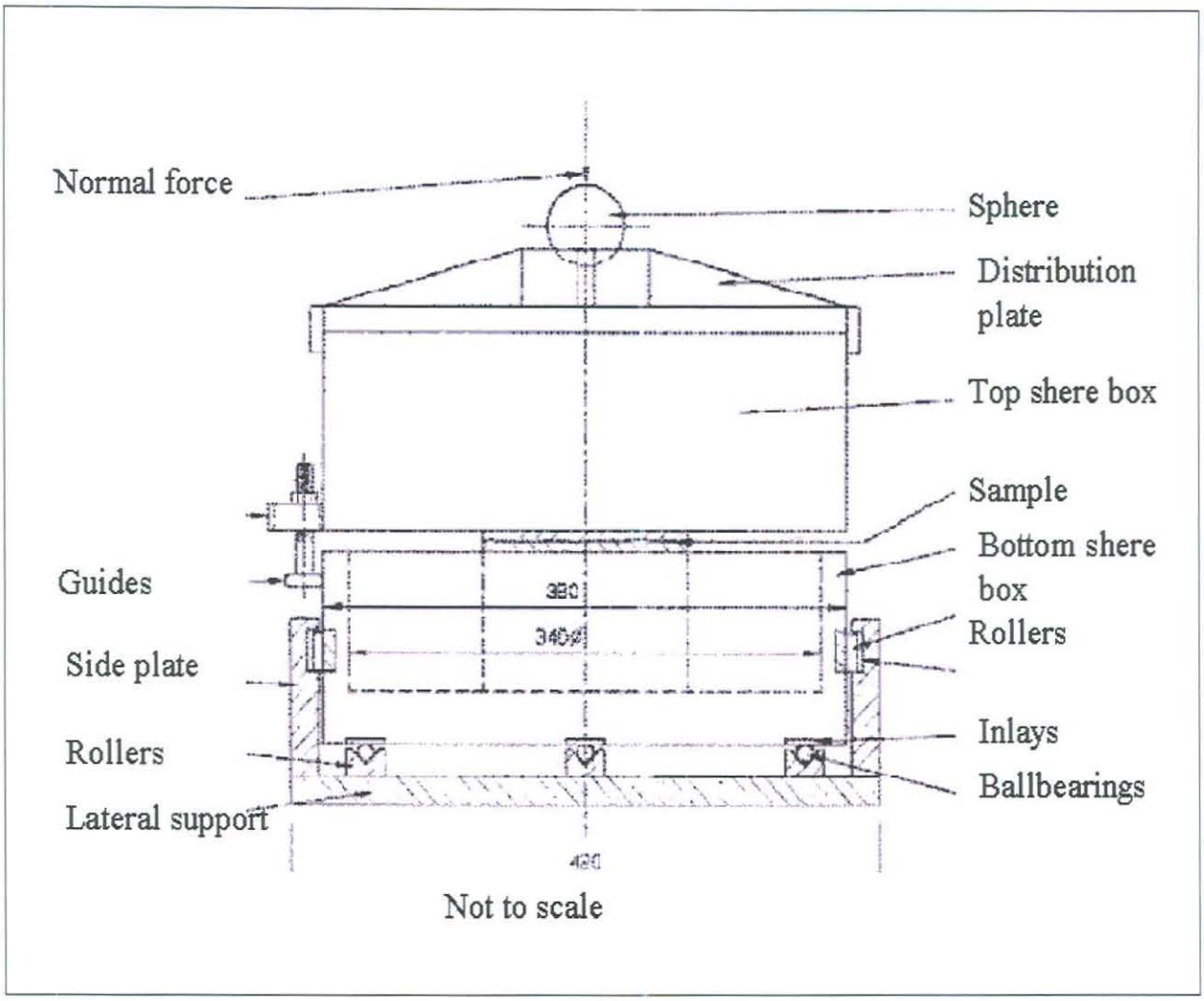

Figure 3. 5 **Schematic sketch of large shear testing machine (front view)**

Shear box assembly (specimen accommodation)

The shear box assembly consists of two different parts, a lower half and a top half. The lower half accommodates one half of the specimen and represents the mobile part of the shear box i.e. shearing takes place underneath the top half, which is kept horizontally stationary. Via a yoke the bottom part is in direct contact with the mechanism which provides the force necessary for shearing.

Suitable roller bearings ensure low friction gliding of the lower half over a rigid, machined base plate. The base plate is fitted to a strong frame, to which all other stationary machine components are fitted. The lateral support of the bottom part is provided by needle bearings.

The top half accommodates the other half of the specimen and is separated from the bottom part by a gap, which is aimed to be 5 mm.

The direction of the shear force is in line with the shear plane. Provision is made for adjusting the gap between the bottom and top parts of the shear box and for adjusting the direction of the shear force to suit the specimen as described above.

To prevent side way drifting of the top part during testing side, guides are provided which are in firm touch with the corresponding outside flats of the bottom part.

Provision is made for testing the sample under wet conditions by a water bath. The water bath allows for immersion of the entire test sample in water. The water bath is designed not to interfere with either the transfer of loads onto the specimen or with the measuring of displacements.

Provision is made to protect the lower shear-box assembly from water and moisture when testing specimens under wet conditions.

Both shear box parts are equipped with clamps for temporary immobilization and hooks are provided at suitable positions on both parts to facilitate the handling of the equipment during assembly, testing and dismantling.

Three shear box assemblies were manufactured, having the following inside dimensions:

Box No. 1: 350 x 350 mm Square
Box No. 2: ø 350 mm Round
Box No. 3: ø 150 mm Round

All three boxes have sufficient wall thickness to minimise deformations caused by loads acting on them. Figure 3.6 illustrates the square box.

Figure 3.6 Bottom half of shear box assembly with test specimen

Load distribution plate

On the top part of the shear box assembly a stiffened load distribution plate is placed. In the geometrical center of the stiffened plate a spherical seating is provided through which the normal loads are applied.

For each of the square or round boxes, two different load distribution plates were manufactured:

(a) one plate which fits loosely over the outside of the top part and

(b) one which fits with enough clearance into the respective square or round cavity of the top part.

The clearance of the plates on the sides of the shear box and the method of providing for vertical movement of the plates is sufficient to ensure free unhindered vertical travel of the load plates up to 10 mm.

Application of normal loads

The normal load is applied on the seating of the load-distribution plate by means of a hydraulic cylinder. The maximum capacity is 200 kN. During the test the mechanism is able to maintain any specified load of up to 200 kN constant, to ± 2 %, regardless of any volume change of the specimen. The apparatus was designed so that no tilting of the shear box with

the specimen during testing was allowed. The reason for this is that on this scale, no tilting takes place under a dam foundation as a result of confinement.

Application of shear forces

The shear force is applied in the horizontal direction. The mechanism that generates the force is a hydraulically operated and strain-controlled hydraulic jack. The shear force is applied continuously and can reach up to 500 kN.

The rate of shearing, i.e. the horizontal displacement, measured at the bottom part of the shear box assembly within a certain period of time, can be pre-selected in steps of 0.2 mm/min. from 0.2 mm/min. to 5.0mm/min. The maximum shear displacement is 50 mm.

Data measurement and acquisition

All forces and displacements are measured electronically. The recording of the voltage outputs is recorded continuously. The measurement of the normal and the shear forces are done by means of suitable load-cells.

A total of five interchangeable load cells with capacities of 50, 100, 150, 200 and 500 kN can be used. Suitable mountings for the load cells are provided. The combined error for linearity and hysteresis of each load cell is less than 0,10 % of the RO (rated output mV/V ± 0,1 %).
The measurement of the relative horizontal movement between the two halves of the shear box assembly (shear displacement) is measured by two LVDT's (linear variable differential transducers), with a stroke of 50 mm and a linearity of better than 0,25 % RO. The LVDT's are positioned at the upper left and right hand corners of the bottom part of the shear box assembly. The electrical wiring of the LVDT's is done in such a way that their combined output represents the average displacement. The mountings (clamps) for the bodies of the LVDT's are rigid and shock resistant. The contact points for the spring-return armatures are smoothened.

The vertical displacement (dilation) is measured by two LVDT's with a stroke of 20 mm and a linearity of better than 0,25 % RO. The two LVDT's are positioned in the middle and at opposite ends of the load distribution plate.

3.2.2 Apparatus for the measurement of roughness

3.2.2.1 Laser apparatus

During the course of this investigation a laser-scanning device was developed and built.

The apparatus

The laser is built on a sturdy frame 750 mm long by 500 mm wide, allowing samples up to 600 mm by 350 mm. Figure 3.7 clearly shows the scanner head which moves in a longitudinal direction above the sample.

A laser displacement sensor is attached to this head, which is moved along the guide rails by a stepper motor driving a toothed belt by means of two toothed gear wheels.
The rotational movement of the stepper motor produces an incremental movement of the

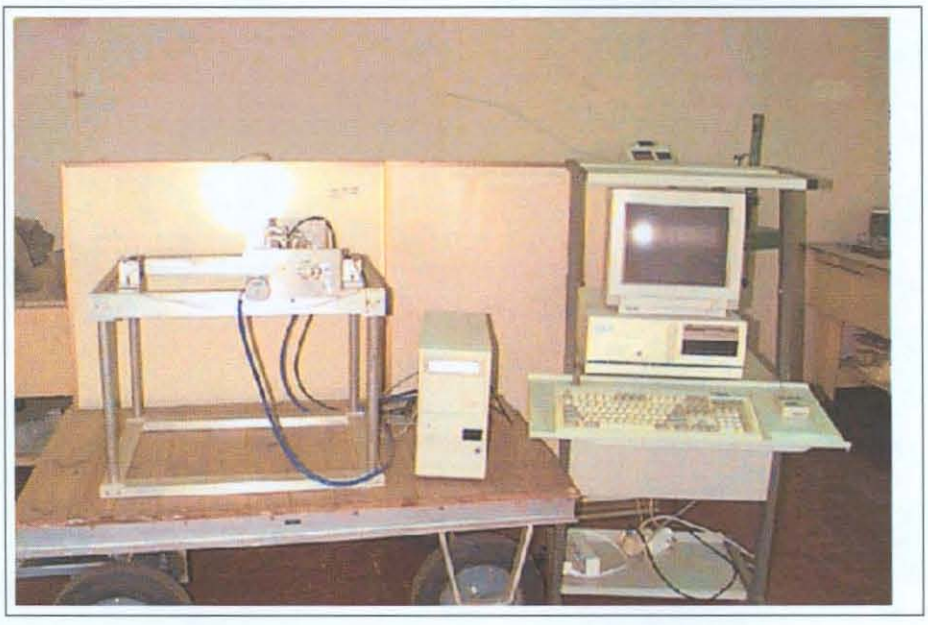

Figure 3. 7 **The laser scanning device**

scanning head which in turn allows the rock sample to be scanned in steps in the X-direction. This longitudinal scanning frame is attached, on one side, to the transverse moveable carriage, which allows movement in the Y-direction. The other end of the longitudinal frame is supported on a linear bearing, along which it moves. The transverse moveable carriage is driven along two guide rails by a second stepper motor arrangement.

The size or number of steps and thus the speed of rotation of the stepper motors are determined by the number of electrical pulses and the frequency of the input signal respectively. The laser displacement sensor uses a 3 mW helium-neon semiconductor laser diode producing a light with a wavelength of 780 nm and a spot diameter less than 2 mm. It can measure distances between 50 and 130 mm, with a resolution of 50 μm at a 100 ms response time, or 150 μm with a 10 ms response time. The light is reflected off the surface to be measured and is received by a position sensing diode, which allows a stepped incremental signal to be output. This voltage output is directly related to the distance measured so that the latter may be simply determined.

Method of operation

The sample to be scanned is placed on the base plate against a reference bar in order to ensure accurate positioning and is oriented such that the direction of shearing is parallel with the longitudinal scanning head. A wide range of sample thicknessess can be accommodated because of the large measuring range of the laser sensor. Once the sample has been positioned the longitudinal and transverse scanning ranges of the apparatus can be set by positioning the micro switches appropriately. In this way only as small an area as required is scanned. The working sequence of the scanner is programmed and completely automated by the use of a PC connected to a control box via an RS-232 serial port.

Once the scan program has been started and the relevant information entered, scanning can commence. Both stepper motors are initially moved so that the laser displacement sensor is positioned at the starting point as dictated by the positions of two micro switches. This point is to the left and below the actual sample to be scanned. The scanning head is then moved incrementally to the right in the X-direction by applying pulses to the stepper motor. When the scanning head reaches a limiting micro switch the head returns to the left limit of its travel and the entire longitudinal scanning frame is moved by one increment in the Y-direction. The scanner head then again begins to move to the right in the X-direction and the process is repeated until a fourth micro switch triggers the end of the scanning process.

The profile of the sample is only measured as the scanner head moves from left to the right in the X-direction. The X- and Y- coordinates are determined from the number of pulses fed to each of the stepper motors and the distance between the scanner head and the joint surface is measured at each increment directly by the laser sensor.
The increment in the X- and Y-directions can be set separately, such that the Y-direction increment can be any multiple of the X-direction increment. For a small joint surface approximately 80 mm by 55 mm in size, and using a scan increment of 0.5 mm, the entire surface can be scanned in 25 minutes, producing a data file containing approximately 18 000 data points.

The accuracy and relevance of the results that are obtained from the scanner are influenced by the increments between individual data points. A large increment will produce a coarse and largely non-representative profile whereas a very small increment may provide too much information for processing and will greatly increase the time taken to build up a complete three dimensional picture of the surface roughness.

3.2.2.2 Alternative method of determining joint roughness.

An alternative method to measure joint roughness is with the use of a carpenter's comb. The carpenter's comb consists of a number of vertical steel or plastic pins that can individually move up or down to resemble the face of a two dimensional surface. This tool can be used to determine the unevenness of a joint surface in two dimensions by placing it directly onto the surface. Fig 3.8 illustrates this principle. This apparatus was used to measure and record the roughness profiles of joint surfaces. These roughness profiles were then compared to Barton's roughness profiles (Figure 2.9) and the joint roughness coefficient (JRC) for each sample determined.

Figure 3. 8 **Carpenter's comb on rough joint surface**

3.3 Tests methods for basic, peak and residual shear strength

Barton (1993) states that both angles of basic (ϕ_b) and residual (ϕ_r) friction represent minimum shear resistance. Conceptually ϕ_b refers to smooth planar surfaces in unweathered rock and can be considered as a material constant. The residual friction angle (ϕ_r) refers to the residual condition of natural joint surfaces, which is attained after large shear displacements. If the natural surface is unweathered, ϕ_r can be taken to be equal to ϕ_b.

3.3.1 Testing basic friction angle with the small shear box

Methods for basic angle of friction (ϕ_b) characterization include the direct shear test or tilt tests on saw cut surfaces (Barton and Choubey, 1977).

These tests were carried out with the converted soil shear box, as described in paragraph 3.2.1.1, on saw cut surfaces of NX size core samples. NX size core samples were cut perpendicular to the core axis with a diamond saw. The saw cut surface was then shaved by brushing the sample under its own weight on a fine sanding paper. The test was carried out under dry conditions. Results of this testing are discussed in chapter four.

3.3.2 Testing shear strength with the large shear box

Sampling procedure

Sampling of rock specimens with associated joint surfaces is a difficult procedure because a joint surface is delicate and that must be preserved in its original state for testing.

The size of the final sample is determined by the size of the shear box assembly. Two boxes were used with the following dimensions: 350 x 350 mm square and 350 mm diameter. Samples were carefully selected in a rock mass on site and the surrounding rock material removed. Samples were taken out by hand with the use of a handspike "koevoet" and "Hilti" drill. Then the two rock material pieces with associated joint surface were carefully wedged out and placed on the floor and packaged for transport to the laboratory. Extra rock samples were taken as to compensate for damage during transportation and casting.

Sample preparation

In the laboratory a suitable sample was selected and tied up with wire, with the joint surfaces in their original relative position. Figure 3.9 illustrates this principle.

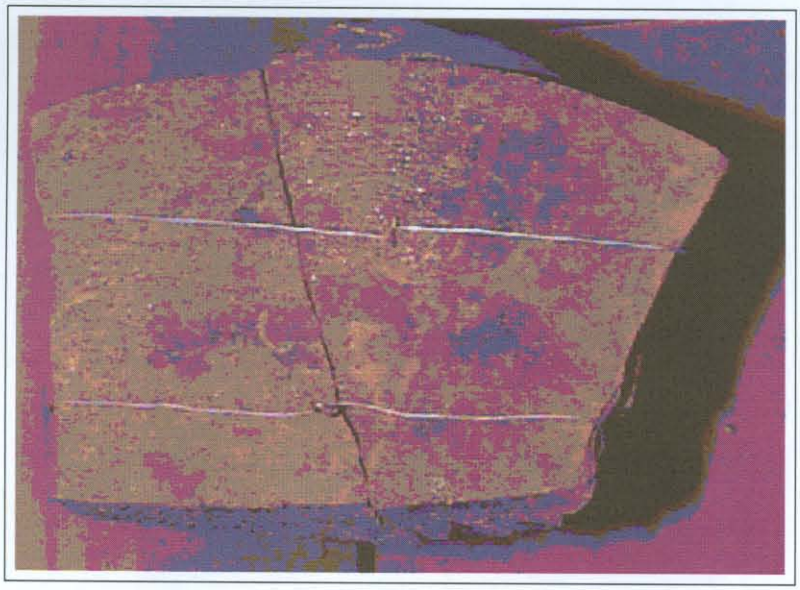

Figure 3. 9 Rock sample with associated joint surface tied, up with wire ready to be cast

The sample is then placed into the top box (upside down position) and the joint surface orientated parallel to the shear plane. It is positioned such that the shear surface is approximately 10 mm above the top of the shear box rim. A casting agent (cement grout) is then prepared and cast into the top half of the box with the sample in position. The grout is poured into the box to about 20 mm below the rim of the box. The grout is made up of the following ingredients: 20 kg building sand, 5,25 kg cement, 2,25 kg slagment, 10 ml plastisizer, and ± 3,9 liters water. The grout is then left for two days to set. Figure 3.9 illustrates a rock sample with joint cast in the shear box.

The bottom part of the box is then bolted onto a special jig to keep it in position and filled with grout to about 40 mm below of the rim of the box. The top part of the box with the sample in place can now be turned around and gently lowered onto the bottom part until the joint surface is about 10 mm above the rim of the bottom part. Now it can be bolted to the jig and left for two days to set. When completely set, the wire holding the sample together can be cut and the moulds removed from the jig and moved to the testing machine.

Testing procedure

The prepared sample in the shear box assembly is placed into the shear box machine. The whole testing operation is computer controlled.

The software supports a variety of shear testing procedures as well as keeping record of all the results. Mounted inside the PC is an ADC/DAC card, which interfaces the software to the testing machine. This interface enables the software to read the load signals and controls the speed of the drive motor. When the software is loaded, the first menu is activated on the screen. Selecting the options on the screen and entering the required information carries out the test by keyboard.

The normal load is applied for at least 20 seconds before the shear load is activated. Normal stresses of 0.6, 0.9 and 1.2 MPa were decided upon and depending on the area of the sample to be tested, the corresponding loads were calculated and fed into the programme. The mass of the top half including the plate for transferring the load to the sample was determined and included in the calculation of the normal load. Shear load is applied at a rate of 2 mm per minute.

The data acquisition unit captures data every two seconds. These data consist of normal load by means of a pressure transducer, vertical movement by means of two vertical LVDT's, horizontal movement by means of two horizontal LVDT's and shear load by means of a load cell. The test was terminated when the horizontal movement reached a maximum of approximately 20 mm.

A test cycle was conducted for each normal load and the corresponding shear load obtained. Thereafter graphs of shear stress vs. normal stress were plotted and values for the angle of friction and cohesion were calculated.

Tests were carried out on basalt, dolerite, granite, sandstone and mudstone samples. Samples were tested a first time through three cycles dry and then photographed (Appendix F). After interpretation of the results, it was decided to run another three cycles of dry testing and then three cycles wet. (Submerged under atmospheric conditions). After the completion of a the "dry" tests, the same samples were saturated and "wet" tests were done to compare the results and to get a "dry - wet" relationship.

Evaluation of the large shear apparatus

The large shear apparatus is the only shear test apparatus of its kind in southern Africa. The **advantages** of the machine are that it can be used to determine the shear strength parameters of relative large rock specimens. The expertise has now been developed to prepare samples, execute the test procedure and interpret the results. The machine can also be used to determine the shear strength parameters of other materials such as gravel's or even simulated rock fill materials.

The **disadvantages** of the method are that it is difficult to take specimens from rock mass while ensuring that both joint surfaces remain intact. Great care should also be taken with transportation. The preparation and testing process is very time-consuming.

It should be noted that the true peak shear strength of a joint could theoretically only be measured if at least three identical specimens can be tested at different normal stresses.
Since three or more identical specimens are never available, true peak shear strength can not be determined in practice. If a single specimen is used, some of its peak shear strength (roughness) is removed after the first shear failure. The second and further shear failures

therefore represent "post-peak" shear strength. After many tests on the same specimen, most of the roughness has been removed, and the residual or basic shear strength is approached. In this test programme, the "maximum post-peak" (max p-p) friction angle is considered to be an conservative measure of the true peak friction angle. The "minimum post-peak" (min p-p) friction angle is taken to fall somewhere between the peak and the basic friction angles.

3.3.2.1 Phase 1 testing

The first phase consisted of three tests at different vertical stresses, i.e. at approximately 600, 900 and 1200 kPa on dry rock samples. It was expected that this test phase would result in the determination of the max p-p shear strengths.

After analysis of the data it was decided to check the large shear apparatus for any possible defects since the results were difficult to interpret. After adjustments to the apparatus and amendments to the software controlling the machine the second and third phases were carried out. Adjustments to the apparatus included repositioning of LVDT attachments, while the software was partially rewritten to change the commands regulating the horizontal and vertical forces. During the first phase of testing the shear and normal forces were initiated simultaneously, which meant these forces, increased simultaneously to the set levels. This was changed to allow the normal force to reach its predetermined level before the shear force was initiated. Results of this testing phase are presented in Appendices C and D, and on the compact disc (CD) included in this report.

The results obtained during the first phase of testing must be regarded as unreliable as they were not conducted in accordance with standard testing methods due to the way the software controlling the application of stresses on the sample. The results are however included and compared with residual shear strength results as obtained from the second and third phases of testing.

3.3.2.2 Phase 2 testing

The second phase consisted of two sub phases, referred to as phases 2A and 2B. Phase 2A was conducted on the same rock specimens as tested in Phase 1. This was done after adjustments to the large shear machine and software controlling the shear process had been

made. The same normal stresses as used during Phase 1 were applied. At the beginning of this stage each specimen had already been sheared three times and it was accepted that the results obtained were approaching the residual shear strength. Supportive documentation is available in Appendix E and F.

Phase 2B was carried out immediately after Phase 2A, without removing the specimen from the apparatus. All tests were conducted in the same manner as during phase 2A but the shear box was filled with water to simulate submerged conditions. Supportive documentation is available in Appendices E and F.

3.3.2.3 Shear strength of joints in Granite - Phase 3

The third phase of the investigation involved the taking of the three new samples. A suitable site for sampling specimens for the third phase of testing was located at the Nandoni Dam presently under construction in the Limpopo (Northern) Province near Thohoyandou. A number of large samples were taken for shear testing in the laboratory. These samples were all taken from the quarry at the dam site as no suitable samples could be found in the dam foundation. They were all excavated from the rock mass with hand held tools. Care was taken that the joint surfaces were not damaged during the sampling process. Table 3.2 gives a description of the three granite specimens tested.

They were numbered Granite 1C, 2C and 3C and prepared as described in chapter two of this report.

Specimen	Surface characteristic	Schmidt rebound Number	JRC
Granite 1C	Rough clean	62	6 – 8
Granite 2C	Rough - FeO_2 stained	61	4 – 6
Granite 3C	Rough - hard joint fill	58	10 – 12

Table 3. 2 Granite specimens tested during the third phase of the investigation

Although the three samples were taken from the same granite site it was not possible to get samples from the same continuous in situ joint surfaces. On closer inspection it was found that there were some variations in the characteristics of the joint surface sampled. Granite 1C had the smallest surface area of 15950 mm^2. The surface was not stained or covered by any joint fill. Granite material formed the contact surface. Granite 2C had a surface area of 30600 mm^2. The surface was lightly stained with iron oxide. No joint fill was present. Slightly weathered granite material formed the contact surface. Granite 3C had a surface area of 31500 mm^2. The surface was covered with joint fill in the form of a greenish secondary mineral. The joint fill material formed the contact surface. The joint roughness (JRC) of the three samples was approximately the same.

Testing during Phase 3A was carried out at effective normal stresses of approximately 600, 900, 1200 and 1500 kPa. It was decided to use four normal loads as this would give greater accuracy with four points on the shear stress vs. normal stress graph. Testing was carried out in a forward direction and then the sample was cleaned (all debris of the previous test removed by blowing it off the surface), turned 180° around, and tested in the opposite direction (reverse). The reverse tests were also carried out at the same normal stresses. Thereafter the samples were tested in the forward direction under submerged conditions, using the same four normal loads. This was Phase 3B of the investigation. Supportive documentation is available in Appendices G and H.

3.4 Self evaluation

In hindsight, the following aspects of the project is worth noting:

- A project of this magnitude should be approached as a team effort and preferably on a full time basis. This project was carried out by on a part time basis over a long period. The minority of research projects in South Africa is carried on a full time basis due to the shortage of expertise. In contrast to researchers in the USA, UK and Europe the majority of researchers (Masters and Doctorate students) at South African tertiary educational institutions are enrolled in a part time capacity. This means that the have divided interests and that the research project is secondary to their daily occupation

and responsibility to their employer. This results in many projects taking much longer and initially planned and loss of coherent ness of data and information in such reports.

- It is important to define the scope of a project at the start of the project and not allow the project to 'grow' during the course of the project. When additional interesting research aspects emerge during the project they should be treated as separate projects.

- A large shear-testing machine was designed and built as part of the research project. This was a time consuming task and many people were involved. These included staff of the Department of Water Affairs and Forestry, different members of the steering committee of the Water Research Commission, the researcher and a contractor. Looking back at the process from initiation to commissioning of the machine, it can be concluded that the whole process was very well organized and the end product very suitable for the purpose it was built. The only problem identified was that the software controlling the stresses, which was rectified after interpretation of the first set of results was analyzed.

- During the taking of large-scale samples for shear test care must be taken as not to damage the shear surface. Large shear tests were carried out on block samples with surface areas ranging from approximately 100 x 100 mm to 300 x 300 mm. The samples are extremely sensitive to disturbance during sample taking, transportation, preparation, and testing. During the project extreme care was taken as not to damage samples and it can be reported that damage to surfaces were very limited and it can be stated that joint surfaces tested were very similar to joints conditions in situ, with the exception of moisture content. Samples were taken that were of a small enough size to fit the laboratory shear box so that cutting and associated damage to the shear surface was limited to a minimum. Generally joint fill material dried out during the period between sample taking and testing that could have been as much as eighteen (18) months. During the final phase of testing water as added to the shear box to test the shear strength under saturated conditions.

- During 1995 a laser-scanning device was built to determine the 3D roughness of joint surfaces. In hindsight, this apparatus should have been used more extensively in the determination of the volume of material that was removed from the joint surface

during each shear. The relationship between volume of material removed during each shear and friction angle will give interesting results and should be investigated further.

CHAPTER FOUR
RESULTS OF THE INVESTIGATION

4.1 Basic friction angle

The basic friction angles of a number of rock types were tested in the laboratory. Testing was carried out on NX size core samples of which the shear surface that was saw cut and polished on sandpaper. Three loading cycles were carried out on each sample. Normal stresses of 40 kPa, 70 kPa and 110 kPa were applied. The results of the testing are presented in table 4.1.

ROCK TYPE	BASIC FRICTION ANGLE (Degrees)	COHESION (kPa)
A. Sedimentary Rocks		
Shale (2A)	31,72	4,14
Sandstone (2B)	27,89	6,7
Mudstone (3C)	32,71	9,93
Shale (4A)	31,9	10,46
Sandstone (4B)	34,9	3,34
Sandstone (5B)	35,95	0
Siltstone (5C)	38,19	8,99
B. Igneous Rocks		
Dolerite (Fine) (3A)	33,33	6,7
Dolerite (Coarse) (3B)	36,32	3,03
Granite (5A)	31,11	6,26
Dolerite (5D)	31,03	0
Riolite (6A)	35,03	11,91
C. Metamorphic Rocks		
Quartzite (1A)	30,42	8,59
Quartzite (1B)	27,85	9,36
Tillite (7A)	32,63	2,74
Quartzite (8A)	28,58	1,96

Table 4. 1 **Basic friction angles and cohesion of various unweathered rocks obtained from flat surfaces of important Southern African rock types**

When the basic shear strength is determined no cohesion is present. During testing of this parameter some cohesion was recorded. This cohesion (apparent cohesion) is relatively small and could be attributed to residual roughness of the saw cut surfaces.
The basic friction angle, determined for all rock types during this project, were in the same range as work done by Coulson (1972). The testing programme gave very encouraging results. These values can be used with confidence further in this report.

4.2 Shear strength of rock types tested

Specimens tested with the large shear apparatus during the first two phases are listed in Table 4.2. This table also contains the results of surface characterization, Schmidt hammer tests and testing performed.

Five rock types were tested. These included three (3) basalt samples, three (3) dolerite samples, seven (7) granite samples, three (3) sandstone samples and three (3) mudstone samples. Some specimens were damaged during the first phase of testing and were not available for the subsequent testing programme.

Specimen	Origin	Surface characteristics	Schmidt Rebound	JRC	First phase	Second phase (dry)	Second phase (wet)
Basalt 1	Lesotho	Rough, hard	54	8-10		Yes	Yes
Basalt 2	Lesotho	Rough, hard	56	8-10	Yes	Yes	Yes
Basalt 3	Lesotho	Rough, hard	52	6-8	Yes	Yes	Yes
Dolerite 1	Qedusizi	Rough, hard	46	4-6	Yes	Yes	Yes
Dolerite 2	Qedusizi	Rough, hard	40	2-4	Yes		
Dolerite 3	Qedusizi	Soft clay 1 mm	51	4-6	Yes	Yes	Yes
Granite 1	Driekoppies	Rough, hard	67	2-4		Yes	Yes
Granite 2	Driekoppies	Rough, hard	58	10-12	Yes		
Granite 3	Driekoppies	Rough, hard	60	8-10		Yes	Yes
Granite 4	Driekoppies	Rough, hard	65	8-10	Yes		
Granite 5	Driekoppies	Rough, hard	61	8-10	Yes	Yes	Yes
Granite 6	Driekoppies	Rough, hard	61	8-10	Yes	Yes	Yes
Granite 7	Driekoppies	Rough, hard	56	6-8	Yes	Yes	Yes
Sandstone 1	Natal	Rough, hard	22	6-8	Yes	Yes	Yes
Sandstone 2	Natal	Rough, hard	28	12-14	Yes		
Sandstone 3	Natal	Rough, hard	26	6-8	Yes		
Mudstone 1	Qedusizi	Rough, hard	28	2-4	Yes	Yes	Yes
Mudstone 2	Qedusizi	Rough, hard	40	2-4	Yes	Yes	Yes
Mudstone 3	Qedusizi	Rough, hard	40	2-4	Yes	Yes	Yes

Table 4. 2 **Specimens tested during the first and second phases of testing**

A detailed analysis of the results of the shear tests on large samples was carried out to determine the shear strength of the different rock types as well as the influence of hardness and roughness of the joint surfaces on the shear strength.

Tests were conducted at normal stresses between 0,5 and 1,5 MPa. Normal stresses under a concrete dam are in this order of magnitude. The test method is described in detail in paragraph 3.3.2.1 of this thesis.

Barton and Choubey (1977) have shown that the relationship between shear stress and normal stress for lower stresses (both under 3 MPa) and smooth joints (JRC = 5) are linear. For higher stresses (shear stress up to 6 MPa and normal stress up to 4 MPa) on rough joints (JRC = 20) the relationship is curved. The relationship in all cases originates at 0.

Analysis of the results of tests on each sample involved the selection of three points on the graph of shear load vs. horizontal displacement (see example below) and evaluating the horizontal load (kN) and vertical load (kN) at each of these points. From the graph (Fig 4.2) vertical displacement vs. horizontal displacement, the deviation from horizontal (positive or negative) in degrees was determined to calculate the "corrected" shear load and normal load. The shear and normal stresses were then calculated. The normal stresses for all the samples were then plotted vs. the shear strength (dry and saturated, see Appendix H). Regression plots were then drawn and the coefficient of correlation and slope and X-intercept (c) calculated. (See Appendix F for tables).

Ranges where three arbitrary maximum values measured.

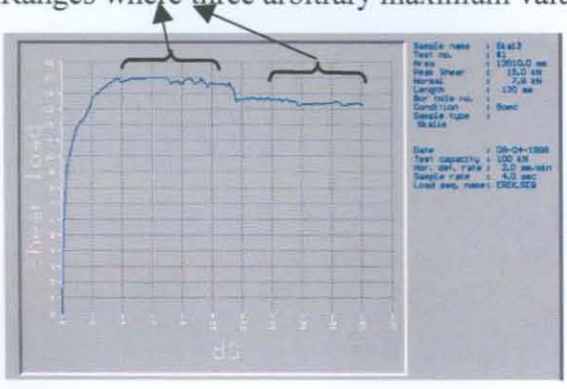

Figure 4.1 Shear load vs. shear displacement showing where readings were taken.

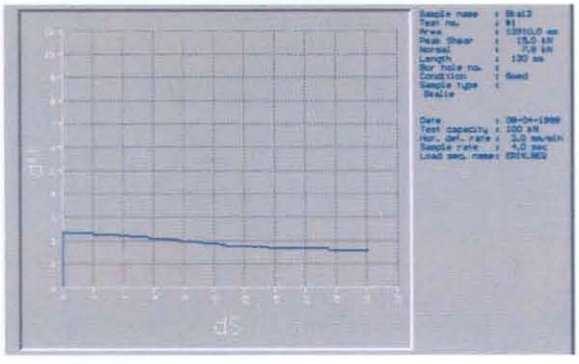

Figure 4.2 Horizontal displacement vs. vertical displacement showing dip angle.

The calculated peak friction angle is the value of the friction angle as calculated with Barton's formula. (See paragraph 2.3.1 of this thesis). The measured maximum p-p friction angle is the friction angle determined by the highest shear load observation points on the shear load vs. displacement graph. The measured minimum p-p friction angle is the friction angle determined by the lowest shear load observation points on the shear load vs. displacement graph. The measured average residual friction angle is the friction angle determined by the average shear load observation points (horizontal part of the graph) on the shear load vs. displacement graph.

4.3 Maximum post peak shear strength - Phase 1

The results obtained during this phase of testing are suspect because the test machine and software controlling the apparatus was faulty. After analysis of the data of phases 1 it was decided to check the large shear apparatus for any possible defects since the results were difficult to interpret. Adjustments were made to the apparatus and amendments to the software controlling the machine were carried out. Adjustments to the apparatus included repositioning of LVDT attachments, while the software was partially rewritten to change the commands regulating the horizontal and vertical forces. During the first phase of testing the shear and normal forces were initiated simultaneously, which meant these forces, increased simultaneously to the set levels. This was changed to allow the normal force to reach its predetermined level before the shear force was initiated. The reliability of the results are in question. It is however discussed as it forms part of the investigation conducted.

4.3.1 Basalt

Two basalt specimens, basalt 2 and basalt 3, were tested during phase 1 of this investigation. The plot of shear stress vs. normal stress for phase 1 is shown in Figure 4.3. Table 4.4 presents a summary of the results obtained for phase1.

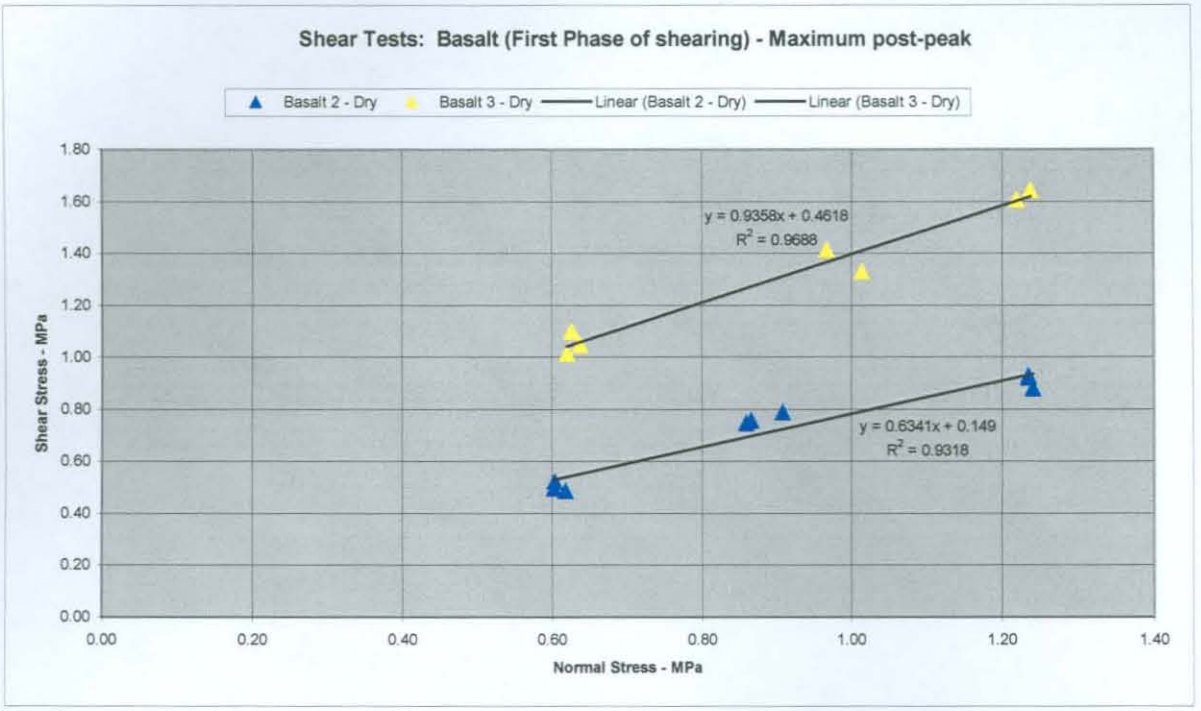

Figure 4. 3 **Shear stress vs. normal stress -Phase 1 of shearing for Basalt 2 and 3**

Specimen	Angle of friction (degrees)	Apparent Cohesion (kPa)	Correlation coefficient of observation points on normal- vs. shear stress graph
Basalt 2 - Phase 1 (dry)	32,4	149	0,93
Basalt 3 - Phase 1 (dry)	43,1	461	0,97

Table 4. 3 **Shear strength parameters of basalt as determined during test Phase 1**

Discussion

The maximum post-peak friction angle of basalt 2 is lower than that of basalt 3 due to the rougher joint surface of basalt 3. The value of basalt 2 is low compared to the basic friction angle for basalt has been reported as being between 35° and 38° (Coulson, 1972).

4.3.2 Dolerite

Only one Dolerite specimen was tested during the first phase of shearing. Figure 4.4 illustrates the normal stress vs. shear stress of Dolerite in the first phase of shearing (dry).

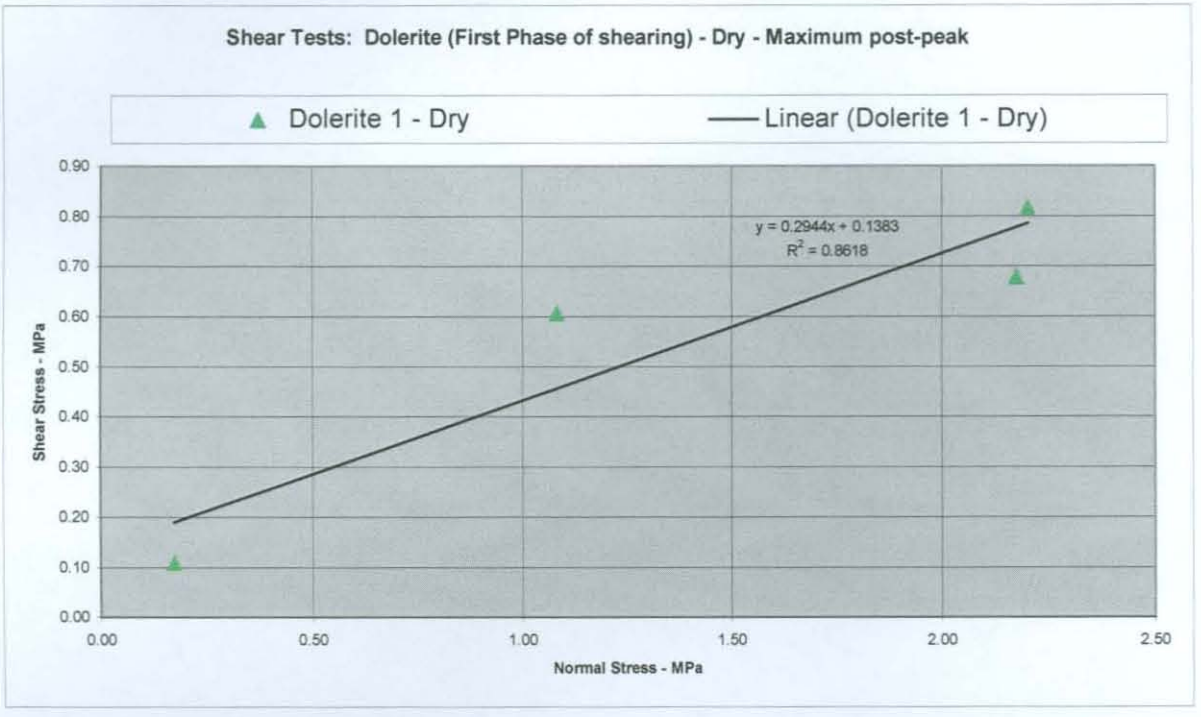

Figure 4. 4 **Shear stress vs. normal stress -Phase 1 of shearing (dry) of Dolerite 1**

The test results are listed in Table 4.5.

Specimen	Angle of friction (degrees)	Apparent cohesion (kPa)	Correlation coefficient of observation points on normal - vs. shear stress graph
Dolerite 1 - Phase 1 (dry)	16,4	138	0,86

Table 4. 4 **Friction angle and apparent cohesion for Dolerite 1**

Discussion

The angle of friction of 16,4° is very low for dolerite. This is probably due to the method of testing as described in paragraph 3.3.2.1. These results could not be used with confidence and are presented here only for record purposes.

4.3.3 Granite

Three specimens of Granite were tested through phase 1 of shear testing. These were Granite samples 5, 6 and 7. The shear stress vs. normal stress observations for phase 1 (dry) is plotted in Figure 4.5.

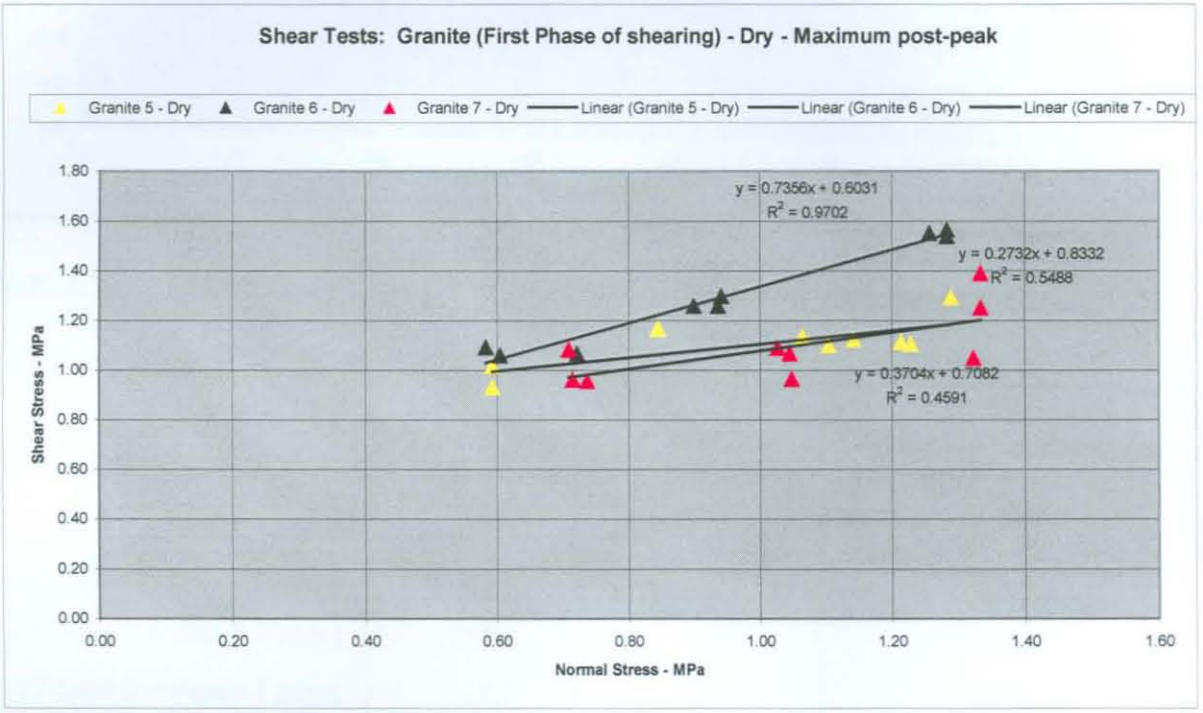

Figure 4. 5 **Shear stress vs. normal stress - Phase 1 of shearing (dry) Granite**

Rock type and test phase	Angle of friction (degrees) Value	Average	Apparent cohesion (kPa)	Correlation coefficient of observation points on normal - vs. shear stress graph
Granite 5 – Phase 1 (dry)	15,3		603	0,55
Granite 6 – Phase 1 (dry)	20,2	23,9	833	0,97
Granite 7 – Phase 1 (dry)	36,3		708	0,46

Table 4. 5 **Shear strength parameters of Granite as determined during Phase 1**

Discussion

The granite specimens were moderately hard with rough surfaces. The friction angles for granite samples 5, 6 and 7 are very low, 15,3°, 20,2° and 36,9° respectively. The basic

friction angle for granite is 31° to 35° as reported by Coulson (1972, in Barton and Choubey, 1977).

4.3.4 Sandstone

Three specimens of Sandstone were tested. The shear stress vs. normal stress observations for phase 1 (dry) is plotted in Figure 4.6.

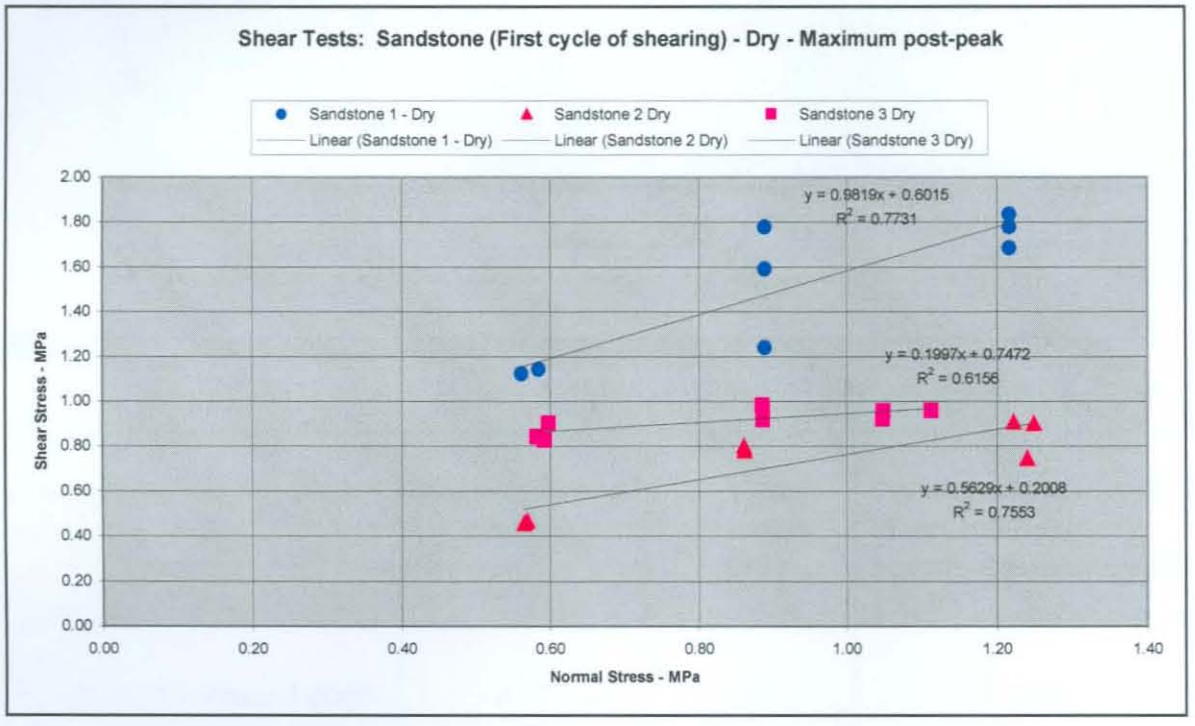

Figure 4. 6 **Shear stress vs. normal stress - Phase 1 of shearing (dry) Sandstone**

Rock type and test phase	Angle of friction (degrees)	Apparent cohesion (kPa)	Correlation coefficient of observation points on normal - vs. shear stress graph
Sandstone 1 – Phase 1 (dry)	44,5	602	0,77
Sandstone 2 – Phase 1 (dry)	29,4	747	0,62
Sandstone 3 – Phase 1 (dry)	11,3	201	0,76

Table 4. 6 **Shear strength parameters of sandstone as determined during Phase 1**

Discussion

These mudstone specimens were tested through Phase 1. Tests on Sandstone 1 gave a very high value for the maximum post-peak friction angle and for Sandstone 2 and 3 very low values.

The basic friction angle for sandstone is 26° - 35° as reported by Coulson (in Barton and Choubey, 1977).

4.3.5 Mudstone

Three specimens of Mudstone (please note: Mudstone is referred to as Shale on the plates in the appendices) were tested, through phase 1. The shear stresses vs. normal stress observations for the first phase (dry) are plotted in Figure 4.7.

Table 4.7 presents the shear strength parameters as determined during this study.

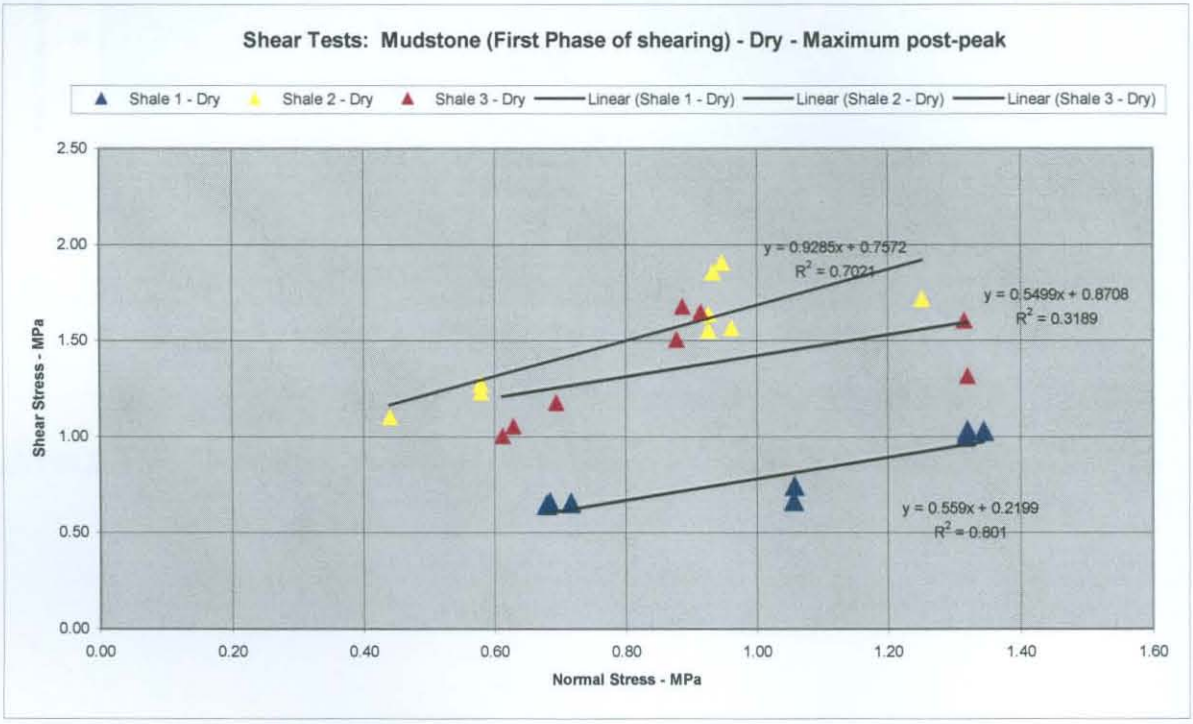

Figure 4. 7 **Shear stress vs. normal stress-phase 1 of shearing (dry) Mudstone**

Rock type and test phase	Angle of friction (degrees)	Apparent cohesion (kPa)	Correlation coefficient of observation points on normal - vs. shear stress graph
Mudstone 1 – Phase 1 (dry)	29,2	220	0,80
Mudstone 2 – Phase 1 (dry)	28,8	871	0,32
Mudstone 3 – Phase 1 (dry)	42,9	757	0,70

Table 4. 7 **Shear strength parameters of mudstone as determined during Phase 1.**

Discussion

Three mudstone specimens were tested. The maximum post-peak friction angle of mudstone 1 and 2 were determined as 29,2° and 28,8° respectively. The peak friction angle of mudstone 3 was determined as 42,9°. The basic friction angle for Mudstone is between 31° and 33° as reported by Coulson, (1972).

4.4 Minimum post-peak shear strength - Phase 2

4.4.1 Basalt

Three basalt specimens were tested, two of which through phases 1, 2A and 2B. The graphs of shear stress vs. normal stress for phase's 2A and 2B are shown in Figure 4.8. The shear strength parameters are listed in Table 4.8.

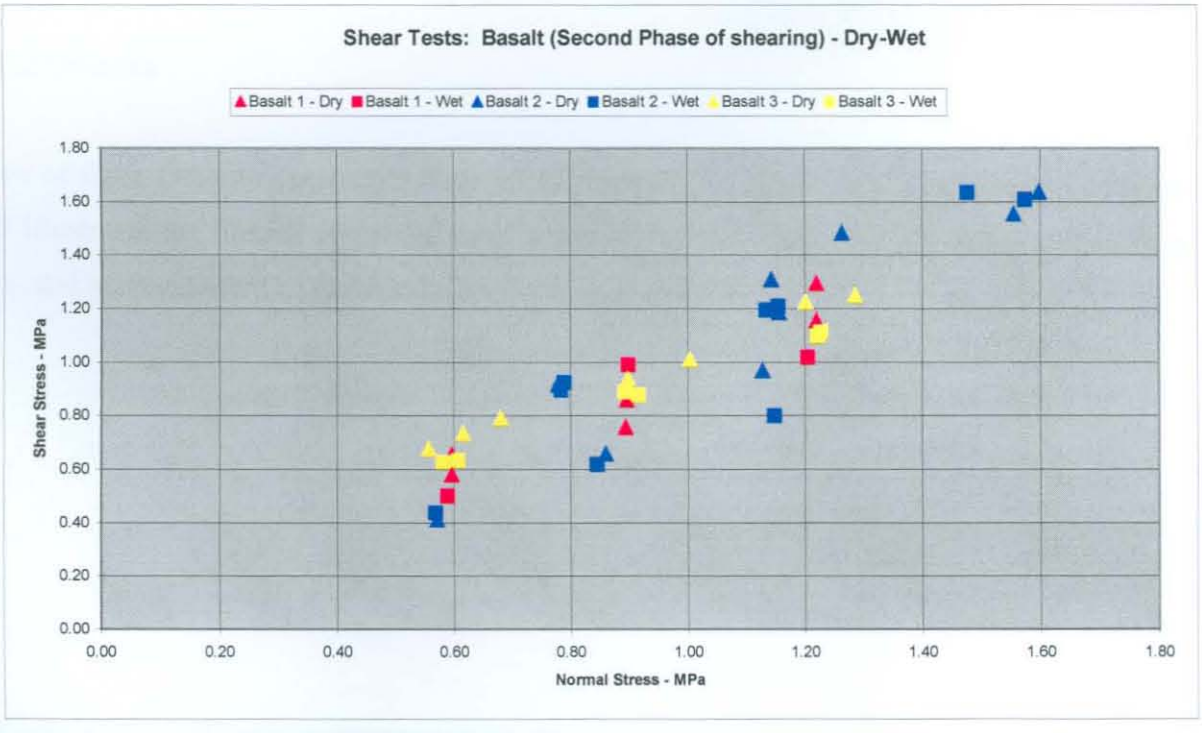

Figure 4. 8 **Shear stress vs. normal stress-Phases 2A and 2B of shearing Basalt 1, 2 and 3**

Specimen	Angle of friction (degrees) Value	Average	Apparent Cohesion (kPa)	Correlation coefficient of observation points on normal - vs. shear stress graph
Basalt 1 - Phase 2A (dry)	44		0	0,93
Basalt 2 - Phase 2A (dry)	49	44	166	0,88
Basalt 3 - Phase 2A (dry)	38		240	0,99
Basalt 1 - Phase 2B (wet)	40		82	0,80
Basalt 2 - Phase 2B (wet)	48	42	137	0,82
Basalt 3 - Phase 2B (wet)	37		190	1,00

Table 4. 8 **Shear strength parameters of Basalt as determined during test Phases 2A and 2B**

Discussion

The average post-peak dry friction angle of 44° seems to be in the order of what can be expected, as the basic friction angle for basalt has been reported as being between 35° and 38° (Coulson, 1972). The average submerged residual friction angle was determined as 42°. This is expected as basalt is a hard rock (UCS or JCS = 200 MPa and Schmidt hardness = 53 - 57) with rough joint surface. The JRC was determined as 9. the reduction of 44° to 42° can also be due to the large cumulative distance of shear.

4.4.2 Dolerite

Two of three Dolerite specimens were tested through the second phase of shearing. Figure 4.9 illustrates the normal stress vs. shear stress of Dolerite in the second phase of shearing (dry and submerged). The test results are listed in Table 4.9.

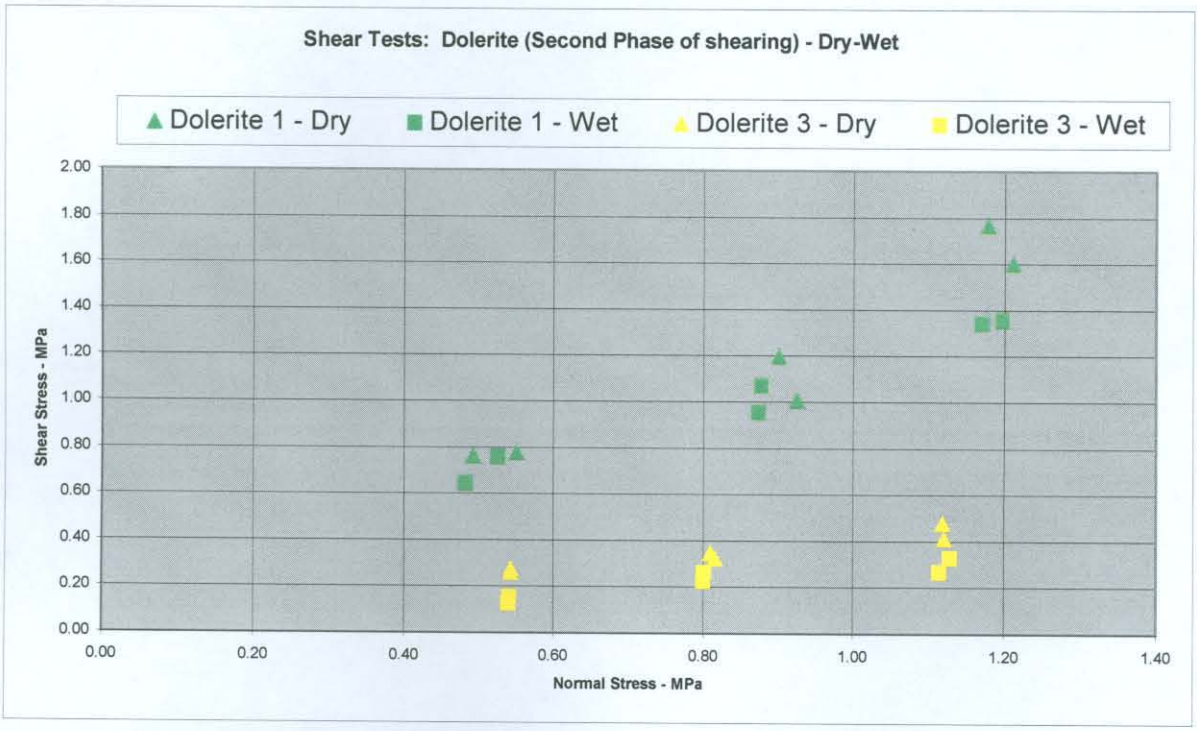

Figure 4. 9 **Shear stress vs. normal stress -Phases 2A and 2B of shearing (dry and submerged) of Dolerite 1 & 3**

Specimen	Angle of friction (degrees)	Apparent cohesion (kPa)	Correlation coefficient of observation points on normal - vs. shear stress graph
Dolerite 1 - Second phase (dry)	52,6	39	0,89
Dolerite 3* - Second phase (dry)	17,0	95	0,82
Dolerite 1 – Second phase (wet)	43,6	205	0,97
Dolerite 3* - Second phase (wet)	14,9	8,5	0,86

Dolerite 3* with 1mm clay layer on joint

Table 4. 9 **Friction angles and apparent cohesion for Dolerite**

Discussion

Two of the three dolerite specimens were tested. There was a distinctive difference between the shear surfaces of the two specimens. Dolerite 1 was a hard, rough surface whilst Dolerite 3 had approximately one millimetre of clay on its surface. Shear strength of the two surfaces can thus not be compared nor correlated.

The minimum p-p angle of friction for Dolerite 1 was determined as 52,6° during phase 2A. This value seems to be high, as the basic friction angle for dolerite is 36°. The maximum post-peak friction angle of Dolerite 1 was determined as 43,6° submerged (test phase 2B). This value seems to be on the high side, however it must be kept in mind that dolerite is a hard rock (UCS = 250 MPa, and Schmidt rebound number: 46). Another factor explaining the medium high friction angle is the roughness of the joint surface. The JRC is between 10 and 12

The minimum p-p friction angle of Dolerite 3 (on the clay filled joint) was determined as 17° dry and 14,9° submerged. These values are low due to the fact that the joint fill is soft clay about 1mm thick. Another factor explaining the low friction angle is the smoothness of the joint surface. The JRC is 4 - 6.

4.4.3 Granite

Seven specimens of Granite were tested, four through phases 1, 2A and 2B of testing. Table 4.10 shows the shear strength parameters obtained. Three other specimens were tested in detail during phase 3 of this project.

The shear stress vs. normal stress observations for phase 2A and 2B (dry and saturated) are plotted in Figure 4.10.

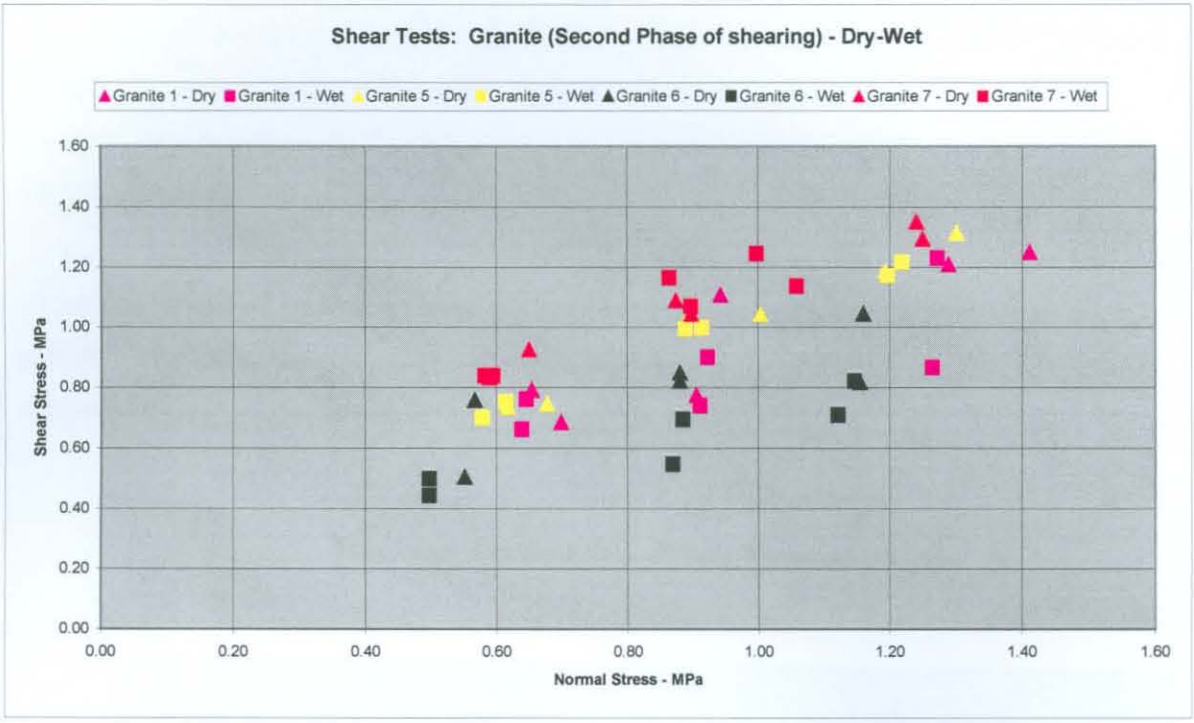

Figure 4. 10 **Shear stress vs. normal stress -Phases 2A and 2B of shearing (dry and submerged) Granite**

Rock type and test phase	Angle of friction (degrees) Value	Angle of friction (degrees) Average	Apparent cohesion (kPa)	Correlation coefficient of observation points on normal - vs. shear stress graph
Granite 1 – Phase 2A (dry)	35,8	34,6	261	0,81
Granite 5 – Phase 2A (dry)	40,0		231	0,98
Granite 6 – Phase 2A (dry)	27,1		56	0,62
Granite 7 – Phase 2A (dry)	35,3		440	0,97
Granite 1 – Phase 2B (wet)	28,8	29,9	343	0,59
Granite 5 – Phase 2B (wet)	37,5		279	0,99
Granite 6 – Phase 2B (wet)	24,9		230	0,84
Granite 7 – Phase 2B (wet)	28,2		394	0,85

Table 4. 10 **Shear strength parameters of Granite as determined during Phases 2A and 2B**

.Discussion

Four of the seven granite specimens were tested during the Phases 2A and 2B of testing. The granite specimens were moderately hard with rough surfaces. The basic friction angle for granite, 31° to 35° as reported by Coulson, (in Barton and Choubey, 1977) is in the same order of magnitude as the results obtained during this project. The minimum p-p friction angle of granite was determined as 34,6° dry and 29,9° submerged. These values seem to be as what could be expected as it must be kept in mind that granite is a moderately hard rock (UCS or JCS = 150 MPa and Schmidt rebound number 56 to 65). Another factor explaining the moderately high friction angle is the roughness of the joint surface. The JRC is 8 - 10. The reduction in shear strength from 34,6° to 29,9° is probably due to a combination of saturation and smoothing of the shear surface as a result of shear distance.

4.4.4 Sandstone

Three specimens of Sandstone were tested of which only one was tested through phases 1, 2A and 2B. The shear stress vs. normal stress observations for phase 2A and 2B (dry and submerged) are plotted in Figure 4.11. Results are listed in table 4.11.

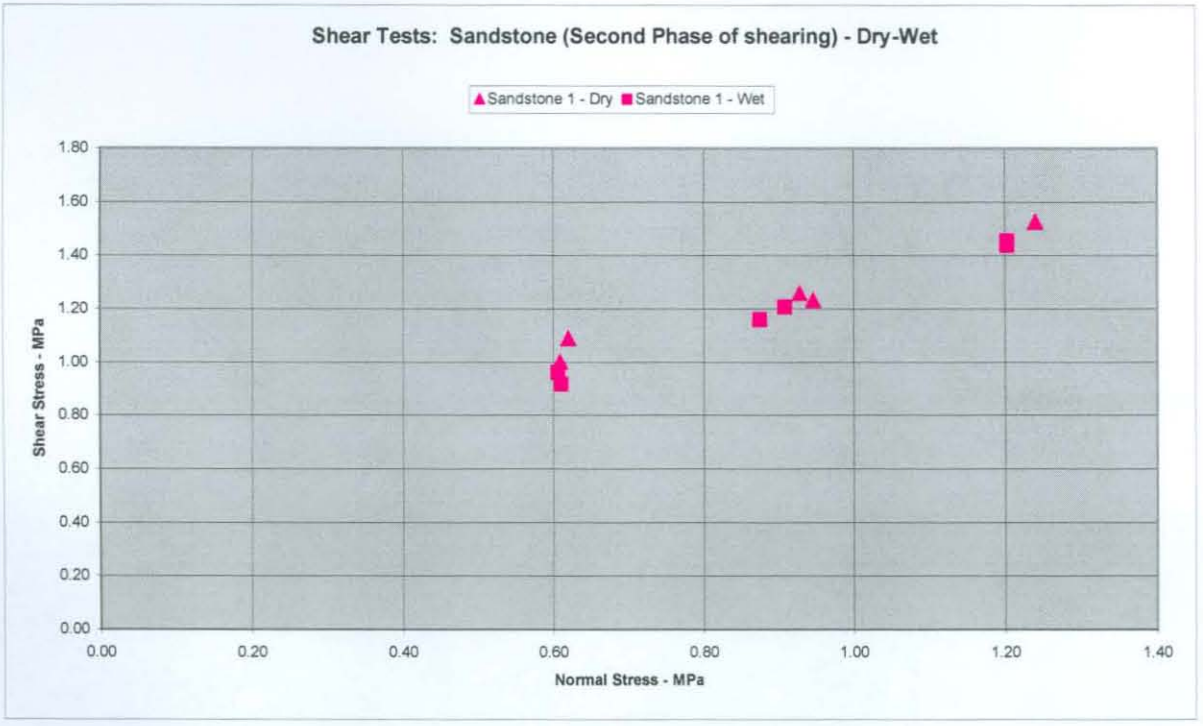

Figure 4. 11 **Shear stress vs. normal stress -Phases 2A and 2B of shearing (dry and submerged) Sandstone**

Rock type and test phase	Angle of friction (degrees) Value	Average	Apparent cohesion (kPa)	Correlation Coefficient
Sandstone 1 – Phase 2A (dry)	37,6	-	558	0,97
Sandstone 1 – Phase 2B (wet)	40,5	-	422	0,99

Table 4. 11 **Shear strength parameters of Sandstone as determined during Phase 2**

Discussion

One sandstone specimen was tested through Phases 1, 2A and 2B. Sandstone 1 had a hard rough surface. The basic friction angle for sandstone is 26° - 35° as reported by Coulson, (in Barton and Choubey, 1977). The minimum p-p friction angle of sandstone 1 was determined as 37,6° dry and 40,5° saturated. These values seem to be moderately high, however it must be kept in mind that sandstone is a hard rock (UCS or JCS = 180 MPa and Schmidt rebound number is 22 - 26). Another factor explaining the high friction angle is the roughness of the joint surface. The JRC is between 10 and 12. The higher value during B2 cannot be explained.

4.4.5 Mudstone

Three specimens of Mudstone were tested, all three specimens through phases 1, 2A and 2B. Table 4.12 presents the shear strength parameters as determined during this study.

The shear stress vs. normal stress observations for the second phases (dry and submerged) are plotted in Figure 4.12.

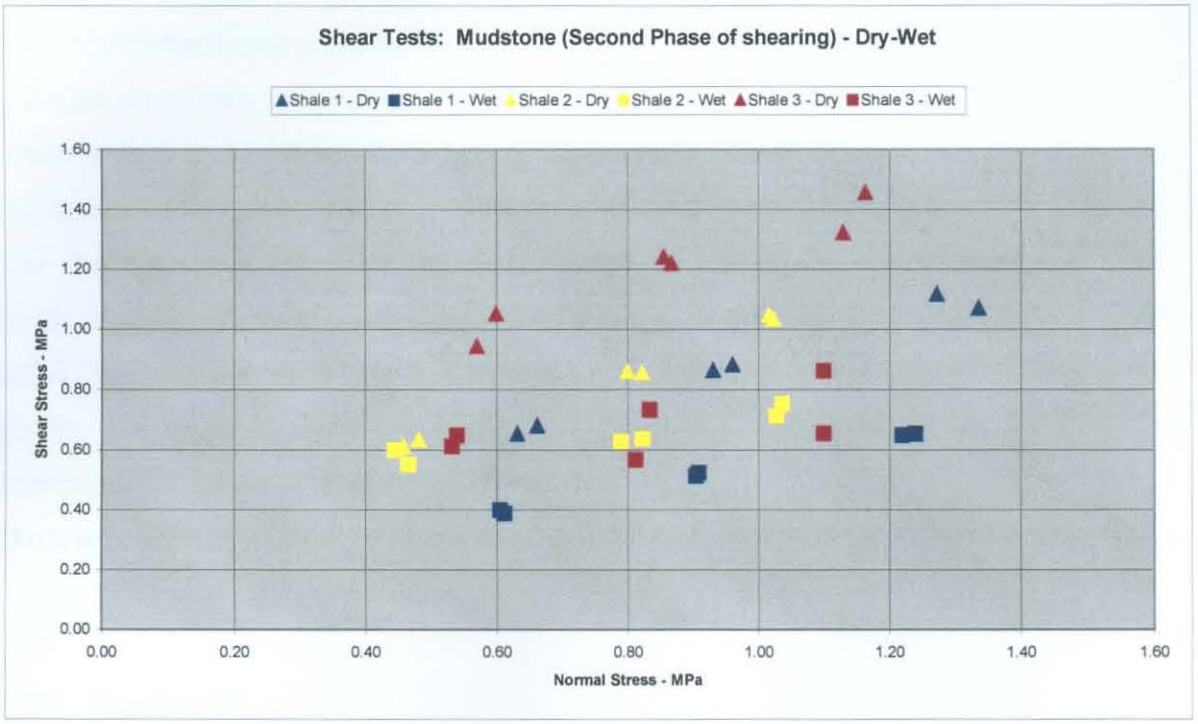

Figure 4. 12 **Shear stress vs. normal stress -Phases 2A and 2B of shearing (dry and submerged) Mudstone**

Rock type and test phase	Angle of friction (degrees) Value	Average	Apparent cohesion (kPa)	Correlation Coefficient of observation points on normal - vs. shear stress graph
Mudstone 1 – Phase 2A (dry)	32,8		257	0,98
Mudstone 2 – Phase 2A (dry)	37,0	34,9	252	0,99
Mudstone 3 – Phase 2A (dry)	35,2		598	0,93
Mudstone 1 – Phase 2B (wet)	22,6		141	1,00
Mudstone 2 – Phase 2B (wet)	14,6	16,8	446	0,85
Mudstone 3 – Phase 2B (wet)	13,2		487	0,32

Table 4. 12 **Shear strength parameters of Mudstone**

Discussion

Three mudstone specimens were tested. The basic friction angle for Mudstone is between 31° and 33° as reported by Coulson, (1972). The minimum post-peak friction angle of

mudstone was determined as 34,9° dry and 16,8° submerged. These values seem to be slightly on the high side (not true residual) during dry testing and very low during saturated conditions, however it must be kept in mind that Mudstone is a soft rock (UCS or JCS = 120 MPa and Schmidt rebound number between 28 and 40). The JRC is between 2 and 4.

4.5 Shear strength of joints in Granite - Phase 3

During the interpretation of the test results of Phase 2 it became clear that there were large variations between the calculated (peak) friction angles (see table 4.20) and the tested maximum minimum p-p friction angles. The reasons for this were unclear. It could be that although the cumulative shear distance was in the order 80 mm after the first test and as much as 180 mm after the sixth test, the residual shear strength had not been reached for some samples with hard joint surfaces.

A further set of rock samples were selected and tested with great care and put through a cycle of four tests to try to determine the shear strength more accurately.

The results of this phase (Phase 3) were tested and evaluated. Correction for the shear angle with the horizontal (as described in paragraph 4.2) from the shear load vs. horizontal displacement graph were made (Appendix J). A maximum, minimum and a general average called "intermediate value" were determined and plotted on a shear stress vs. normal stress graphs. The angle of friction, cohesion and correlation coefficient for the trend line was determined for the forward, reverse and wet tests.

The test results of the third phase are discussed for each sample in the following paragraphs.

4.5.1 Granite 1C

Figure 4.13 is a graph of the shear stress vs. normal stress. The diamonds present the forward test result, the triangles the reverse and the circles the saturated test results. In each case a maximum (blue), minimum (red) and intermediate (yellow) value is presented. The results for Granite 1C are summarised in Table 4.13.

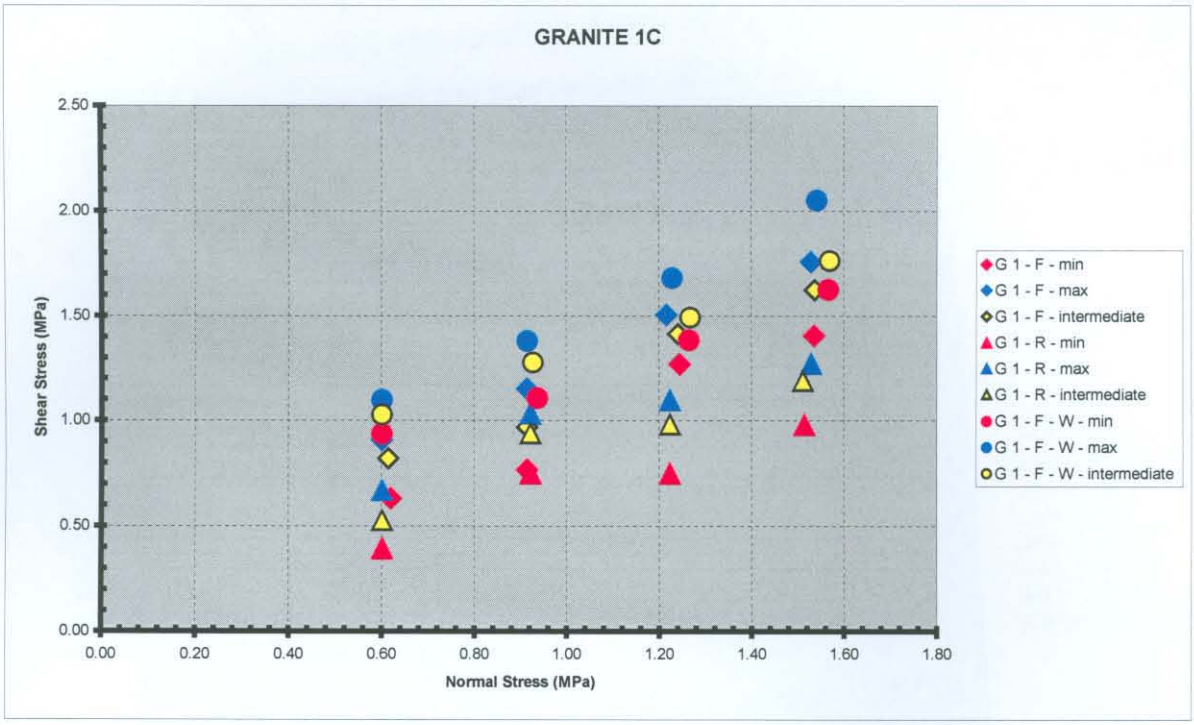

Figure 4. 13 **Shear stress vs. normal stress for Granite 1C**

Shear direction and size	Apparent cohesion KPa	Friction angle Degrees	Correlation coefficient of observation points on normal - vs. shear stress graph
Forward – minimum	228	42,7	0,95
Forward – maximum	333	43,1	0,99
Forward – intermediate	215	42,7	0,97
Reverse – minimum	99	30,3	0,89
Reverse – maximum	369	31,3	0,92
Reverse – intermediate	192	34,0	0,90
Forward (Wet) – minimum	476	35,8	0,99
Forward (Wet) – maximum	471	45,2	1,00
Forward (Wet) – intermediate	575	36,7	1,00

Table 4. 13 **Results of shear testing on Granite 1C**

Discussion

The test in a forward direction yielded an angle of friction of between 42,7 and 43,1 degrees. The value for reverse is approximately 10 degrees lower, between 30,3 and 34 degrees. The value for the saturated sample's minimum and intermediate is between 35,8 and 36,7 degrees. The maximum value of 45,2° is unexpected and no reasonable explanation could be found. The higher values for the forward test can also not be explained.

4.5.2 Granite 2C

Figure 4.14 is a graph of the shear stress vs. normal stress. The diamonds present the forward test result, the triangles the reverse and the circles the saturated test results. In each case a maximum (blue), minimum (red) and intermediate (yellow) value is presented.

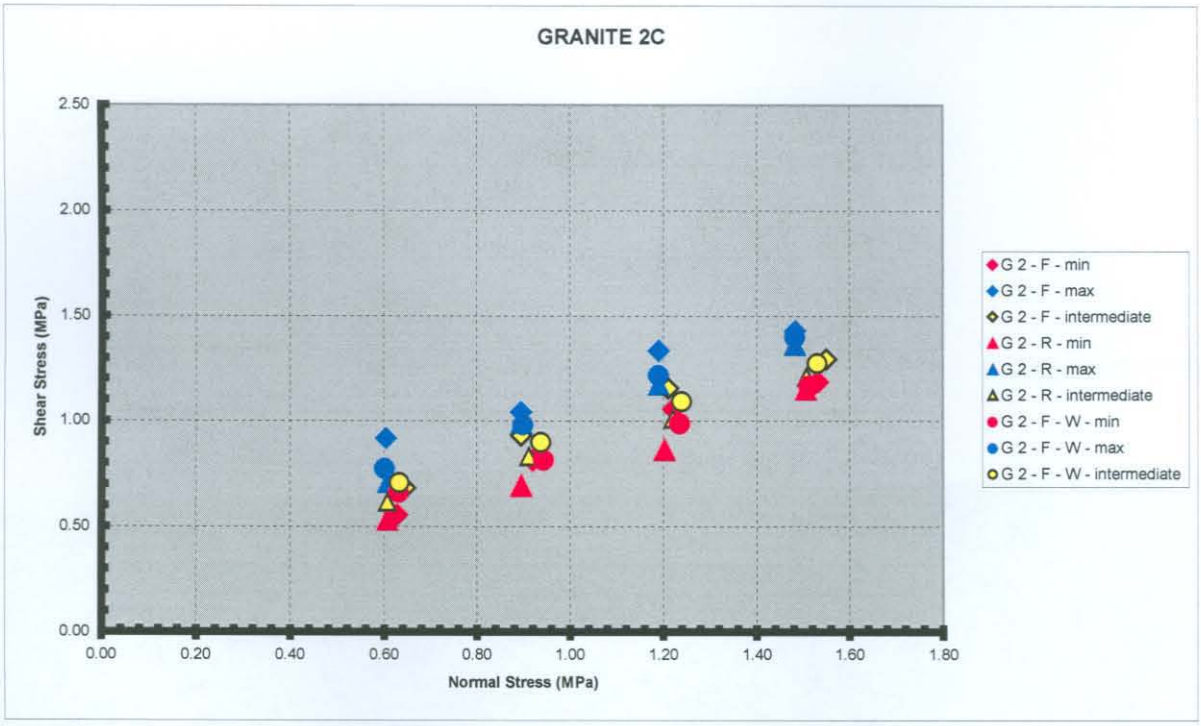

Figure 4. 14 **Shear stress vs. normal stress for Granite 2C**

.

The results for Granite 2C are summarised in Table 4.14.

Shear direction and size	Apparent cohesion kPa	Friction angle Degrees	Correlation coefficient of observation points on normal - vs. shear stress graph
Forward – minimum	145	31,8	0,98
Forward – maximum	536	35,2	0,96
Forward – intermediate	290	34,0	0,97
Reverse – minimum	101	34,0	0,98
Reverse – maximum	297	36,3	0,99
Reverse – intermediate	222	33,2	1,00
Forward (Wet) – minimum	294	29,8	1,00
Forward (Wet) – maximum	350	35,7	1,00
Forward (Wet) – intermediate	309	32,4	1,00

Table 4. 14 **Results of shear testing on Granite 2C**

Discussion

The test in a forward direction yielded an angle of friction of between 31,8 and 34,0 degrees. The value for reverse is approximately the same, between 33,3 and 36,3 degrees. The value for the saturated sample's minimum and intermediate is between 29,8 and 35,7 degrees.

4.5.3 Granite 3C

Figure 4.15 is a graph of the shear stress vs. normal stress. The diamonds present the forward test result, the triangles the reverse and the circles the saturated test results. In each case a maximum (blue), minimum (red) and intermediate (yellow) value is presented.

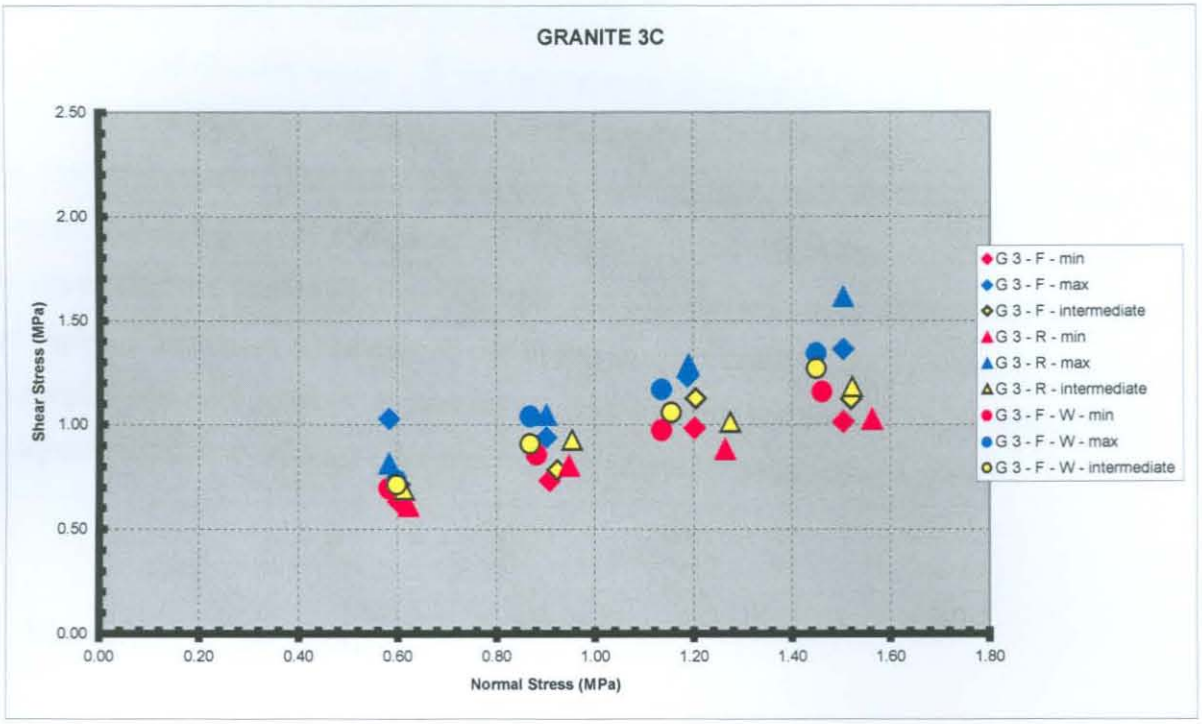

Figure 4. 15 **Shear stress vs. normal stress for Granite 3C**

Shear direction and size	Apparent cohesion kPa	Friction angle Degrees	Correlation coefficient of observation points on normal - vs. shear stress graph
Forward – minimum	355	24,8	0,92
Forward – maximum	705	22,7	0,74
Forward – intermediate	392	27,1	0,84
Reverse – minimum	382	22,8	0,98
Reverse – maximum	290	40,9	0,99
Reverse – intermediate	393	27,1	0,97
Forward (Wet) – minimum	394	27,5	1,00
Forward (Wet) – maximum	376	34,6	0,96
Forward (Wet) – intermediate	339	32,5	1,00

Table 4. 15 **Shear stress vs. normal stress for Granite 3C**

Discussion

The joint surface of Granite 3C was covered by approximately 1 mm of joint fill material. The joint fill comprised of a secondary green mineral, probably chlorite in an unweathered form. The joint surface had prominent striations in the direction of shearing. The test in a forward direction yielded an angle of friction of between 22,8 and 27,1 degrees. The values obtained for the reverse tests were 22,8°, 27,1° and 40,9°. The friction angle of 40,9° is very high and cannot be explained. This test result is regarded as credible as the observations on the Normal stress vs. Shear stress graph gave a coefficient of correlation of 0,9930. The values obtained for the saturated sample's minimum is 27,5° and for the intermediate value 22,8°. This could not be explained.

Ideally, calculated peak friction angles (with Barton's empirical formula) should be compared with tested peak friction angles. When testing rock specimens for shear strength in a large shear apparatus where high normal stresses are applied, only the result of the first shear is a true peak test result. The following cycles of testing take place on a surface damaged by previous testing. To obtain the angle of friction (ϕ) and the cohesion of a joint surface at least three (3), but preferably four (4), tests must be carried out at different normal loads. The angle of friction of a test carried out in this manner can thus not be called a "peak". In this chapter post-peak refers to the results obtained as described above. There is thus merit in the argument of comparing the peak and "maximum post-peak" friction angles.

4.6 Discussion of test results

As part of the research project a comparison was made between the calculated peak shear strength according to Barton and Choubey (1977) and the shear strength during testing.

It can be assumed that the effective normal stress (σ_n) under a concrete dam foundation of moderate size is in the order of 1 MPa or 1000 kPa. This was the reasoning for choosing effective normal stresses of 600, 900, 1200 kPa for testing during the phase 2 and effective normal stresses of 600, 900, 1200 and 1500 kPa during the phase 3.

Roughness was determined with a carpenter's comb and compared with Barton and Choubey's (1977) roughness profiles and the joint roughness coefficient (JRC) was so

obtained. The hardness of joint surfaces was determined with a Schmidt hammer and the joint wall compressive strength (JCS) calculated using Barton and Choubey's (1977) formula.

4.6.1 Discussion of test results of Phase 1 and 2

The contribution to the angle of friction by roughness and hardness was determined by using Barton's formula (paragraph 2.3.1) and subtracting the maximum post-peak value. By adding the basic friction angle to this value, the total peak friction angle can be determined. Table 4.16 presents these results of this calculation for rock types tested for Phase 2 of the investigation.

Rock type	JRC	JCS (MPa)	Calculated peak friction angle Barton (degrees)	Basic friction ϕ_b *(degrees)* Tested values	Calculated contribution of JRC & JCS to friction angle (degrees)
Basalt 1	9	234	56	35	21
Basalt 3	7	188	51	35	16
Dolerite 1	5	163	47	36	11
Granite 1	5	347	44	31	13
Granite 5	9	280	53	31	22
Granite 6	9	280	53	31	22
Granite 7	7	213	47	31	16
Mudstone 1	3	42	36	31	5
Mudstone 2	3	76	37	31	6
Mudstone 3	3	51	36	31	5
Sandstone 1	7	32	41	31	10

Table 4. 16 **Friction angles for rock types as calculated with the Barton and Choubey (1977) empirical equation for shear strength at normal stress σ_n = 1000 kPa.**

The contribution of hardness and roughness of the joint surfaces to the peak friction angle of the joint plane varied between a minimum of 5° and a maximum of 22°. The minimum

values of 5° and 6° are for the Mudstone with smooth and moderately hard joint plane surfaces. The basic friction angle for Mudstone is about 31°. The peak friction angle is thus 36° to 37°. The maximum values of 13° to 22° were found to be that for granite where the joint surfaces were rough and hard. The basic friction angle for Granite is also about 31°. The peak friction angle is thus 44° to 53°.

The calculated peak friction angles were then compared with the maximum post-peak friction angles as determined by testing of joint planes during this study. Table 4.17 presents the results of this comparison. Normally calculated peak friction angles should not be compared with post-peak friction angles. However, in this case they were the maximum values determined with the available specimens.

Rock type	Calculated peak friction angle (Barton) *(Degrees)*	Tested max post-peak friction angle (dry) *(Degrees)*	Difference in friction angle	
			Degrees	*Percentage*
Basalt 1	56	44	-12	-21,4
Basalt 2	56	49	-7	-12,5
Basalt 3	51	38	-13	-25,5
Dolerite 1	47	52,6	+6	+12,8
Dolerite 3 (Clay)	48	17	-	-
Granite 1	44	36	-8	-18,2
Granite 5	53	40	-13	-24,5
Granite 6	53	27	-26	-49
Granite 7	47	35	-12	-25,5
Mudstone 1	36	33	-3	-8,3
Mudstone 2	37	37	0	0
Mudstone 3	36	35	-1	-3
Sandstone 1	41	38	-3	-7,3

Table 4. 17 **Difference between the calculated peak and tested residual friction angles for rock types tested during Phase 2. (Calculated peak friction angle = 100 %)**

It is obvious from Table 4.17 that the differences between calculated and tested maximum post-peak friction angles are small, between 0° and 3° for rock with smooth moderately hard joint surfaces (in this case Mudstone 1, 2 and 3). Greater differences, 7° to 13° were found for rock with very hard and rough joint surfaces (Basalt 1,2 and 3) as well as for Granite (phase 2 testing) where the difference varies between 8° and 26°.
An even greater difference was found for Dolerite 3 (see Table 4.17). A peak friction angle of 48° was calculated but the cycle of three tests gave a minimum post-peak friction angle of 17°. This is because Dolerite 3 had a clay layer as joint fill material for which Barton's equation does not make provision.

The conclusion from this research is that Barton's equation can be used to predict maximum post-peak friction for smooth and moderately hard joint surfaces. Higher friction angles were calculated by Barton's equation than were determined in the laboratory for hard rough joint surfaces. It is generally accepted that Barton's formula is not applicable for filled joints.
The effect of water on the shear strength is demonstrated in Table 4.18 where the tested friction angle (dry) and tested friction angle (submerged) are listed.

Rock type	Tested min p-p friction angle $\phi_{(Dry)}$ *(degrees)*	Tested min p-p friction angle $\phi_{(Saturated)}$ *(degrees)*	Difference between dry and saturated friction angles ϕ *(degrees)*
Basalt 1	44	40	-4
Basalt 2	49	48	-1
Basalt 3	38	37	-1
Dolerite 1	52,6	43,6	-9
Dolerite 3 (Clay)	17	14,9	-2,1
Granite 1	35,8	28,8	-7
Granite 5	40,0	37,5	-2,5
Granite 6	27,1	24,9	-2,2
Granite 7	35,3	28,2	-7,1
Mudstone 1	32,8	22,6	-10,2
Mudstone 2	37	14,6	-22,4
Mudstone 3	35,2	13,2	-22
Sandstone 1	37,6	40,5	+2,9

Table 4. 18 **Difference between dry and saturated friction angles**

The effect of water on the friction angles of different rock types is illustrated in Table 4.19. From this table it is evident that as can be expected, rock types with hard, rough joint surfaces are only slightly influenced by the presence of water as far as friction angles are concerned. This is especially true for Basalt (with JRC = 7 - 9 and JCS = 188 - 234 MPa) where the difference between dry and submerged is between 1 and 4 degrees.

The influence of water is the greatest on friction angles of smooth moderately hard joint surfaces JRC = 3 and JCS = 43 - 76 MPa where the differences between dry and saturated is 10,2 degrees for Mudstone 1 and 22 to 22,4 degrees for Mudstone 2 and 3.

The friction angles for clay filled joints is affected by water. The friction angle of a clay filled joint tested for Dolerite 3 is as low as 17°. Submerged in water it falls to 14,9°.

4.6.2 Discussion of test results of Phase 3

To confirm the results obtained in phases 1 and 2, it was decided to investigate a further set of rock samples with great care and through four cycles of testing to try to determine the shear strength more accurately. The test method employed is described on page 3.18 of this thesis. The test results are presented in Table 4.19.

Rock type	JRC	JCS (MPa)	Calculated peak friction angle Barton (degrees)	Basic friction ϕ_b (degrees)	Calculated contribution of JRC & JCS to friction angle (degrees)
Granite 1C	7	185	46,9	31	15,9
Granite 2C	5	190	42,4	31	11,4
Granite 3C	11	205	56,4	31	25,4

Table 4. 19 **Friction angles for Granite as calculated with the Barton and Choubey (1977) empirical equation for shear strength at normal stress σ_n = 1000 kPa**

From Table 4.19 it is evident that all three granite samples had the different roughness profiles. The JRC values ranged form 5 to 11. The joint compressive strengths were very much the same, in the order of 200 kPa. The contribution of these two characteristics to the friction angle in all three examples is given in Table 4.19. The calculated contribution was between 11,4° and 25,4°. However, the tested intermediate minimum post-peak friction angle was between 4,2° for Granite 1C; 8,4° for Granite 2C and 29,3 lower than the calculated peak angle of friction. The tested angle of friction is lower than the calculated peak for Granite 3C with joint fill material present. See Table 4.20 for this information.

Rock type	Calculated peak friction angle (Barton) *(degrees)*	Tested maximum post-peak friction angle (dry) (by testing – intermediate) *(degrees)*	Difference in friction angle	
			Degrees	*Percentage*
Granite 1C	46,9	42,3	-4,2	-10
Granite 2C	42,4	34,0	-8,4	-25
Granite 3C	56,4	27,1	-29,3	-108

Table 4. 20 **Difference between the calculated peak and residual friction angles for Granite tested during Phase 3 (Percentages calculated in relation to calculated peak)**

The influence of water on the residual friction angle is shown in Table 4.21. From this table it is evident that water saturated joints have a negative effect on the friction angle. This influence is between 1,6 and 6 degrees. However, during testing of granite 3C (with a secondary mineral as joint fill material) it was found that the presence of water had a positive effect on the angle of friction. The minimum post-peak angle of friction in a saturated state was 5,4° higher than the dry residual friction angle.

Rock type	Tested post-peak friction angle ϕ *(Dry)* *(degrees)*	Tested post-peak friction angle ϕ *(Saturated)* *(degrees)*	Difference between dry and saturated friction anglesϕ *(degrees)*
Granite 1C	42,7	36,7	-6
Granite 2C	34,0	32,4	-1,6
Granite 3C	27,1	32,5	+5,4

Table 4. 21 Difference between dry and saturated friction angles of Granite samples tested

4.7 Relationships investigated.

4.7.1 The relationship between shear displacement and joint roughness.

In theory, it is expected that there should be a relationship between the cumulative shear displacement and residual joint roughness. The farther a joint surface is sheared along a joint plane the smoother that plane becomes as a result of abrasion. If a joint surface is sheared far enough, it should theoretically become a smooth plane (with a residual friction angle equal to the basic friction angle – as described by Rengers envelope) That is if the normal stress is high enough or the joint wall material is so soft that all asperities are sheared. If the asperities are overridden this will not be the case, as part of the sheared asperities will determine the shear strength, probably by rolling, ect. The normal stress acting on the joint plane also has an influence on the distance a joint surface can move before abrasion has removed all asperities and reduced the surface to smooth plane. The higher the normal stress (for a given rock hardness) the shorter the shear displacement. This relationship can be expressed as JCS/σ_n. Where normal stresses are very low, $JCS/\sigma_n > 1000$ and where normal stresses are very high $JCS/\sigma_n \leq 1$.

This principle is presented in Figure 4.16

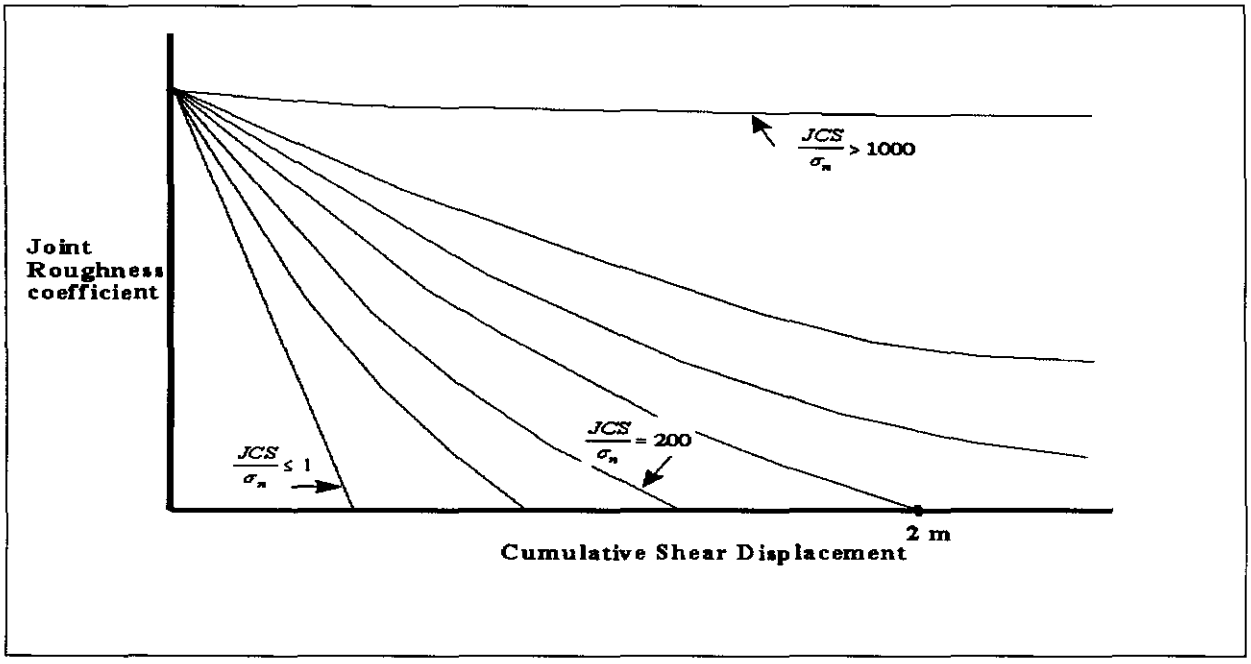

Figure 4.16 **The theoretical relationship between joint roughness coefficients and shear displacement.**

Under high normal stresses (σ_n) shear will normally take place through intact rock material (asperity), whereas for low normal stresses (σ_n) asperities will be overridden and not be damaged or be slightly damaged.

The relationship between joint roughness (in this case JRC was used) and shear displacement was investigated during this study. The influence of high normal stresses were not taken into consideration as testing was limited to normal stresses of maximum 1 MPa.

Figure 4.17 is a representation of Joint Roughness Coefficient (JRC) vs. cumulative shear displacement as determined for the three granite samples tested.

The JRC for each consecutive shear was determined by visually comparing the joint roughness profile as determined with the laser apparatus (as described in chapter 3) with Barton's (1971) joint roughness profiles and assigning a JRC value to each profile. A copy of each profile created by laser measurements was produced on an transparency and put on top of profiles prepared by Barton (1977) and compared visually. The measured JRC valves for Granite 1A, 1B and 1C deteriorated form 8 to 6, 6 to 4 and 12 to 10 respectively.

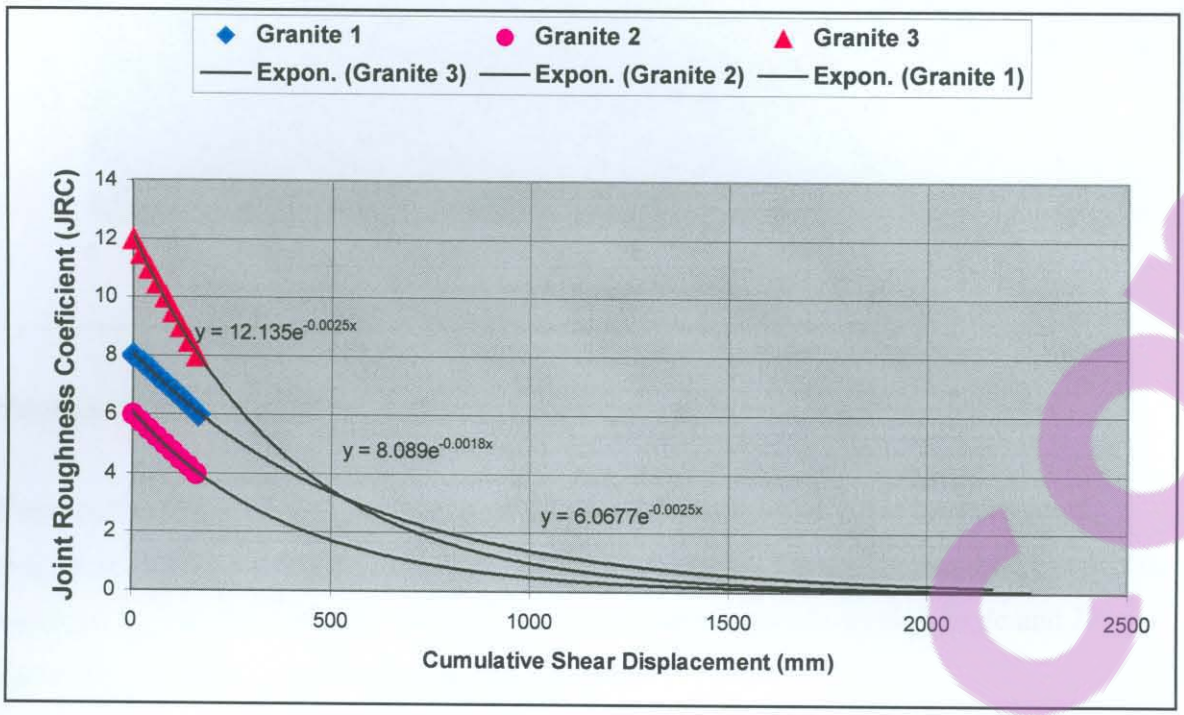

Figure 4.17 **Relationship between JRC and cumulative shear displacement.**

The deterioration of joint roughness of each of the three granite samples were measured visually, with an overlay on Barton's roughness profiles and the JRC value for each consecutive shear determined. The JRC values of each granite sample was the plotted vs. the cumulative shear displacement. An exponential regression was fitted to the points plotted on Figure 4.17. From this figure it can be seen that at the applied normal stress levels a cumulative shear displacement of more than 2,0 meter will be required to make the joint surface smooth as a result of friction. Only then will the friction angle be equal to the true residual or basic friction angle.

Conclusion: From the JRC / Cumulative shear displacement graphs it should be possible to predict the deterioration in joint roughness for different distances of shear displacement at specified levels of normal stress.

4.7.2 The relationship between friction angle and joint roughness.

From a theoretical point of view there should be a relationship between friction angle and joint roughness. This relationship was investigated for the all rock types tested during this project and included the peak and basic friction angles.

Figure 4.18 is a plot of JRC vs. Friction angle.

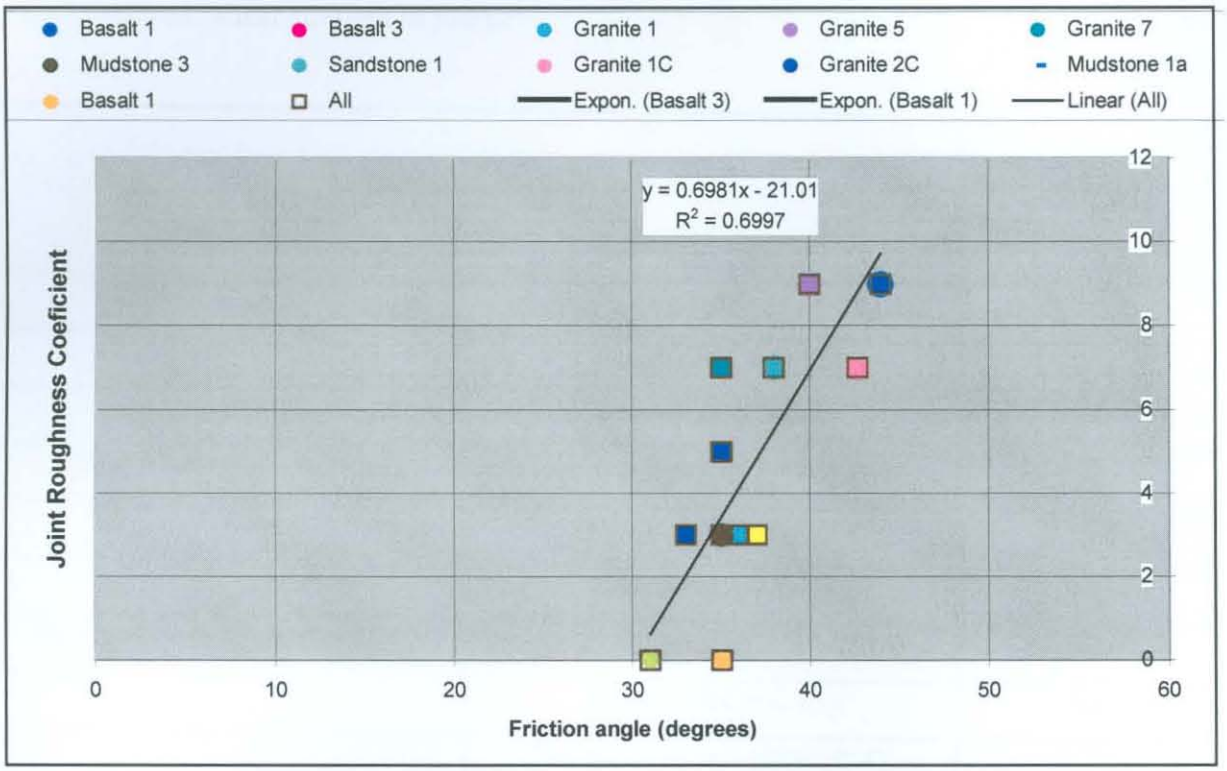

Figure 4.18 Graph of JRC vs. friction angle

Conclusion: A reasonable correlation (with a confidence limit of 70%) between joint roughness and friction angle exists for the rock types tested. The rock types tested varied in hardness, origin, structure and strength. The relationship between friction angle and JRC under dry conditions can be expressed as follows:

$$\phi = \phi_b + f\,(JRC) \qquad \text{where } \phi_b = 30° \qquad \ldots\ldots\ldots\ldots\ldots\ldots \quad (4.1)$$

f = is the slope of the line = 1,43

The graph can be used to estimate the friction angle (dry) when the joint roughness coefficient (JRC) is known. In practice this means that a rock mechanics practitioner can measure joint surface roughness on site with a carpenters comb, determine the joint roughness coefficient (JRC) with Barton's (1977) joint roughness profiles and use equation 4.1 to estimate the friction angle of the joint surfaces.

4.7.3 Field estimation of shear strength of joint surfaces in rock

An experienced engineering geologist or rock mechanics practitioner should be able to estimate the hardness (according to Table 5.1) and roughness (Figure 2.9) of a joint surface in the field. He or she would also be able to measure waviness of continuous joints. From these parameters together with the basic friction angle the peak friction angle can be estimated.

The shear strength of Patton's saw-tooth specimens is represented by:

$$\tau = \sigma_n \tan (\phi_b + i) \quad \ldots\ldots\ldots\ldots\ldots\ldots\ldots\ldots (2.10)$$

where ϕ_b is the basic friction angle of the surface and i is the angle of the saw-tooth face.

The basic friction angle for any rock material can be determined from Table 2.2 or Table 4.1. The angle of friction of the saw tooth face is determined by the hardness and roughness of the surface. From work done during this research the following guidelines (rule of thumb) can be used to estimate shear strength of joints:

Surface characterization		*i* value
Hardness	Roughness	
Very hard (> 200 MPa)	Very rough (JRC= 14-20)	8°-13°
	Rough (JRC= 6-12)	0°-9°
	Smooth (JRC=0-4)	5°
Hard (100-200 MPa)	Very rough (JRC= 14-20)	Na
	Rough (JRC= 6-12)	2°-16°
	Smooth (JRC=0-4)	Na
Moderately hard (50-75MPa)	Very rough (JRC= 14-20)	Na
	Rough (JRC= 6-12)	Na
	Smooth (planar) (JRC=0-4)	4-7°

*Na – not available

Table 4.22 **Estimation of *i* value contribution to angle of friction**

When this calculated data of the rock types tested in the laboratory are used to plot angle of friction due to surface characteristics (i.e. hardness and roughness) vs. JRC, the result is Figure 4.1.

The results of the laboratory shear testing does not appear to give satisfactory results. For that reason it was decided to use Barton's (1977) empirical formula (2.11).

$$\tau = \sigma_n \tan [JRC \log_{10} (JCS/\sigma_n) + \phi_b] \ldots\ldots\ldots\ldots (2.11)$$

Where τ = peak shear strength σ_n = effective normal stress

JRC = joint roughness coefficient JCS = joint wall compressive strength

ϕ_b = basic friction angle (obtained from residual shear tests on flat unweathered rock surfaces)

The contribution of roughness and hardness are presented in the following part of the formula: $JRC \log_{10} (JCS/\sigma_n)$ ..... (4.2)

This formula was used to calculate the contribution of the hardness (JCS) in terms of Uniaxial Compressive Strength (UCS) vs. the roughness (JRC). The roughness (JRC) was use as values between 1 and 20 and the UCS values from 50 to 350 MPa in multiples of 50.

If it is accepted that σ_n = 1 MPa (equal to the stresses normally associated in the foundations of dams and other civil engineering structures) then the value of *i* can be calculated for different JRC vs. JCS values and a graph be drawn as shown in Figure 4.19

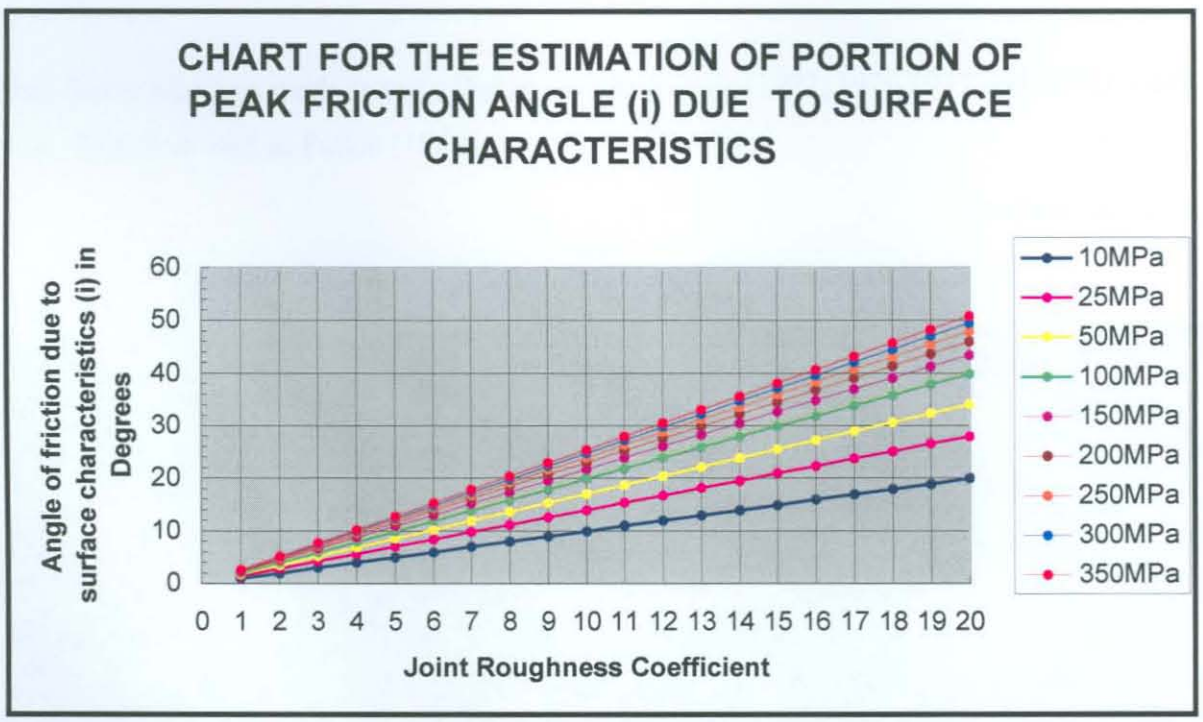

Figure 4.19 **Chart for the estimation of peak friction angle (*i*) due to surface characteristics, for σ_n = 1 MPa**

Any experienced engineering geologist or rock mechanics engineer can now estimate [by estimating (or measuring) in the field] the JRC and the JCS (in terms of UCS) of a joint surface and by using this chart, determine the contribution of the surface characteristics (medium scale roughness) to the angle of friction.

The contribution of waviness could contribute further to the value of *i*. The contribution of this component could be determined by using Hack, et. al.'s (2002) large scale roughness (waviness) profiles. It is especially applicable to large-scale foundations as for dams. Table 4.23 could be used to determine the contribution of waviness to the shear strength of large surfaces.

Large scale roughness (waviness)	Amplitude	Shear strength contribution in degrees
Straight	0 cm	0°
Slightly curved	1,5 – 3,5 cm	2° – 4°
Curved	3,5 – 7 cm	4° – 8°
Slightly wavy – wave length ±1 m	5 – 9 cm	9° - 14°
Wavy – wave length ± 0,5m	5 – 9 cm	14° - 20°

Table 4.23 Shear strength contribution due to large-scale roughness (waviness) – (After Hack et. al. , 2002)

By adding the basic friction angle (from Fable 4.1) to this value, the total friction angle, is obtained.

$$\phi_t = \phi_b + i_a + i_w \quad \text{.....4.3}$$

where ϕ_t = total friction angle and ϕ_b = basic friction angle,

i_a = the angle of the asperity (saw-tooth face, Patton, 1966) and

i_w = is the angle of the waviness (Hack et. al., 2002)

The research has shown that this simple tool will be of use to engineering geologists and rock mechanics practitioners who require a rapid method to determine the angle of friction of a joint surface in the field.

This tool is based on work done by Barton and co-authors (1972, 1976,1977 and 1991), Hack et. al. (2002) as well as Patton (1966).

4.7.4 The influence of true cohesion, rock bridging and waviness on shear strength

Barton and Choubey (1977) does not take into account:

(i) the presence of discontinuity filling with true cohesion (c_t)

(ii) rock bridging (c_b)

(iii) the effect of waviness resulting in change of direction (i)

Van Schalkwyk (1999) therefore suggested that the equation be written as follows:

$$\tau = c_t + c_b + \sigma_n \tan [JRC \cdot JMC \cdot \log_{10}(JCS/\sigma_n) + \phi_b + i]$$

Where: τ = peak shear strength; σ_n = effective normal stress; *JRC* = joint roughness coefficient; *JCS* = joint wall compressive strength; ϕ_b = basic friction angle; JMC = joint matching coefficient; c_t = true cohesion (fill); c_b = bridging strength; i = effect of waviness resulting in change of direction

Where fill is present on a joint surface, the fill thickness is of great importance. It is postulated that there is a relationship (FTC) between fill thickness JRC which has a value between 0 – 1.

For filled joints the modified Barton & Choubey equation becomes:

$$\tau = c_t + c_b + \sigma_n \tan [JRC \cdot JMC \cdot (1\text{-}FTC) \log_{10}(JCS/\sigma_n) + (1+FTC)\,\phi_b + (FTC \cdot \phi_f) + i]$$

Where: τ = peak shear strength; σ_n = effective normal stress; *JRC* = joint roughness coefficient; *JCS* = joint wall compressive strength; ϕ_f = friction angle of fill; JMC = joint matching coefficient; c_t = true cohesion (fill); c_b = bridging strength; i = effect of waviness resulting in change of direction; FT = Fill thickness in mm; FTC = -0,07 ln (JRC+1/FT+1) + 0,5; ϕ_b = basic friction angle of rock

4.8 Further research and conclusion

This research has provided the framework within further research can be undertaken. The infrastructure is now available in South Africa to investigate the following:

The relationship between shear displacement and joint roughness should be investigated further. Testing should be carried out with low (1 MPa) to High (10 MPa) normal stresses. This could provide a graph the relationship of joint roughness (JRC) vs. shear displacement.

The relationship between fill thickness, joint roughness and shear strength should be investigated further.

This study contributes to the knowledge of shear strength on southern African rock types, in particular on the sampling of specimens, preparation of specimens for testing in the large shear apparatus, the measurement of the roughness and hardness of the joint surface, the testing procedure and the interpretation and application of the results. To a lesser extent the study provides typical values of the shear strength characteristics of the rock joints.

CHAPTER FIVE
CLASSIFICATION OF SHEAR STRENGTH OF JOINTS IN ROCK

5.1 Introduction

The shear strength of joint surfaces in a rock mass is a difficult parameter to determine. Several researchers, including Amadei and Seab (1990), Barton and Choubey (1977), Goodman (1976), Nicholson (1983) and others have investigated this problem. The shear strength parameters of joints in a rock mass are affected by a number of factors as described in chapter two. To simulate these factors in a laboratory is virtually impossible and in this study only the most important factors have been considered.

Geotechnical characteristics of joint surfaces in a rock mass can be described in terms of hardness, roughness filling and water considerations. Sampling and testing of these joints is difficult and time consuming. Design engineers usually need an estimate of the shear strength of joints early during the design stage of a structure in a rock mass. If the shear strength could be linked to a geotechnical description of the joints, then a first estimate of the shear strength could be made which would satisfy the immediate need of the design engineer. This research concentrated on classifying joints in order to estimate the shear strength of joints at the early stage of an investigation. The findings are discussed in this chapter. This chapter contributes to the existing knowledge of shear strength by describing the results of shear tests on a number of southern African rock types tested on the large shear machine described in chapter four. The rock types used for the investigation were Basalt, Dolerite, Granite, Mudstone and Sandstone.

The major factors influencing shear strength are:

(i) hardness of the joint surface

(ii) roughness of the joint surface

(iii) the influence of water

(iv) the effects of joint fill material

An attempt was made to estimate the shear strength parameters by describing geotechnical properties of the joint surface, including hardness, roughness, joint fill material present and the presence of water. These factors were correlated with the shear strengths measured during large scale shear testing.

A correlation between the calculated peak angle of friction and the tested angle of friction was made for each of the rock types tested. The method described by Barton and Choubey (1977) for calculating the empirical relation of shear strength of joints in rock is as follows:

$$\tau = \sigma_n \tan [JRC \log_{10} (JCS/\sigma_n) + \phi_b]$$

where

	τ	=	peak shear strength (kPa)
	σ_n	=	effective normal stress (kPa)
	JRC	=	joint roughness coefficient
	JCS	=	joint wall compressive strength (kPa)
	ϕ_b	=	basic friction angle (obtained from residual shear tests on flat unweathered rock surfaces) (degrees)

From this relation it is apparent that there are three important factors determining the shear strength of joints in rock.

They are:

(i) the basic friction angle of the rock material

(ii) the joint roughness (JRC)

(iii) the joint wall compressive strengths (JCS)

The following portion of the formula used above can express the contribution of roughness and hardness of the joint surface to the peak friction angle:

$$[JRC \log_{10} (JCS/\sigma_n)]$$

5.2 Classification of joints according to this study

In order to classify joint surface characteristics it was necessary to investigate work done on unconfined compressive strength (Deere and Miller,1966), joint wall compressive strength (Barton and Choubey, 1977) and joint roughness (Barton and Choubey, 1977).

5.2.1 Classification of joint wall compressive strength

The value of the joint wall compressive strength (JCS) is of fundamental importance in the determination of rock slope stability since it is largely the thin layer of rock adjacent to the joint wall that controls the shear strength. This parameter can be determined using a Schmidt Hammer. The relationship between the Schmidt rebound number and the unconfined compressive strength is discussed in chapter two of this thesis. The UCS is used if the joint wall has no alteration. Miller (1965) found a reasonable correlation between the rebound number and unconfined compressive strength. The unconfined compressive strength (UCS) classification of rock material by Deere is displayed in Table 5.1.(Deere and Miller,1966)

Rock classification	Unconfined compressive strength (UCS)	Rock type
Very weak rock	1 – 25 MPa	-
Weak rock	25 – 50 MPa	-
Moderately hard rock	50 – 100 MPa	Mudstone, Sandstone
Hard rock	100 – 200 MPa	Basalt
Very hard rock	> 200 MPa	Dolerite, Granite

Table 5.1 **Classification of intact rock strength (Deere and Miller, 1966)**

5.2.2 Classification of roughness profiles

The roughness profile is another fundamental parameter in the determination of shear strength. Table 2.4 (after Barton and Choubey, 1977) of roughness profiles with associated JRC values was used as guide to roughness profiles.

5.3 Shear strength classification based on roughness and hardness of joint surfaces.

5.3.1 Joints in hard rock filled with clayey material of more than 2 mm thickness

In the case where joints are filled with a secondary mineral or soft fill material, the peak shear strength cannot be determined by the empirical formula of Barton and Choubey (1977).

Joint description

During the testing programme a Dolerite sample was tested. The Dolerite material was hard and the joint filled with completely weathered (residual) doleritic material. The joint fill material was more than 2mm thick.

Test results

The results are illustrated in Table 5.2 below.

Characteristic	Dolerite (Phase 2)
Measured dry min. post-peak friction angle	17,0°
Measured saturated min. post-peak friction angle	14,9°

Table 5. 2 Friction angles of clay filled joint in hard rock (dolerite)

Discussion of results

In this case the joint fill material (a 2 mm thick layer of clay) resulted in a maximum post-peak friction angle much lower than the basic friction angle of the rock. The basic friction angle is 36°. The measured maximum post-peak friction angle was tested as 17,0° and the saturated post-peak friction angle as 14,9°.

Conclusion

For filled joints in moderate to hard rock or joints in soft rock, the following conclusions can be made:

(i) the basic friction angle of the rock material is **not** the minimum friction angle of a filled joint.

(ii) the dry minimum post-peak friction angle is much lower than the basic.

(iii) the angle of friction is affected negatively by the presence of water if the infill consists of clay.

5.3.2 Joints in hard to very hard rock with stained joint surfaces

Joint description

Joints in granite (Granite 2C) were tested. These joints were in hard to very hard rock and the joint surfaces were stained, presumably with iron staining.

Test results

The results of empirical calculations as well as test results are shown in Table 5.3.

Characteristic	Empirical value Peak	Tested value
Basic friction angle		31°
JRC $\log_{10}$ *(JCS/*σ_n*)*	12°	
Peak or max. p-p angle of friction	43°	35,2°
Min. post-peak angle of friction		31,8°
Min. post-peak angle of friction (saturated)		29,8°

Table 5. 3 **Friction angles of joints in hard to very hard rock with stained joint surfaces (Granite 2C)**

Conclusions

The following conclusions could be made for unfilled joints and joints that are lightly stained in hard rock:

(i) the basic friction angle is the minimum friction angle of a particular joint

(ii) the contribution of the roughness and hardness of the joint can be added to the basic friction angle to obtain a design parameter.

(iii) the angle of friction is not significantly affected negatively by the presence of water.

(i) the max. post-peak is considerably lower than the calculated peak.

5.3.3 Smooth, planar, bedding joints with unweathered surfaces in moderately hard rock

Joint description

Joints consisted of smooth planar bedding joints with unweathered surfaces in a moderately hard mudstone.

Results

The results of empirical calculations as well as test results are shown in Table 5.4.

Characteristic	Empirical value	Tested value
Basic friction angle		31°
JRC $\log_{10}$ *(JCS/*σ_n*)*	4,5°	
Max. post-peak angle of friction	35,5°	34,9°
Min. post-peak angle of friction (saturated)		16,8°

Table 5.4 **Friction angle of smooth, planar, bedding joints with unweathered surfaces in moderately hard rock (Mudstone)**

The tested angle of friction of the three samples is between 37,0° and 32,8° with an average of 34,9°. The calculated peak friction angle is between 35,3° and 35,8° with an average of 35.5°. There is a difference of less than one degree between the calculated and the tested value of the peak friction angle.

There is a marked difference between the angle of friction determined under dry conditions and that of under saturated conditions. For Mudstone 1 the difference is 10°. For Mudstone 1 and 2 the difference is even greater namely 22° and 22,4° respectively.

The influence of water on the shear strength (angle of friction) of mudstone was larger than expected and this phenomenon should be taken into consideration in the design of dams on mudstone.

Conclusions

(i) The empirical formula developed by Barton and Choubey (1977) to calculate peak angle of friction was found to be applicable to the rock type tested in this case under dry conditions.

(i) The influence of water on the shear strength (angle of friction) of mudstone was larger than expected and this phenomenon should be taken into consideration in the design of dams on mudstone.

5.3.4 Rough, planar, unweathered surfaces in hard rock

In a rock mass where joint surfaces are characterised by moderate to high joint roughness coefficient values (JRC above 6 according to Barton and Choubey, 1977) and high joint wall compressive strength values (UCS above 100 MPa), the shear strength is determined by these characteristics. The peak shear strength can be calculated using Barton and Choubey's empirical formula (1977). In essence the peak angle of friction consists of the basic friction angle plus the contribution of the hardness and roughness.

Joint description

Unweathered joints in hard rock (Granite) were investigated. The joints were rough and planar.

Results

Results are shown in Table 5.5.

Characteristic	Empirical value By Barton	Tested value
Basic friction angle	-	31°
$JRC \log_{10} (JCS/\sigma_n)$	10°	-
Max. post-peak angle of friction	41°	43,1°
Min. post-peak angle of friction	-	37,0°
Min post-peak angle of friction (saturated)	-	27,5°

Table 5.5 **Friction angle of rough, planar, tectonic, unweathered surfaces in hard rock (Granite 1C)**

Discussion of results

The tested maximum post-peak and calculated peak friction angle for the specimen are almost the same. The effect of water is that the friction angle under saturated conditions is about 10° lower than under dry conditions.

Conclusion

(i) In hard rock with relatively rough surfaces the calculated peak friction angle is much the same as the tested maximum post-peak value.

(ii) The influence of water on the angle of friction is relative large, in this case almost 10°.

5.3.5 Rough, irregular joints in unweathered hard rock (Basalt, Dolerite)

Two hard to very hard rock types were investigated that had rough, irregular joints. Basalt has a unconfined compressive strength in the order of 160 MPa and Dolerite 260 MPa.

Joint description

The joint surfaces of Basalt samples tested were rough, irregular with a JRC of between 6 and 10. The Schmidt rebound number was between 53 and 57. The joint surfaces of Dolerite samples tested were rough, irregular with a JRC of between 4 and 8. The Schmidt rebound number was between 46 and 51.

Results

Tables 5.6 and 5.7 are summaries of the results of Basalt and Dolerite respectively.

Characteristic	Empirical value By Barton	Tested value
Basic friction angle	-	35 - 38°
$JRC \log_{10} (JCS/\sigma_n)$	14°	-
Max. post-peak angle of friction (dry)	49°	44,0°
Min. post-peak angle of friction (saturated)	-	42°

Table 5.6 **Friction angle of rough, irregular, joints in unweathered hard rock (Basalt)**

Characteristic	Empirical value By Barton	Tested value
Basic friction angle	-	36°
JRC $\log_{10}$ *(JCS/*σ_n*)*	11°	-
Max. post-peak angle of friction (dry)	47°	52,6°
Min. post-peak angle of friction (saturated)	-	43,6°

Table 5.7 **Friction angles of rough, irregular, joints in unweathered hard rock (Dolerite)**

Discussion of results

The peak calculated and tested maximum post-peak values of angle of friction are very high namely 49° and 44° for Basalt and 47° and 52,6° for Dolerite respectively. The minimum post-peak friction angles for both rock types are also very high namely 42° and 43,6° respectively.

Conclusions

(i) The peak shear strength of joints in rock with rough and hard joint surfaces are very high.

(ii) The minimum post-peak shear strength under saturated conditions are also very high. Water has little effect on the friction angle of hard and rough joints.

5.4 Proposed classification of joints according to roughness and hardness.

Table 5.8 is a proposed classification of joints according to roughness and hardness as determined during this study.

Joint description	Peak angle of friction Calculated	Max. post-peak angle of friction Tested	Min. post-peak angle of friction Saturated
1. Joint in hard rock filled with clayey material of 2mm thickness	-	-	14,9°
2. Joints in hard rock with stained surfaces	43°	35,2°	29,8°
3. Smooth, planar, bedding joints with unweathered surface	35,5°	34,9°	16,8°
4. Rough, planar, joints with unweathered surfaces	41°	43,1°	27,5°
5. Rough, irregular, with unweathered surfaces	46- 49°	44 – 52,6°	42 – 43,6°

Table 5.8 **Classification of joints according to roughness and hardness of joint surfaces.**

5.5 Application of shear strength in the design of concrete dam foundations

In the design of the stability of a concrete dam foundation the design must include parameters for even the worst possible situations. This includes joint sets with unfavourable dip, full water uplift pressure acting on joint surfaces and the maximum force on the concrete structure as a result of water in the reservoir at maximum overflow conditions.

Important parameters used in the design of concrete dam foundations include the following:

- the orientation of important joint sets in the rock foundation
- the shear strength of joints in the rock mass
- the direction and magnitude of the forces acting on the rock foundation as a result of:

(i) the concrete structure

(ii) the water in the reservoir

(iii) the uplift pressure of the water

(iv) external forces (e.g. Seismic)

Instability can occur as a result of sliding of the concrete structure along an unfavourable joint set with insufficient shear strength or rotation of the concrete structure around the toe of the structure. The design of every structure including the foundation as part of the structure should be treated separately and investigated in detail.

CHAPTER SIX
CONCLUSIONS AND RECOMMENDATIONS

6.1 The objectives of this research project were to determine and to analyze the shear strength of joints in a number of rock types, sampled at different locations. The objective was also to link these strengths to the conditions of the foundations and in particular the condition of the surfaces of the rock joints. The information so obtained can then serve as a data bank for the design of new dams and for the evaluation of the safety of existing dams. The results were obtained for a number of rock types, including dolerite, granite and mudstone and to some extent for basalt and sandstone

6.2 A comprehensive literature study was conducted and it showed that although engineering characteristics of rock material are investigated on a continuous basis for civil and other engineering applications, this information is not readily available to the engineering community because clients and contractors regard it as confidential information. This thesis is a source that describes the shear strength characteristics of southern African rock types available today.

6.3 The emphasis was placed on the shear strength of discontinuities in rock. The basic shear strength parameters of the different rock materials were determined as part of the determination of rock material characteristics. The angles of friction obtained for the different materials correspond very well with those in the literature.

6.4 It was also envisaged to determine the peak and residual shear strength parameters of important southern African rocks. To achieve this objective the Department of Water Affairs and Forestry, in association with a technical subcommittee of the Water Research Commission, had a large shear box apparatus built that was used for the testing of large specimens as well as rock fill material for this project. This thesis describes the design and construction of the apparatus, the test method, the results as well as the interpretation and application of shear testing on large specimens.

6.5 It was impossible to determine the true peak and residual shear strength due to practical limitations. Peak values are therefore approximated by determining the "maximum post-peak" strength, whilst residual values were approximated by "minimum post-peak" values.

6.6 The testing of the specimens with the large shear box apparatus was conducted in three phases. During the first phase the "maximum post-peak" shear strength parameters were determined under dry conditions. The second phases (2A and 2B) involved determination of the "minimum post-peak" shear strength parameters under dry and submerged conditions and the third phase (granite) a record of the polishing effect after repeated testing of three granite samples under dry and submerged conditions. The same specimens were used through phases 1, 2A and 2B.

6.7 The first phase was carried out between 28 September 1995 and 10 June 1996. It was intended to determine the peak shear strength parameters during this phase. This phase of testing consisted of three cycles of shear testing under increasing normal stress. Normal stresses for the testing were in the order of 600, 900 and 1200 kPa.

6.8 Evaluation of the test results of the first phase revealed certain problems. The shear load vs. shear displacement graphs was difficult to interpret. Further detailed investigation discovered a problem with the software controlling the shear- and normal load actuators. It was found that at the start of the shear test, the normal and shear loads increased simultaneously. The normal load should have been at a set maximum before the shear load was applied.

6.9 Before the second and third phases the shear apparatus was inspected and all the bolts and LVDT's were fastened properly. The software used to drive the apparatus was scrutinised to ensure correct instruction during testing.

6.10 The second and third phases were carried out between 25 March 1998 and October 2000. The aim was to determine the residual shear strength parameters during this phase. These tests were conducted under dry and submerged conditions. Each phase of testing consisted of three cycles of shear testing under increasing normal stress.

Normal stresses for the testing were in the order of 600, 900 and 1200 kPa for Phase 2 and 600, 900, 1200 and 1500 kPa for Phase 3.

6.11 The results showed that the shear strength parameters of joints in rock are mainly influenced by (i) the hardness and (ii) the roughness of the joint surfaces. Both these parameters were measured during the study. The hardness of each joint surface was determined with a Schmidt hammer and related to the uniaxial compressive strength as reported by Barton and Choubey, 1977.

6.12 As part of this research project a three-dimensional laser-scanning device was developed. The Department of Civil Engineering of the University of Natal was commissioned to build this apparatus to measure the roughness of joint surfaces. This device measures x, y and z co-ordinates on a rock joint surface on a grid pattern. This information can be manipulated with software on a computer to produce a contour diagram of the joint surface area. From this joint roughness profiles can be obtained.

6.13 A third phase of investigation was undertaken to determine the validity of the test results during the second phase of testing. This was the final phase and concluded the project during October 2000. Three Granite samples were tested in detail. Every sample was tested in a forward as well as reverse direction. Tests were also carried out with the sample saturated. Four normal loads were applied to have four observation points on the graph. It was concluded that although problems were encountered during the second phase of testing, the results obtained can now be used with confidence.

6.14 Emphasis was placed on the shear strength parameters of joints, especially the angle of friction. Two types of joints are recognised in nature: (a) joints with no or little fill material where the shear strength is strongly influenced by the characteristics of the rock material and (b) joints with fill material where the shear strength is determined by the characteristics of the fill material. The major part of this research concentrated on (a) joints with no or little fill material. The three major characteristics determining the shear strength parameters of this type of joint are (i) the base shear strength of the rock material, (ii) the roughness profile along the joint surface and (iii) the hardness of the material on the joint surface.

6.15 A classification system for joints in terms of hardness and roughness were developed. The classification system is described in Table 5.20

6.16 The relationship between joint roughness (in this case JRC was used) and shear displacement was investigated during this study. The influence of high normal stresses were not taken into consideration as testing was limited to normal stresses of maximum 1 MPa. An exponential regression was fitted to the points plotted. After a cumulative shear displacement of more than 2,0 meter will the joint surface be smooth as a result of friction. Then only will the friction angle be equal to the residual friction angle.

6.17 A reasonable correlation (with a confidence limit of 70%) between joint roughness and friction angle exists for the rock types tested. The rock types tested varied in hardness, origin, structure and strength. The conclusion that can be made from this is that rough joints have higher friction angles, with a minimum (basic) friction angle at 30° under dry conditions. In practice this means that a rock mechanics practitioner can measure joint surface roughness on site with a carpenters comb, determine the joint roughness coefficient (JRC) with Barton's joint roughness profiles and use the graph to read of the friction angle of the joint surface for rocks with a hardness of approximately 200 MPa.

6.18 This research has provided the framework from which further research can be undertaken. The infrastructure is now available in South Africa to investigate the relationship between shear displacement and joint roughness. Testing should be carried out under the conditions of low (1 MPa) to high (10 MPa) normal stresses. This could provide a graph showing the relationship of joint roughness (JRC) vs. shear displacement. A reasonable correlation (with a confidence limit of 70%) between joint roughness and friction angle exists for the rock types tested. The rock types tested varied in hardness, origin, structure and strength. The relationship between friction angle and JRC under dry conditions can be expressed as follows:

$$\phi = \phi_b + f(JRC) \qquad \text{where } \phi_b = 30°$$

$$\text{and } f = 1{,}43$$

The graph can be used to estimate the friction angle (dry) when the joint roughness coefficient (JRC) is known. In practice this means that a rock mechanics practitioner can measure joint surface roughness on site with a carpenters comb, determine the joint roughness coefficient (JRC) with Barton's joint roughness profiles and use the equation to estimate the friction angle of the joint surfaces.

6.19 This study contributes to the knowledge of shear strength on southern African rock types, in particular on the sampling of specimens, preparation of specimens for testing in the large shear apparatus, the measurement of the roughness and hardness of the joint surface, the testing procedure and the interpretation and application of the results. The roughness index developed from this research as a measure of joint roughness was developed during this research project. To a lesser extent the study provides typical values of the shear strength characteristics of the rock joints.

6.20 It is recommended that a further research be initiated to investigate the shear strength of representative southern African rock types in further detail in a systematic manner. Such an investigation can build on the knowledge obtained in this investigation. It is important to keep the variables such as rock type, weathering, and hardness as few as possible and to investigate the influence of joint roughness.

6.21 A simple tool has been developed that will be of use to engineering geologists and rock mechanics practitioners who require a rapid method to determine the peak angle of friction of a joint surface in the field. If it is accepted that σ_n = 1 MPa (equal to the stresses normally associated in the foundations of dams and other civil engineering structures) then the value of *i* can be calculated for different JRC vs. JCS values and a graph be drawn as shown in Figure 4.19 on page 4.34.

6.22 Any experienced engineering geologist or rock mechanics engineer can now estimate [by estimating (or measuring) in the field] the JRC and the JCS (in terms of UCS) of a joint surface and by using this chart, determine the contribution of the surface characteristics to the portion of peak angle of friction. By adding the contribution of the waviness (Table 4.23 on page 4.35) as well as the basic friction angle, the total peak friction angle can be calculated.

6.23 Where fill is present on a joint surface, the fill thickness is of great importance. It is postulated that there is a relationship (FTC) between fill thickness JRC which has a value between 0 – 1.

For filled joints the modified Barton & Choubey equation becomes:

$$\tau = c_t + c_b + \sigma_n \tan [JRC \,.\, JMC \,.(1\text{-}FTC) \log_{10}(JCS/\sigma_n) + (1+FTC)\,\phi_b + (FTC \,.\, \phi_f) + i]$$

Where: τ = peak shear strength; σ_n = effective normal stress; JRC = joint roughness coefficient; JCS = joint wall compressive strength; ϕ_f = friction angle of fill; JMC = joint matching coefficient; c_t = true cohesion (fill); c_b = bridging strength; i = effect of waviness resulting in change of direction; FT = Fill thickness in mm; FTC = $-0{,}07 \ln (JRC+1/FT+1) + 0{,}5$; ϕ_b = basic friction angle of rock.

This relationship could further be investigated.

CHAPTER SEVEN

REFERENCES

Amadei, B. and Seab, S (1990) Constitutive models of rock joints. Rock Joints, Balkema, Rotterdam, 1990.

Bandis, S.C., Lumsden, A.C. and Barton, N.R. (1983) Fundamentals of Rock Joint Deformation. Int. J. Rock Mech. Min. Sci. & Geomech. Abstr. Vol. 20, No. 6 pp 249-268.

Bandis, S.C (1990) Mechanical properties of rock joints. In Rock Joints, proc. Int. symp. On rock joints, Loen, Norway, (eds. N. Barton and O. Stephansson), pp. 125-140. Rotterdam: Balkema.

Barton, N. (1971a) A relation between joint roughness and joint shear strength. Proc. Int. Symp. on Rock Mech. Rock Fracture. Nancy. Paper I-8

Barton, N. (1971b) Estimation of in situ shear strength from back analysis of failed rock slopes. Proc. Int. Symp. on Rock Mech. Rock Fracture. Nancy. Paper I-8

Barton, N. (1972) A model study of rock joint deformation. Int. J. Rock Mech. Min. Sci. Vol. 9, pp 579-602.

Barton, N. (1973) Review of a new shear strength criterion for rock joints. Engng. Geol. No. 7, pp287-332.

Barton, N.R. (1974) A review of the shear strength of filled discontinuities. Publication 105. Norwegian Geotechnical Institute, Oslo.

Barton, N. (1976) The shear strength of rock and rock joints. Int. J. Rock Mech. Min. Sci. & Geomech. Abstr. 13, 1 – 24.

Barton, N. and Choubey, V (1977) The Shear Strength of Rock Joints in Theory and Practice. Rock Mechanics 10, 1 - 54, 1977

Barton, N. (1982) Modelling Rock Joint Behaviour from In Situ Block Tests: Implications for Nuclear Waste Repository Design. Technical Report ONWI-308, Terra Tek, Inc, September 1982.

Barton, N.R. and Bandis, S.C. (1982) Effects of block size on the shear behaviour of rock joints. 23rd U.S. symp. On rock mechanics, Berkley, pp. 739-760.

Barton, N.R. and Bandis, S.C. (1990) Review of Predictive Capabilities of JRC-JCS Model in engineering practise. In Rock Joints, proc. Int. symp. On rock joints, Loen, Norway, (eds. N. Barton and O. Stephansson), pp 603-610. Rotterdam: Balkema.

Barton, N.R. and Bandis, S.C. (1991) Review of Predictive Capabilities of JRC-JCS Model in Engineering. Norwegian Geotechnical Institute, Publication Nr 182, Oslo, 1991.

Brown, E. T. (Ed) (1981) Rock characterisation, Testing and Monitoring. International Society for Rock Mechanics (ISRM) suggested methods, Pergamon Press.

Broch. ,E., and Franklin, J.A. (1972) Point load testing of rock. Int. J. Rock Mech. Min. Sci. Vol. 9, pp. 669-697, 1972.

Coulson, J.H. (1972) Shear strength of flat surfaces in rock. Proc. 13th Symposium on Rock Mechanics. Urbana, Ill., 1971 (E.J. Cording, Ed.). pp 77 – 105 (1972)

Cutnell, J.D. and Johnson, K.W. (2001) Physics. John Willey and Sons, Inc

De Toledo, P.E.C. and De Freitas, M.H. (1993) Laboratory testing and parameters controlling the shear strength of filled rock joints. Geotechnique 43, No 1, pp 1 - 19.

Deere, D.U. and Miller, R.P. (1966) Engineering classification and index properties of rock. Technical report No. AFNL-TR-65-116 Air Force Weapons Laboratory, New Mexico.

Duzgun, H.S.B., Yucemen, M.S. and Karpuz, C. (2002) A probabilistic model for the assessment of uncertainties in the shear strength of rock discontinuities. Int. J. Rock Mech. Min. Sci. Vol. 39, pp 743-754, 2002.

Fecker, E and Rengers, N. (1971) Measurement of large scale roughness of rock planes by means of profilograph and geological compass. Proc. Int. Symp. on Rock Fracture, Nancy (ISRM) Paper 1 – 18.

Fookes, P.G. and Denness, B. (1969) Observational studies on fissure patterns in Cretaceous sediments of South East England. Geotechnique, 19, No 4, pp 453 - 477.

Fourmaintraux, D. (1975) Quantification of discontinuities in rock from mafic origin. Rock Mechanics, 7, pp83 - 100

Fox, D.J., Kana, D.D. and Hsiung, S.M. (1998) Influence of Interface Roughness on Dynamic Shear Behavior in Jointed Rock. Int. J. Rock Mech. Min. Sci. Vol. 35, No. 7, pp. 923-940, 1998.

Geertsema, A.J. (2000) The Engineering Characteristics of Important Southern African Rock Types with special reference to the Shear Strength of Concrete Dam Foundations. Report to the Water Research Commission, Pretoria, 2000.

Gentier, S., Riss, J., Archambault, G., Flamand, R. and Hopkins, D. (2000) Influence of fracture geometry on shear behaviour. Int. J. Rock Mech. Min. Sci. Vol. 37, pp. 161-174, 2000.

Goodman, R.E. (1970) Determination of the in-situ modulus of deformation of rock. Deformability of Joints Symposium. American Society for Testing Materials, S.T.P. 477, pp 174 –196.

Goodman, R.E. (1976) Methods of Geological Engineering in Discontinuous Rocks, West, St Paul.

Grasselli, G., Wirth, J. and Egger, P. (2002) Quantitative three-dimensional description of a rough surface and parameter evolution with shearing. Int. J. Rock Mech. Min. Sci. Vol. 39, pp 789-800, 2002.

Hack, H., Price, D. and Rengers, N. (2002) A New Approach to Rock Slope Stability - a probability classification – SSPC. Bulletin of Engineering Geology and the Environment. Springer-Verlag, 2002.

Halliday, D., Resnick, R. and Walker, J. (1993) Fundamentals of Physics. Forth edition, John Wiley & Sons, Inc.

Hoek, E (2000) Practical rock engineering. Rocscience.

Hoek, E and Bray, J. (1977) Rock slope engineering. The Institution of Mining and Metallurgy, London.

Hoek, E and Brown, E.T. (1980) Underground Excavation in Rock. London: Institute of Mining and Metallurgy 527 pages.

Hudson, John A. (1993) Comprehensive Rock Engineering. Volume 1 - 5. Pergamon Press

ISRM (1978) Suggested method for determining the Uniaxial Compressive Strength of Rock Materials. ISRM Committee on Laboratory Tests, September 1978.

ISRM (1974) Suggested method for Determining Shear Strength. Committee on standardisation of Laboratory and Field tests, February 1974.

ISRM suggested method for the quantitative description of discontinuities in rock masses. Int. J. Rock Mech. Min. Sci. & Geomech. Abstr. 15, 319-368 (1978)

Katz, O., Reches, Z. and Roegiers, J.-C. (2000) Evaluation of mechanical rock properties using a Schmidt Hammer. Int. J. Rock Mech. Min. Sci. Vol.37, pp. 723-728, 2000.

Kulatilake, P.H.S.W. and Um, J. (1999) Requirements for accurate quantification of self-affine roughness using the roughness-length method. Int. J. Rock Mech. Min. Sci. Vol. 36, pp. 5-18, 1999.

Kutter, H.K. (1974) Rotary shear testing of rock joints. In: Advances in rock mechanics, pp 254 - 262. Proc. 3rd Congr. Int. Soc. Rock Mech, Denver.

Ladanyi, H.K. and Archambault, G. (1977) Shear strength and deformability of filled indented joints. Proc. 1st Int. Symp. Geotech, pp 317 - 326. Structural Complex Formations, Capri.

Lee, H.S., Park, Y.J., Cho, T.F. and You, K.H. (2001) Influence of asperity degradation on the mechanical behavior of rough rock joints under cyclic shear loading. Int. J. Rock Mech. Min. Sci. Vol. 38, pp. 967-980, 2001.

Lupini, J.F, Skinner, A.E. and Vaughan, P.R. (1981) The drained residual strength of cohesive soils. Geotechnique, No 2, pp 181 - 213.

Maertz N. H. and Franklin J. (1990) A. Roughness scale effects and fractal dimension. In Proc. 1st Workshop on Scale Effects in Rock Masses, Leon Norway. (Edited by A. Pinto da Cunha), pp 121 – 126. Balkema, Rotterdam.

Maksimovic, M. (1996) The Shear Strength Components of a Rough Rock Joint. Int. J. Rock Mech. Min. Sci. Vol. 33, No. 8, pp 769-783, 1996.

Miller, R.P. (1965) Engineering classification of index properties for intact rock. Ph.D. Thesis. University of Illinois, 1965.

Nicholson, Glenn A. (1983) In situ and laboratory shear device for rock: A comparison. Technical Report GL-83-14. Geotechnical Laboratory. U S Army Engineer Waterways Experimental Station, Vicksburg, Mississippi.

Patton, F.D. (1966) Multiple modes of shear failure in rock and related materials. Ph. D. Thesis. University of Illinois. Pp 1 – 282.

Pegram, G.G.S. and Pennington, M.S. (1996) A Method for Estimating the Hydraulic Roughness of Unlined Bored Tunnels. Report to the Water Research Commission by the Department of Civil Engineering, University of Natal. WRC Report No 579/1/96.

Pereira, J.P. (1990) Mechanics of filled discontinuities. Proceedings of an International Conference on mechanics of jointed and faulted rock, pp 375 - 380. Vienna.

Rengers, N (1971) Unebenheit und der Reibungswiderstand von Gesteintrennflächen. Diss. Tech. Hochschule Frindericiana, Karlsruhe, Ins. Bodenmech. Felsmech. Veroff, pp 1-129.

Priest, Stephen D. (1993) Discontinuity analysis for rock engineering. Chapman & Hall, London.

Richards, L.R. (1975) The shear strength of joints in weathered rock. Ph.D. Thesis. University of London, Imperial College, pp 1 – 427.

Roko, R.O., Daemen, J.J.K. and Myers, D.E. (1997) Variogram Characterization of Joint Surface Morphology and Asperity Deformation During Shearing. Int. J. Rock Mech. Min. Sci. Vol.34, No. 1, pp. 71-84.

Seidel, J.P. and Haberfield, C.M. (2002) A theoretical model for rock joints subjected to constant normal stiffness direct shear. Int. J. Rock Mech. Min. Sci. Vol. 39. pp 539-553.

Scavia, C. and Re, F. (1999) Determination of contact areas in rock joints by X-ray computer tomography. Int. J. Rock Mech. Min. Sci. Vol. 36, pp. 883-890, 1999.

Stacey, T.R. (1980) A simple device for direct shear testing of intact rock. Jnl. of the SA Institution of Mining and metallurgy. March, 1980.

Sun, W.H, Zheng, T.M. and Li, M.Y. (1981) The mechanical effect of the thickness of weak intercalary layers. Proceedings of an International symposium on weak rock, pp 49 - 54, Tokyo.

Szwedzick, T. (1998) Indentation Hardness Testing of Rock. Int. J. Rock Mech. Min. Sci. Vol. 35, No. 6, pp 825-829, 1998.

U S Bureau of Reclamation. Procedure for performing Direct and Sliding Friction Testing of Rock Core. Draft Internal report USBR 6250-92.

Van der Walt, A. (1992) Specifications for Large Shear Machine. Internal report of the Department of Water Affairs, Pretoria, 1992

Van Loon, A.J. (2003) How 'hard' are hard-rock deformations. Earth Science Reviews Vol 61, pp. 181-188, 2003.

Van Schalkwyk, A. (2002) Engineering Geology (STX 723) class notes. University Pretoria.

Vogler, U. W. (1985) Code of practice for determining the punch shear strength on plates of intact rock material. Geomechanics Division, CSIR, Pretoria 1985. pp 1 - 5.

Yang, Z.Y. and Chiang, D.Y. (2000) An experimental study on the progressive shear behavior of rock joints with tooth-shaped asperities. Int. J. Rock Mech. Min. Sci. Vol. 37, pp. 1247-1259, 2000.

Zhao, J. (1997a) Joint Surface Matching and Shear Strength. Part A: Joint Matching Coefficient (JMC) Int. J. Rock Mech. Min. Sci. Vol. 34, No. 2 pp173-179, 1997.

Zhao, J. (1997b) Joint Surface Matching and Shear Strength. Part B: JRC-JMC Shear Strength Criterion. Int. J. Rock Mech. Min. Sci. Vol. 34, No. 2 pp179-185, 1997.

Additional reading

Barton, N. (1991) Scale effects of Sampling Bias? Norwegian Geotechnical Institute, Publication Nr 182, Oslo, 1991.

Boulton, M., Armand, G., Hoteit, P. and Divoux, P. (2002) Experimental investigations and modelling of shearing calcite healed discontinuities of granodiorite under typical stresses. Engineering Geology Vol. 64, pp. 117-133, 2003.

Bridges, M.C. (1975) Presentation of fracture data for Rock Mechanics. Proceedings of the 2nd Australian - New Zealand Conference on Geomechanics. Brisbane.

Cook N. G. W. (1988) Natural joints in rock: Mechanical, Hydraulic and Seismic Behaviour and Properties under Normal Stress. Int. J. Rock Mech. Min. Sci. & Geomech. Abstr. Vol. 29, No 3, pp 198-223, 1992.

Gabrielsen, R.H. (1990) Characteristics of joints and faults. Proceedings of the International Son Rock Joints, Loen. Balkema, Rotterdam.

Gillette, D. R., Sture, S., Ko, H., Gould, M. C. and Scott, G. S. (1983) Dynamic Behaviour of Rock Joints. 24th U S Symposium on Rock Joints, June 1983.

Hack, H.R.G.K. (1996) Slope Stability Probability Classification – SSPC. PhD thesis, Technische Universiteit, Delft, The Netherlands.

Hakami, E and Barton, N. (1991) Aperture Measurement and Flow experiments Using Transparent Replicas of Rock Joints. Norwegian Geotechnical Institute, Publication Nr 182, Oslo, 1991

Haverland, M. L. and Slebir, E. J. (1971) Methods of performing and interpreting in situ shear tests. Engineering and Research Centre, Bureau of Reclamation, U S Department of the Interior. Proceedings of the 13th Symposium on Rock Mechanics. University of Illinois at Urbana-Champaign, August 30 - September 1, 1971.

Hoek, E. and Brown, E.T. (1997) Practical Estimates of Rock Mass Strength. Int. J. Rock Mech. Min. Sci. Vol. 34, No. 8, pp 1165-1186, 1997.

Jaeger, J.C. (1959) Frictional properties of joints in rock. Geofis. Pura Appl. Milano. pp 148 - 158.

Jaeger, J.C. (1971) Friction of rocks and stability of rock slopes. Geotechnique 21, pp 97-134.

Makurat, A., Barton, N., Rad, N. S. and Bandis, S. (1991) Joint Conductivity variation due to normal and shear deformation. Norwegian Geotechnical Institute, Publication Nr 182, Oslo, 1991.

Makurat, A., Barton, N., Tunbridge, T. and Vic, G.. (1991) The Measurement of the Mechanical and Hydraulic Properties of Rock Joints at Different Scales in the Stripa project. Norwegian Geotechnical Institute, Publication Nr 182, Oslo, 1991.

Makurat, A., Barton, N., Vic, G., Chryssanthakis, P. and Monsen, K. (1991) Jointed Rock Mass Modelling. Norwegian Geotechnical Institute, Publication Nr 182, Oslo, 1991.

Price, N.J. (1966) Fault and Joint development in Brittle and semi-Brittle rock. Pergamon, Oxford.

Sonmez, H, Ulusay, R. and Gokceoglu, C. (1998) A Practical Procedure for Back Analysis of Slope Failures in Closely Jointed Rock Masses. Int. J. Rock Mech. Min. Sci. Vol. 35, No. 2 pp 219-233, 1998.

Whitten, D.G.A. and Brooks, J.R.V. (1972) A Dictionary of Geology. Penguin, Harmondsworth.

Wilbowo, J. T., Amadei, B., Sture, S., Robertson, A. B. and Price, R. (1992) Shear Response of A Rock Joint Under Different Boundary Conditions: An Experimental Study. The Proceedings of an International Conference on Fractured and Jointed Rock Masses, Lake

Ziegler, T.W. (1972) In Situ Testing for the Determination of Rock Mass Shear Strength. Technical Report S-72-12 U.S. Army Engineer Waterways Experimental Station, Vicksburg, Miss.

APPENDICES